Astbury Centre for Structural Molecular Biology

UNIVERSITY OF LEEDS

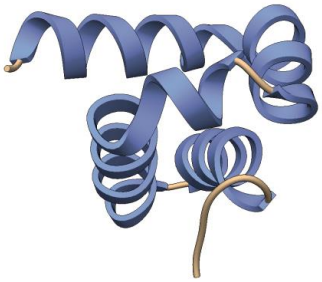

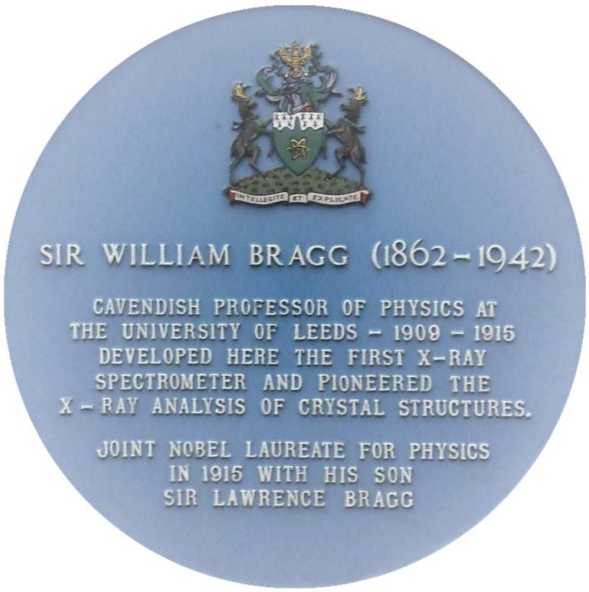

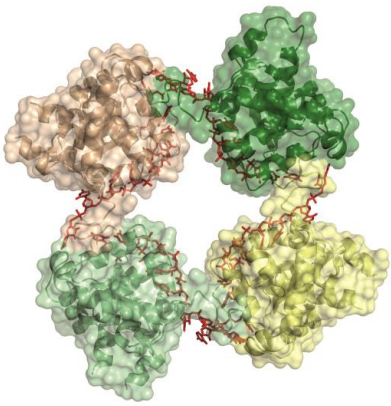

A century of crystallography at Leeds

ASTBURY CENTRE

Annual Report 2013

Front cover illustration: 100 years of crystallography at Leeds. Centre: blue plaque commemorating the development of X-ray crystallography. Left and right: protein structures solved using X-ray crystallography by the Astbury members (the Wright and Edwards groups, respectively) in 2013. More details can be found on pages 20 and 74 of this report.

Acknowledgement

The Astbury Centre for Structural Molecular Biology thanks its many sponsors for support of the work and its members for writing these reports. The report is edited by David Brockwell.

This report is also available electronically via http://www.astbury.leeds.ac.uk

Mission Statement

The Astbury Centre for Structural Molecular Biology will promote interdisciplinary research of the highest standard on the structure and function of biological molecules, biomolecular assemblies and complexes using physico-chemical, molecular biological and computational approaches.

Introduction

2013 showed that the Astbury Centre continues to be a thriving hub of scientific achievement, as this letter and the scientific reports that follow portray. I would like to take this opportunity to thank all Astbury members: the principal investigators, facility managers, technicians, students and postdocs for all of your efforts in generating this success. Without your enthusiasm, hard work, collegiality and excellent science that bring different disciplines together, this could not have happened. We also acknowledge, with thanks, the support of the University of Leeds; the Faculties of Biological Sciences and Maths and Physical Sciences and the Schools of Chemistry, Molecular and Cellular Biology and Physics and Astronomy for their support of the Centre. We are also much indebted to an array of funding agencies for supporting our science, including BBSRC, EPSRC, MRC, the Wellcome Trust, other charities, ERC, EU and Industry.

Our annual report provides summaries on-going scientific projects from the Astbury Centre's research outputs in 2013, chosen for highlight by the participating members. In its pages you will find new and exciting research which spans fundamental research in Structural Molecular Biology, Biophysics, Chemical Biology and Cell Biology, alongside the exploitation of the results obtained in biotechnology, bioengineering and medicine, each made possible by the inter- and multidisciplinary research within the Centre.

During 2013 the Centre continued in its quest of "Understanding Life in Molecular Detail" through multiple different activities, including seminars, publications, public lectures and other events. We continued to enjoy an excellent seminar series (organised by Arwen Pearson), hosting 11 lectures during 2013 with speakers from the UK, Germany, Belgium and the USA. The Centre also continued its "Research Theme" events for PIs, with topics this year including "Synthetic Biology", "Biomembrane and Membrane Proteins", "Antimicrobials and Astbury", and "Astbury Facilities". The Centre's Biennial Residential Research Retreat, held this year on September 19th/20th at the Shrigley Hall Hotel in Cheshire was a sell-out, with 149 attendees enjoying excellent seminars from students, post-docs and PIs. This year's retreat also included sessions highlighting new research equipment within the Centre and popular 'Flash Poster' presentations. We again welcomed representatives from the Wellcome Trust to the retreat, who led a session on "Careers and Fellowships" for the post-docs and students, whilst the PIs discussed "Opportunities for engagement with Industry" in a session led by Adam Nelson and Kate Langton from the University's Pharmaceutical and Biopharmaceutical Innovation Hub. A "Zombie Apocalypse", organised by the Astbury Society provided the stimulus for an amusing, challenging and excellent team-building event. Thank you to the Astbury Society for a memorable event!

The Centre welcomed five new academic staff members in 2013 (Andy Tuplin (RNA structure and virology), Anastasia Zhuravleva (Biological NMR of large complexes), Stephanie Wright (cancer biology and eukaryotic gene regulation), Jamel Mankouri (virus pathogenesis and ion channels) and Adrian Goldman (crystallography of membrane proteins)). We were sorry to lose Sarah Staniland and Peter Olmsted from the membership in 2013, as they took up academic positions elsewhere. We wish them well in their future careers. We were delighted to welcome many PhD students and postdocs to the Centre this year. This takes our current numbers to 65 academic staff, 144 PhD students, 77 postdoctoral researchers and 11 research fellows.

Astbury Centre members published their research in a wide range of journals in 2013, with a total of 123 manuscripts being published, including >10 papers in the high impact journals *Nature Communications*, *PNAS*, *Nature Chemistry*, *PLoS Biol and JACS*. In terms of grant income, Astbury members also enjoyed success in 2013. Highlights included the University's first ERC "Proof of Concept" Grant (€125k to Andy Wilson); a €2.5M ERC Advanced Grant (to Sheena Radford); a BBSRC Alert 13 grant to Adrian Goldman and Astbury colleagues for

new equipment for membrane protein crystallisation (~£1M investment); and the renewal (valued at ~£4.5M) of our Wellcome Trust funded 4 year PhD in "The Molecular Basis of Biological Mechanisms" led by Alan Berry. Together with >£11.6M new grant income raised for project and programme grants, this brings the Astbury portfolio to a £38M share of £60M of grants in 2013: an impressive figure that is testament to the hard work and success of our members.

2013 saw continuing success of the members of the Astbury Centre in terms of peer recognition. Our student and post-doc members again received several awards, including the Sir Howard Dalton Young Microbiologist of the Year award of the Society of General Microbiology to Sophie Schumann in Ade Whitehouse's group. Our members were also winners of the BBSRC DTP business plan competition (Tony Palmer (Stephen Baldwin's group) and Jess Haigh (Jim Deuchars' group)); whilst prizes for poster presentations and oral presentations were awarded to Georgia Magnatti, Richard Doveston and Daniel Foley (Adam Nelson's group); David Yeo (Andy Wilson's group), James Ross (Bruce Turnbull and Emanuele Paci's group) and Kayzaryna Makowska and Adriana Klyszeijko (Michelle Peckham's group). Congratulations also to our PI members who received honours: Lorna Dougan (the Royal Society of Chemistry's (RSC) Macro Group UK Young Researcher's Medal); Sheena Radford (the Carl Branden award of the Protein Society) and Bruce Turnbull (2013 Carbohydrate research Prize of the RSC). Others continued to play an active role in outreach activities: Tom Edwards was interviewed on Radio 4 with Eddie Mair and again with Melvyn Bragg in the aptly termed programme "Bragg on Braggs" to celebrate 100 years of crystallography; Bruce Turnbull and his group took part in the Royal Society's Summer Science Exhibition; Peter Henderson's work on "superbugs" was highlighted by the Yorkshire Evening Post; and Michelle Peckham took part in the Radio 4 programme "In our Time" on the topic "The Microscope". Outreach is an important part of the Centre's activities. Thank you to all who have participated in these events.

The Astbury Society, led by the presidents Sasha Derrington and Megan Hughes in 2013, alongside the current presidents Claire Windle and Katherine Horner, played a magnificent role in Astbury activities in 2013. The first May Ball was a spectacular hit and a highlight of the year. Other activities in 2013 involved the now-famous Christmas quiz night, a Film Night and the much-enjoyed cake bakes and coffee mornings. Together these events have raised more than £1,300 for the "Leeds Children's Charity". The Astbury Society also hosted the barbeque and Sports Day at the Seventh Annual Astbury Lecture which was given by Professor Frances Ashcroft, F Med Sci, FRS (University of Oxford) on "Metabolic Regulation of K-ATP Channels: From Molecules to Disease". This annual event was its usual success, with a brilliant lecture, much fun and physical exertion at the sports day, and a much enjoyed barbeque. Photos of these events can be seen at www.astbury.leeds.ac.uk/about/society.php. Do take a look!

I hope that you enjoy reading this Annual Report whether you are a member of the Centre, a visitor, a member of our Industrial Advisory Board, a member of a funding agency that supports our activities or a passing reader with an interest in Structural Molecular Biology and the activities of our Centre. Finally, thank you to David Brockwell for editing this report, everyone who contributed to it, and all who participated in the Astbury Centre's activities in 2013. I look forward to continuing our successes in 2014.

Sheena E. Radford
Director, Astbury Centre for Structural Molecular Biology,
Leeds, April 2014

Please note that this report (as well as those from previous years) is also available as a PDF document which can be downloaded from our website (www.astbury.leeds.ac.uk).

Contents

Contributions indexed by Astbury Centre Principal Investigator

Biomolecular mass spectrometry

James Ault, Helen Beeston, Antonio Calabrese, Paul Devine, Henry Fisher, Patrick Knight, Negar Rajabi, Charlotte Scarff, Tom Watkinson, Lydia Young and Alison Ashcroft

Introduction

Our research is focussed on the development and application of mass spectrometry (MS) to investigate the structure and function of biomolecules. We use non-covalent electrospray ionisation (ESI)-MS and tandem mass spectrometry (MS/MS) to determine the mass, conformational properties, stoichiometry, stability, and binding characteristics of biomolecules and their complexes. We are pioneers of ion mobility spectrometry (IMS)-MS, a technique that can separate co-populated biomolecular species on the basis of their shape and measure their mass and cross-sectional area in a single, rapid ($\leq$ 2 mins) experiment. The main focus of our research is on protein folding, function and self-aggregation, protein-ligand interactions, biomolecular complex assembly, and oligonucleotide structure.

Results

We have developed a robust mass spectrometric method for sequencing RNA molecules. After using ESI-MS to measure the mass of the RNA, we determine its sequence using collision-induced dissociation MS/MS. This generates a plethora of overlapping product ions which are difficult to interpret. Using IMS after MS/MS separates the fragment ions according to their charge state, allowing us to decipher the sequence more readily (Figure. 1).

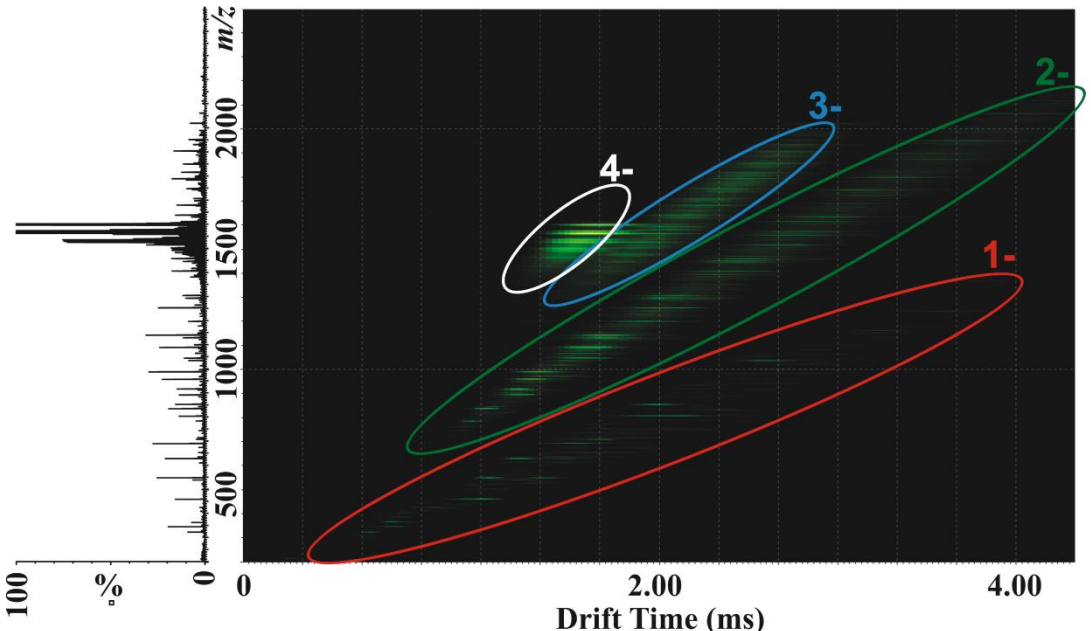

Figure 1: ESI-MS/MS-IMS-MS Driftscope plot (m/z vs IMS drift time (ms) vs intensity) of a 20-nucleotide RNA (6405 Da), following MS/MS dissociation of the m/z 1600 quadruply charged precursor ions. The data show the separation of four groups of product ions: the singly charged ions are encircled in red, the doubly charged ions in green, the triply charged ions in blue, and the quadruply charged ions in white. From these product ions, the sequence was found to be 3'-CCC UAG GAC AGU ACC UAG GG-5'.

Publications

Alexander, C., Juergens, M., Shepherd, D., Freund, S., Ashcroft, A. & Ferguson, N. (2013) Thermodynamic origins of protein folding, allostery, and capsid formation in the human hepatitis B virus core protein. *Proc. Natl. Acad. Sci. USA* **110**: 2782-2791.

Ariza, A., Tanner, S., Walter, C., Dent, K., Shepherd, D., Wu, W., Matthews, S., Hiscox, J., Green, T. , Luo, M., Elliott, R., Fooks, A., Ashcroft, A., Stonehouse, N., Ranson, N., Barr, J. & Edwards, T. (2013) Nucleocapsid protein structures from orthobunyaviruses reveal insight into ribonucleoprotein architecture and RNA polymerization. *Nucleic Acids Res.* **41**: 5912-5926.

Fisher, H., Smith, M. & Ashcroft, A. (2013) De novo sequencing of short interfering ribonucleic acids facilitated by use of tandem mass spectrometry with ion mobility spectrometry. *Rapid Commun. Mass Spectrom.* **27**: 2247-2254.

Juergens, M., Voeroes, J., Rautureau, G., Shepherd, D., Pye, V., Muldoon, J., Johnson, C., Ashcroft, A., Freund, S. & Ferguson, N. (2013) The hepatitis b virus pres1 domain hijacks host trafficking proteins by motif mimicry. *Nat. Chem. Biol.* **9**: 540-U532.

Knapman, T., Valette, N., Warriner, S. & Ashcroft, A. (2013) Ion mobility spectrometry-mass spectrometry of intrinsically unfolded proteins: Trying to put order into disorder. *Curr. Anal. Chem.* **9**: 181-191.

Lewis, M., Arnot, C., Beeston, H., Mccoy, A., Ashcroft, A., Gay, N. & Gangloff, M. (2013) Cytokine spatzle binds to the drosophila immunoreceptor toll with a neurotrophin-like specificity and couples receptor activation. *Proc. Natl. Acad. Sci. USA* **110**: 20461-20466.

Ndlovu, H., Ashcroft, A., Radford, S. & Harris, S. (2013) Molecular dynamics simulations of mechanical failure in polymorphic arrangements of amyloid fibrils containing structural defects. *Beilstein Journal of Nanotechnology* **4**: 429-440.

Pritchard, C., O'connor, G. & Ashcroft, A. (2013) The role of ion mobility spectrometry-mass spectrometry in the analysis of protein reference standards. *Anal. Chem.* **85**: 7205-7212.

Shepherd, D., Holmes, K., Rowlands, D., Stonehouse, N. & Ashcroft, A. (2013) Using ion mobility spectrometry-mass spectrometry to decipher the conformational and assembly characteristics of the hepatitis b capsid protein. *Biophys. J.* **105**: 1258-1267.

Funding
This work was funded by the BBSRC, the EPSRC, the Wellcome Trust, Waters UK Ltd., LGC, AZ, GSK, UCB, & Medimmune. We thank the BMSS for student travel grants.

Collaborators
Leeds: J. Barr, T. Edwards, S. Harris, P. Henderson, S. Radford, D. Rowlands, P. Stockley, N. Stonehouse, S. Warriner, A. Wilson.

External: S. Arscott (CNRS, Lille, France), G. O'Connor (LGC, UK), M. Morris & K. Giles (Waters UK Ltd.), N. Ferguson (UCD, Eire), S. Macedo Ribeiro (IBMC, Portugal), D. Raleigh (Stonybrook, NY, USA) and A. Pastore (King's College London, UK).

Using ion mobility mass spectrometry to probe amyloid formation

Lydia Young, Charlotte Scarff, Lucy Woods, Patrick Knight, Claire Sarell,
Sheena Radford and Alison Ashcroft

Introduction

More than twenty five proteins or peptides are associated with amyloid disease. The precise mechanism by which these soluble monomers assemble into highly-ordered fibrillar deposits is unknown. One example is amylin (also known as islet amyloid polypeptide) which is the amyloid peptide associated with type II diabetes. It is found *in vivo* as amyloid deposits in the pancreatic islets of sufferers and its self-aggregation is thought to be a pathogenic factor in the disease. Human amylin (hAmylin) forms amyloid readily at neutral pH *in vitro*, while rat amylin (rAmylin) does not, despite differing in sequence at only six out of 37 amino acid positions (Figure 1a). We have used electrospray ionisation-ion mobility spectrometry-mass spectrometry (ESI-IMS-MS) to probe oligomer formation from human amylin *in vitro*. This enabled the identification of oligomeric intermediates of human and rat amylin assembly and determination of the mechanisms of two small molecule inhibitors of amyloid formation.

Results

hAmylin and rAmylin oligomers up to, and including, hexamer were detected using ESI-IMS-MS (Figure 1b). An IMS calibration allowed collision cross-sections (CCS) of the oligomers to be estimated, indicating that they are extended in conformation. The gas-phase stabilities of the co-populated, transient, oligomers formed from both peptides were also compared. The results revealed significant differences in the stability of otherwise similarly organized oligomers of hAmylin and rAmylin that are likely related to their difference in amyloid propensity. The binding of small molecule inhibitors to specific conformers within a dynamic ensemble of amylin has also been measured using ESI-IMS-MS and the progress of

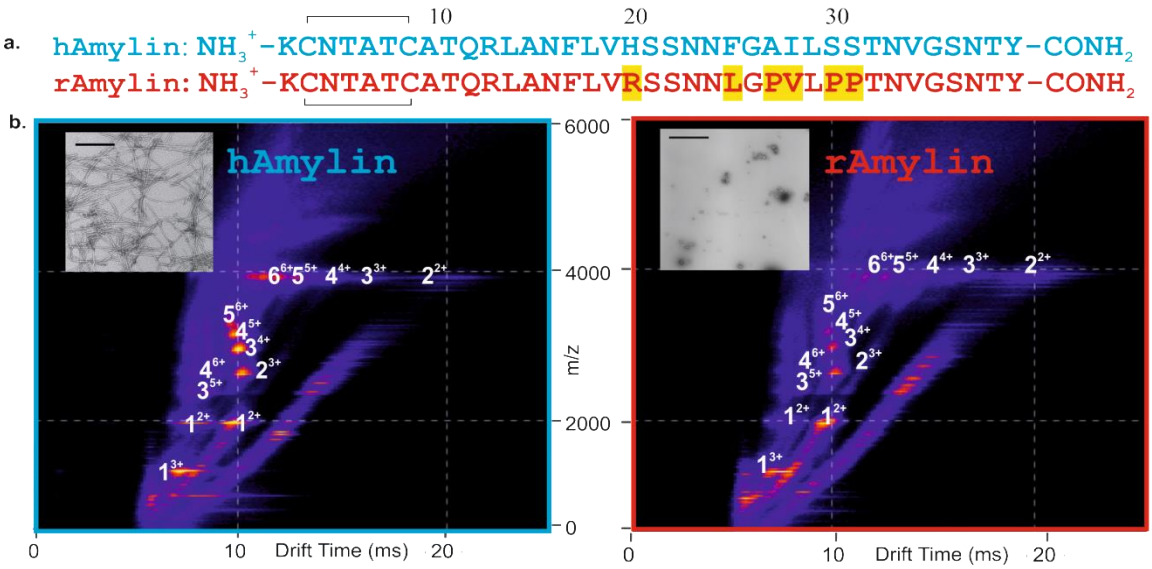

Figure 1: (a) Comparison of human amylin (hAmylin) and rat amylin (rAmylin) sequences. Both peptides have a disulphide bridge between Cys-2 and Cys-7 and an amidated C-terminus. Residues that differ from those of the human peptide are highlighted in yellow in the rat sequence. **(b)** ESI-IMS-MS data showing oligomers formed from the peptides.

oligomer formation and fibril assembly in the presence of inhibitors monitored. The results (Figure 2) indicate that EGCG and silibinin are effective inhibitors of hAmylin assembly into amyloid, binding to monomeric hAmylin and preventing its self-assembly into oligomers and amyloid fibrils.

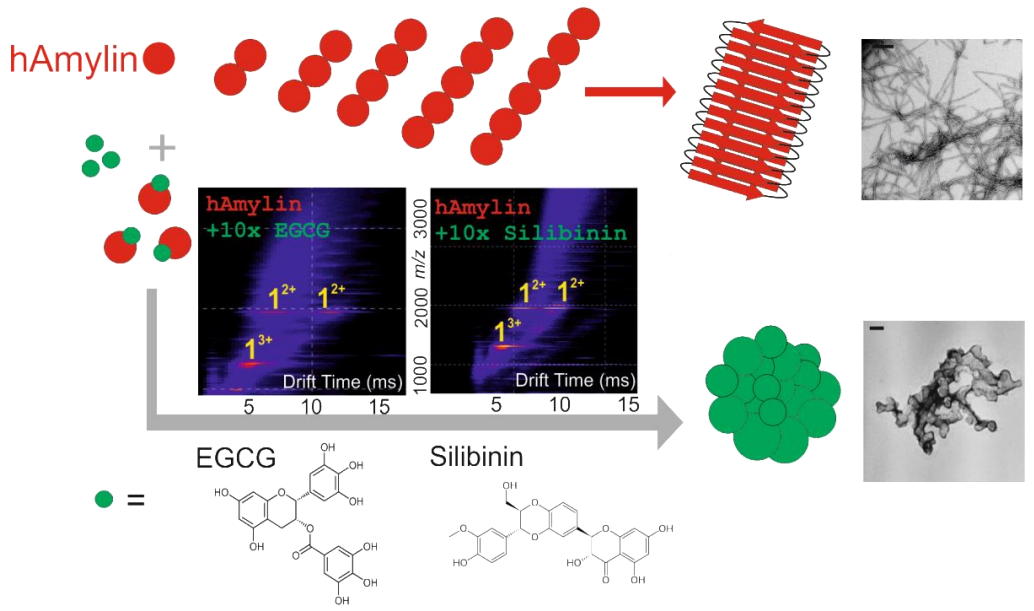

Figure 2: Schematics of hAmylin amyloid formation in the absence and presence of inhibitors (EGCG and silibinin). In isolation, hAmylin forms monomer through hexamer and long-straight fibrils. When bound by inhibitor, hAmylin self-assembly is redirected, resulting in the absence of oligomers and the formation of amorphous aggregate.

We are now using the approaches developed to investigate the assembly mechanisms of other proteins into amyloid fibrils, including β_2-microglobulin and ataxin-3, as highlighted in the references below.

Publications

Sarell, C., Woods, L., Su, Y., Debelouchina, G., Ashcroft, A., Griffin, R., Stockley, P. & Radford, S. (2013) Expanding the repertoire of amyloid polymorphs by co-polymerization of related protein precursors. *J. Biol. Chem.* **288**: 7327-7337.

Scarff, C., Sicorello, A., Tome, R., Macedo-Ribeiro, S., Ashcroft, A. & Radford, S. (2013) A tale of a tail: Structural insights into the conformational properties of the polyglutamine protein ataxin-3. *Int. J. Mass spectrom.* **345**: 63-70.

Woods, L., Radford, S. & Ashcroft, A. (2013) Advances in ion mobility spectrometry-mass spectrometry reveal key insights into amyloid assembly. *Biochimica Et Biophysica Acta-Proteins and Proteomics* **1834:** 1257-1268.

Funding

This work was supported by the BBSRC, EPSRC, Micromass UK Ltd/Waters Corpn. (Manchester, UK) and the Wellcome Trust.

Collaborators

External: S. Macedo Ribeiro (IBMC, Porto), J. Baum (Rutgers University, New Jersey), A. Pastore (Kings College, London), D. Raleigh (Stonybrook University, New York).

Phase behaviour and transitions in complex biological systems

Stefan Auer

Introduction

My research is focused on the application of theoretical computational tools developed in soft condensed matter physics to investigate the phase behaviour and transitions of complex systems of biomolecules. The research highlights in the year 2013 was our reconsideration of nucleation theory to describe amyloid fibrils nucleation.

Confounding the paradigm: peculiarities of amyloid fibril nucleation

Fibrils of amyloid proteins are currently of great interest because of their involvement in various amyloid-related diseases and nanotechnological products. In a recent kinetic Monte Carlo simulation study [Cabriolu, R., Kashchiev D., Auer, S. (2012) *J. Chem. Phys.*, 137, 204903], we found that our simulation data for the rate of amyloid fibril nucleation occurring by direct polymerization of monomeric protein could not be described adequately by nucleation theory. It turned out that the process occurred in a peculiar way, thus confounding the nucleation paradigm and demanding a new theoretical treatment. In the present study, we reconsider the theoretical approach to nucleation of amyloid fibrils and derive new expressions for the stationary rate of the process. As these expressions provide a remarkably good description of the simulation data, using them, we propose a theoretical dependence of the amyloid-β_{40} fibril nucleation rate on the concentration of monomeric protein in the solution. This dependence reveals the existence of a threshold concentration below which the fibril nucleation in small enough solution volumes is practically arrested, and above which the process occurs vigorously, because then each monomeric protein in the solution acts as fibril nucleus. The presented expressions for the threshold concentration and for the dependence of the fibril nucleation rate on the concentration of monomeric protein can be a valuable guide in designing new therapeutic and/or technological strategies for prevention or stimulation of amyloid fibril formation.

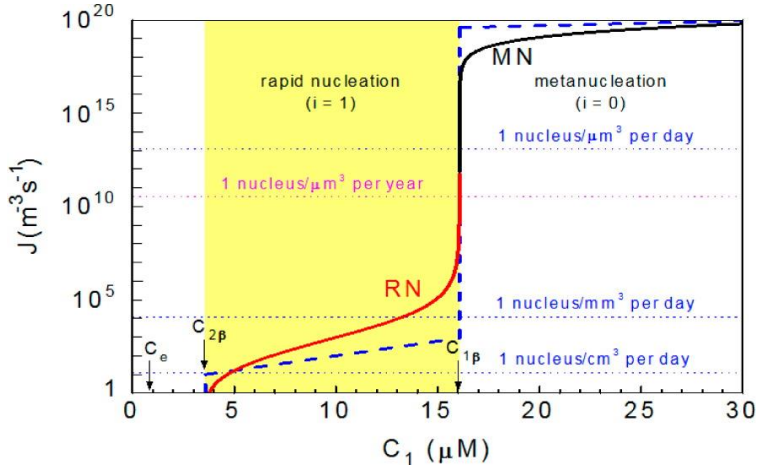

Figure 1: illustration of the sharp jump of the nucleation rate of amyloid fibrils at a certain threshold concentration.

Publications

Kashchiev, D., Cabriolu, R. & Auer, S. (2013) Confounding the paradigm: peculiarities of amyloid fibril nucleation. *J. Am. Chem. Soc.* **135**: 1531-1539.

Funding

This work was supported by the EPSRC-GB Grant No. EP/G026165/1.

This work was funded by the BBSRC, the EPSRC, the Wellcome Trust, Waters UK Ltd., LGC, AZ, GSK, UCB, & Medimmune. We thank the BMSS for student travel grants.

Collaborators
External: D. Kashchiev (Sofia), R. Cabriolu (Washington).

DNA-directed assembly of lipid nanodiscs into BioNanoStack architectures

Paul Beales

We have used Nature's three primary building blocks (lipids, proteins and nucleic acids) to assemble 1D supramolecular polymers with a controllable periodic repeat distance. Lipid nanodiscs are formed, which consist of a 10 nm diameter lipid bilayer that is stabilized at its edges by two copies of an amphipathic, α-helical scaffold protein (a truncated form of apolipoprotein A-1). These nanodiscs are further functionized with lipid-DNA conjugates to create the monomeric sub-unit of our self-assembled architectures. When two populations of nanodiscs, functionalized with complementary oligonucleotide sequences, are mixed, the shape anisotropy of the nanodiscs dictates the formation of quasi-1D superstuctures, which we refer to as BioNanoStacks (Figure 1a,b). The periodicity between nanodiscs is controllable by tuning the length of the DNA sequences and BioNanoStack formation is reversible by heating above the T_m of the duplexed DNA.

We have demonstrated the application of BioNanoStacks for templating the assembly of nanoparticles by taking advantage of a nickel-mediated interaction between NTA-functionalized gold nanoparticles and the His-tags of the scaffold proteins (Fig. 1c). Further applications are anticipated in tissue engineering scaffolds and the serial assembly of transmembrane transporter proteins into biological nanowires.

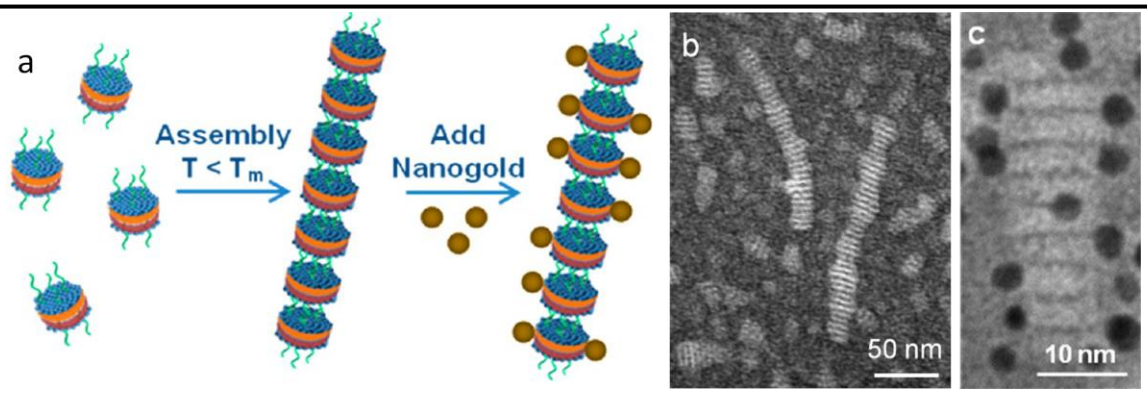

Figure 1: (a) scheme demonstrating the 1D assembly of DNA-functionalized lipid nanodiscs into periodic BioNanostack fibres below the Tm of the DNA sequence and their application as templates for gold nanoparticle patterning. **(b)** Negative-staining TEM image of POPC nanodiscs with an average of 4 DNA per disc assembled in 100 mM NaCl. **(c)** Negative-staining TEM image of the nickel-mediated assembly of 5 nm NTA gold nanoparticles on a BioNanostack template.

Publications

Beales, P., Geerts, N., Inampudi, K., Shigematsu, H., Wilson, C. & Vanderlick, T. (2013) Reversible assembly of stacked membrane nanodiscs with reduced dimensionality and variable periodicity. *J. Am. Chem. Soc.* **135**: 3335-3338.

Geerts, N., Schreck, C., Beales, P., Shigematsu, H., O'hern, C. & Vanderlick, T. (2013) Using DNA-driven assembled phospholipid nanodiscs as a scaffold for gold nanoparticle patterning. *Langmuir* **29**: 13089-13094.

Funding

This work was supported by Yale University.

Collaborators

External: T. Vanderlick, C. Wilson, C. O'Hern, H. Shigematsu and N. Geerts, Yale University.

Cytochrome *c* can permeabilize model mitochondrial membranes

Paul Beales

Introduction

Cytochrome *c* (cyt *c*) is released into the cytosol as an early signalling molecule during intrinsic cell apoptosis, where it complexes with APAF-1 to trigger a downstream cascade of caspase protein activation. The exact mechanism by which cyt *c* escapes from the inter-membrane space of mitochondria is still unknown and is usually refered to as mitochondrial outer membrane permeabilisation (MOMP). We have investigated the interaction of cyt *c* with model mitochondrial membranes (GUVs and droplet interface bilayers) containing the lipid cardiolipin (CL) and, in particular, focused on quantifying changes in membrane permeability.

Results

Confocal fluorescence microscopy studies of GUVs revealed the kinetics of permeabilisation of membranes to macromolecules at the single vesicle level. We observed stochastic permeabilisation of CL-containing membranes induced by cyt *c* (Fig. 1a,b). Once permeabilized, cyt *c* and a passive leakage marker (a 10 kDa fluorescent dextran) rapidly leaked into the GUV, strongly indicative of the formation of pores large enough for macromolecules to translocate through. Notably, a larger 70 kDa fluorescent dextran did not leak simultaneously with the cyt *c*, which suggests a size-limit to the pores that form. The formation of nanoscale pores capable of macromolecular transport was also supported by quantitative measurement of the membrane permeability by analysing the dye influx kinetics.

We have suggested a mechanism for cyt *c*-induced pore formation based on local changes in membrane spontaneous curvature when it binds to the membrane. We propose that cationic cyt *c* electrostatically clusters anionic CL lipids beneath it upon membrane association. CL lipids have bulky acyl tails which intrinsically gives the molecules a significantly large negative spontaneous curvature such that CL prefers to form non-bilayer phases in unitary systems. Therefore clustering of CL will decrease the local spontaneous curvature of the membrane. We theoretically analyzed the impact caused by local generation of negative curvature stress using Helfrich's ansatz for the curvature elastic energy of the membrane. This model revealed a significant reduction in the energy between a planar bilayer state and the formation of a toroidal lipid pores in the membrane, where the pore radius had a strong energy minimum at a finite nanoscale size (Fig. 1c), consistent with our experimental findings.

We further investigated cyt c's permeabilizing properties using the droplet interface bilayer experimental model system, which allows simultaneous electrochemical recording and direct microscopy imaging. We used this system to explore a wide concentration parameter space of cyt *c*, CL and ionic strength. We found that the effect of cyt *c* on the membrane is dose dependent: a critical concentration is required before permeabilisation occurs, the incidence of pores then increases up to a cyt *c* concentration where the density of pores leads to the complete breakdown of the membrane (lysis). However, to our great surprise, at higher still cyt *c* concentrations, the stability of the membrane between droplets returns but with massive ion flux through the membrane such that the recorded current was overloaded (Fig. 1d). The droplets could be mechanically separated and the contact area reformed, with the high membrane permeability quickly reestablished. Cationic PAMAM dendrimers with a similar size and charge to cyt *c* could permeabilize CL-containing membranes in a similar dose-dependent manner, except for the final highly permeable, non-lytic state described above. Therefore this unusual phenomenon appears to be specific to cyt *c*. Most significantly, the highly permeable, non-lytic state occurs under conditions which most closely match those expected to found in the mitochondria of apoptotic cells.

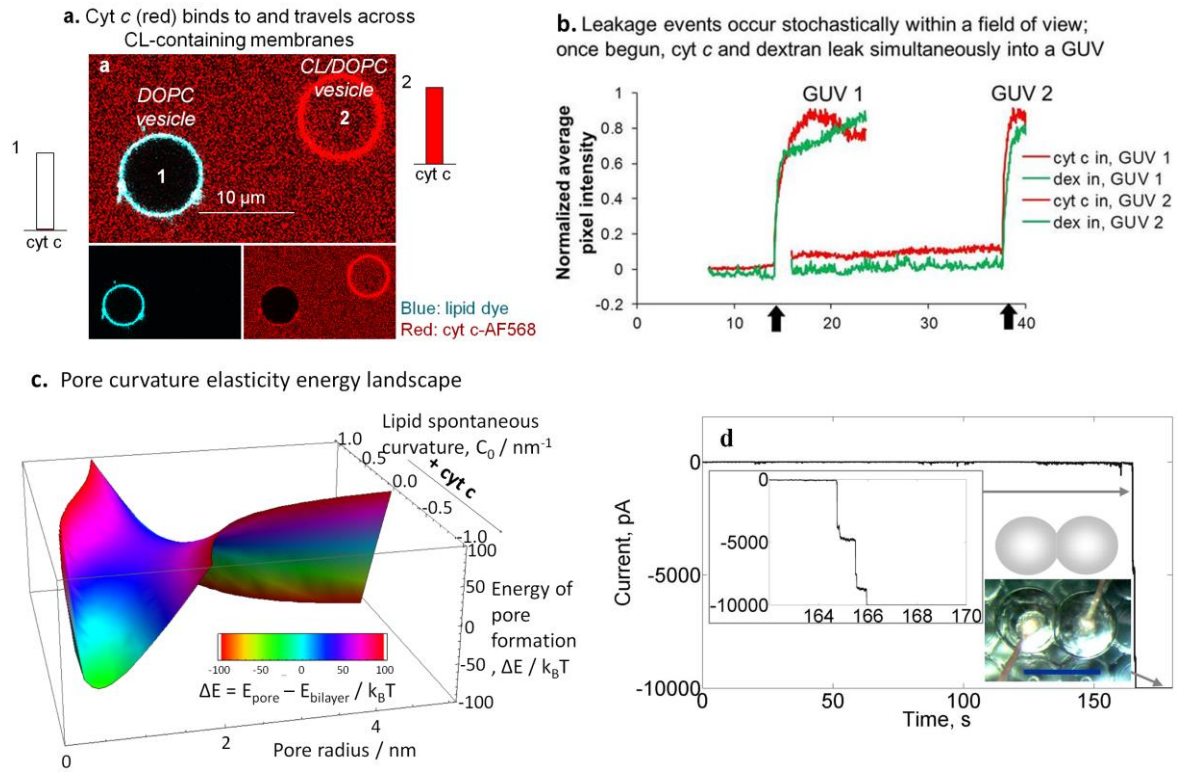

Figure 1: (a) Fluorescent cyt *c* (red) can translocate across CL-containing membranes, but not pure DOPC membranes. DOPC membranes are labelled with a lipid dye (blue), CL/DOPC membranes are unlabelled. Bar charts at sides represent the fraction of cyt *c* that has leaked into each numbered GUV (compared to background fluorescence). **(b)** Normalized fractional leakage of labelled cyt *c* and a 10 kDa dextran into two separate vesicles in the same field of view, showing the stochasticity of pore formation and the simultaneous transport of cyt *c* and dextran. **(c)** Model curvature elastic energy landscape for the energy difference between a pore and a planar bilayer for varying pore radius and membrane spontaneous curvature (C_0). A clear, finite sized energy minimum appears as C_0 reduces. **(d)** Electrochemical measurements using droplet interface bilayers reveal a highly permeable, non-lytic state with a stable bilayer between droplets, yet the current is overloaded (2.5 µM cyt *c*, 20% CL, 200 mM KCl).

It has previously been established that significant proportions of CL transfer to the outer mitochondrial membrane during apoptosis. Therefore our recent findings are strongly indicative that cyt *c* may play a role in MOMP such that it can instigate or amplify its own release into the cytosol during apoptosis.

Publications

Bergstrom, C., Beales, P., Lv, Y., Vanderlick, T. & Groves, J. (2013) Cytochrome *c* causes pore formation in cardiolipin-containing membranes. *Proc. Natl. Acad. Sci. USA* **110**: 6269-6274.

Xu, J., Vanderlick, T. & Beales, P. (2013) Lytic and non-lytic permeabilization of cardiolipin-containing lipid bilayers induced by cytochrome c. *PLoS One* **8:** e69492.

Funding

This work was supported by the NIH, Eli Lily, Princeton University and Yale University.

Collaborators

External: T. Vanderlick and J. Xu, Yale University. J. Groves and C. Bergstrom, Princeton University.

Improving on Nature: protein engineering and design

Sasha Derrington, Claire Windle, Laura Cross, Christopher Rowley, Marion Mueller, Rob Smith, Johannes Schoombie, Chi Trinh, Adam Nelson, Arwen Pearson and Alan Berry

Introduction

We are using protein engineering and directed evolution in a wide range of projects. These methods are used to engineer both enzymes and protein-protein interactions.

Aldolases with fluorosubstrates

Aldolases catalyse carbon-carbon bond formation between a nucleophilic donor and an electrophilic aldehyde acceptor. As the resulting aldol product can have up to two new stereocentres, aldolases have become attractive biocatalysts for the synthesis of key chiral building blocks. Aldolases are generally quite flexible in their acceptance of different aldehyde acceptor substrate butchanging the donor specificity is challenging because of the high specificity of aldolases for their donors. Despite this, we want to find aldolases which accept fluorinated donor substrates. The enzymatic aldol reaction with fluorinated substrates leads to organofluorine compounds which are widely used in industry, e.g. for the synthesis of pharmaceutical drugs. Organofluorine compounds are extremely rare in Nature and their chemical synthesis is difficult. Therefore, the use of aldolases could be a smart and environmentally friendly alternative.

Modifying the activity of *N*-acetylneuraminic acid lyase using non- natural amino acids

N-Acetylneuraminic acid lyase (NAL) catalyses the reversible aldol condensation of *N*-acetyl-D-mannosamine and pyruvate to form *N*-acetylneuraminic acid, through a mechanism that involves the formation of a Schiff base with a lysine residue at position 165. This enzyme has previously been the focus of many traditional directed evolution experiments. Now by using a chemical mutagenesis strategy it has been possible to incorporate non-natural amino acids into the active site of NAL. The chemical mutagenesis strategy works through a dehydroalanine intermediate which then undergoes a Michael addition with a thiol to produce the side chain of the non-natural amino acid. Position 165 was initially targeted and converted into a γ-thialysine. Now that the method has been established a variety of non-natural amino acids have been inserted at various positions throughout the active site, to create many different modified enzymes. These enzymes have then been screened for altered substrate specificity using a thiobarbituric acid assay.

mRNA display

mRNA display is a powerful technique for the exploration of large areas of sequence space in the search for functional peptides and proteins, and has recently proven an invaluable tool in the discovery of novel enzymes. mRNA display selection techniques are being explored as a method of engineering novel enzymes that catalyse the Diels-Alder reaction - a [4+2] cycloaddition that results in the generation of two new carbon-carbon bonds and up to four new stereogenic centres. Biologically catalysed Diels-Alder reactions are of great interest, as although it is an important reaction in synthetic organic chemistry, there are currently no known natural enzymes widely accepted to catalyse this powerful [4+2] cycloaddition.

Polyketide synthases and non-ribosomal peptide synthases.

Polyketide synthases (PKS) and non-ribosomal peptide synthases (NRPS) are large multi-modular proteins responsible for the formation of polyketides (PK) and non-ribosomal peptides (NRP), respectively. The compounds produced as secondary metabolites often have additional properties useful to us in everyday life. They are produced in an assembly-like fashion, adding small units together to form a larger compound. Our interests lie in the

structure-function relationships of these enzymes that allow the selection of building blocks to make vastly different compounds. In the future we wish to edit this selection in a predictable manner. Initial work has focussed on cloning and expression of proteins responsible for the formation of a starting unit of a PK/NRP.

We have successfully purified the apo and holo species of the non-catalytic protein which is responsible for housing the extending PK/NRP chain, the carrier protein. We have used NMR spectroscopy to elucidate the solution structure of the carrier protein. We have analysed approximately 800 models. Figure 1 shows the five lowest energy models. We have also begun to use NMR to investigate any structural changes that may occur the carrier protein is post-translationally modified.

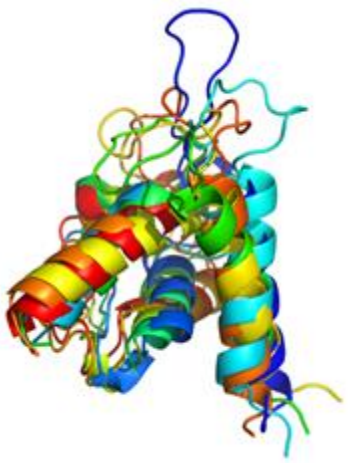

Figure 1: overlay of the five lowest energy models of the carrier protein in the apo form.

Creating novel binding motifs for orthogonal receptors

This project looks at the interaction between the peroxisomal receptor PEX5 and its signal sequence PTS1 (peroxisomal targeting signal 1) which allows targeting of proteins to the peroxisome. The aim is to develop an orthogonal PEX5-PTS1 binding interaction, which will be termed PEX5*-PTS1*. A selection of candidate PTS1* sequences have been synthesised and are being screened against a library of PEX5 mutants.

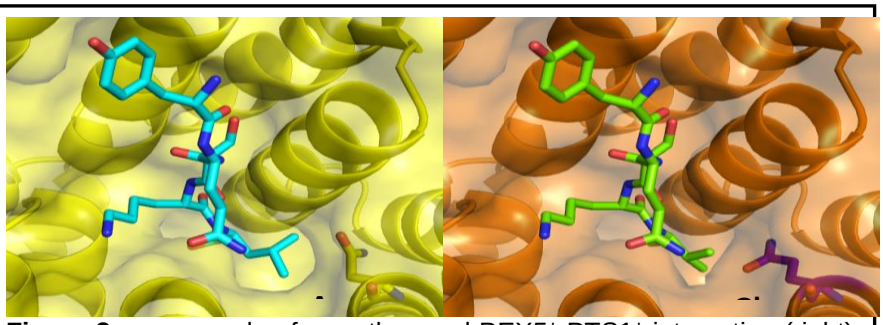

Figure 2: an example of an orthogonal PEX5*-PTS1* interaction (right) in comparison to the PEX5-PTS1 interaction (left). Here, Asn 601 has been mutated to Gln 601 which should reduce the size of the hydrophobic binding pocket and favour binding of valine over leucine on the binding peptide.

Publications

Timms, N., Windle, C., Polyakova, A., Ault, J., Trinh, C., Pearson, A., Nelson, A. & Berry, A. (2013) Structural insights into the recovery of aldolase activity in N-acetylneuraminic acid lyase by replacement of the catalytically active lysine with gamma-thialysine by using a chemical mutagenesis strategy. *ChemBioChem* **14**: 474-481.

Yi, D., He, N., Kickstein, M., Metzner, J., Weiss, M., Berry, A. & Fessner, W.-D. (2013) Engineering of a cytidine 5 '-monophosphate-sialic acid synthetase for improved tolerance to functional sialic acids. *Adv. Synth. Catal.* **355**: 3597-3612.

Funding

Our work is funded by BBSRC, the Wellcome Trust and The Leverhulme Trust, GlaxoSmithKline

Collaborators

Leeds: P. Stockley, A. Baker, A. Cuming, S. Warriner and J. Adams.

Solid phase synthesis of functionalised SAM-forming alkanethiol-oligoethyleneglycols

James Murray, Dominika Nowak, Laurynas Pukenas, Mathieu Guillorit, Christoph Wälti, Kevin Critchley, Steven Johnson and Robin Bon

Introduction

Self-assembled monolayers (SAMs) based on functionalised long chain alkanethiols-oligoethyleneglycols (LCAT-OEGs) provide an excellent platform for studies of well-defined surfaces (or functionalised nanoparticles) containing (bio)molecules through techniques such as surface Plasmon resonance, electrochemical spectroscopy, Plasmon-enhanced fluorescence and mass spectrometry. This makes them very interesting for the development of new biosensors and diagnostics. Easy access to LCAT-OEGs with different functionalities and OEG lengths is crucial to the optimisation of SAMs in sensing studies. However, their commercial availability is limited, and they tend to be difficult to handle/purify. To allow quick optimisation of SAM properties for biosensing applications, we decided to develop a flexible solid phase synthesis approach. In addition, because some of the few LCAT-OEGs that are commercially available give inconsistent results upon SAM formation, we carefully characterised mixed SAMs formed with our new LCAT-OEGs.

Results

LCAT-OEGs were made on 2-chlorotrityl resin by elaboration of immobilised building blocks **3** (Scheme 1). The solid phase approach allowed quick access, in good overall yields, to a range of LCAT-OEGs with different functionalities, such as alcohols, azides, amines, peptides, and the redox probe methylene blue (MB), and the isolated LCAT-OEGs were of high purity.

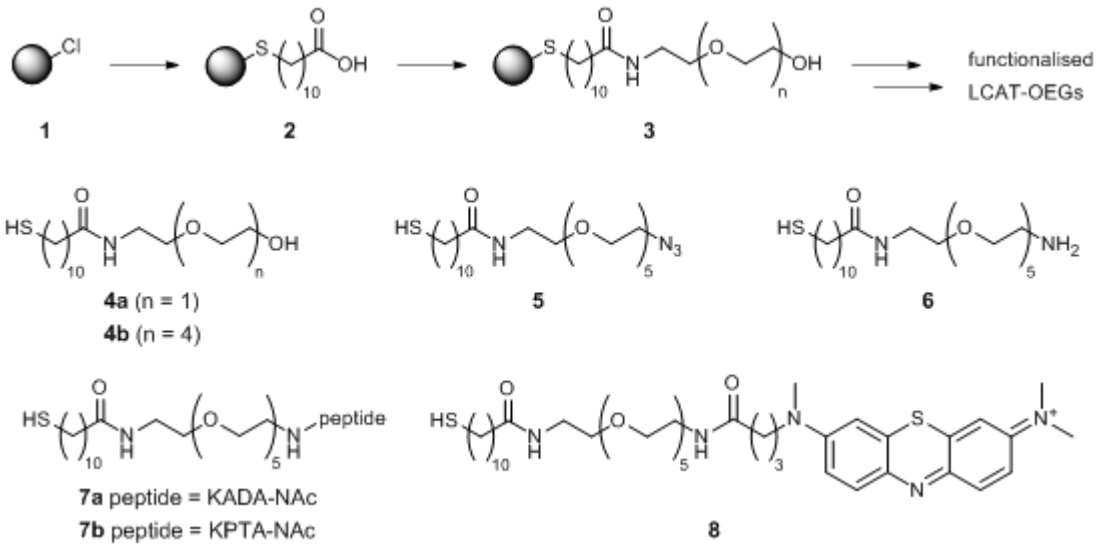

Scheme 1: LCAT-OEGs were synthesised on solid support by functionalisation of intermediate **3**. LCAT-OEGs functionalised with alcohols (**4**), azide (**5**), amine (**6**), peptides (**7**) or the redox probe methylene blue (**8**) were made.

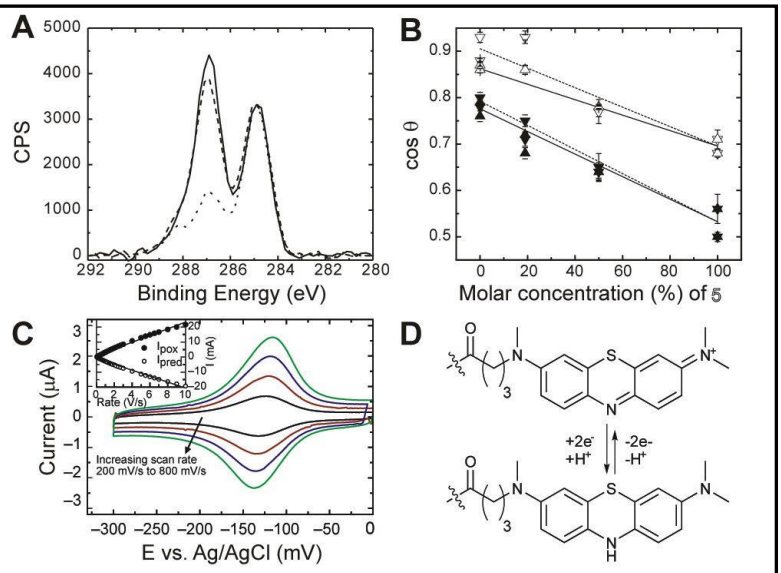

Figure 1: characterisation of LCAT-OEG SAMs. A) XPS data of C 1s region for reference SAMs of **4a** (dotted), **4b** (dashed) and 5 (solid) normalised to the alkyl chain peak at 284.9 eV. B) A linear change in cosine of the contact angle with molar ratio of azide **5** in mixed SAMs was observed. Triangles facing down represent **4a**:**5**; facing up – **4b**:**5** SAMs; advancing and receding angles are filled and open symbols, respectively. C) Typical cyclic voltammograms (left) for the 2-electron oxidation/reduction of SAM-bound methylene blue (right). The inset shows the linear relationships between current and scan rate.

Next, we analysed the quality of SAMs based on our functionalised LCAT-OEGs. X-ray photoelectron spectroscopy (XPS) showed S 2p peaks of SAMs of **4a**, **4b**, and **5** with binding energies consistent with the formation of thiolate bonds. The C 1s region consisted of three peaks for all SAMs, corresponding to the alkyl chain, the OEG chain and carbonyls (Figure 1A). Surface contact angle measurements showed that the ratios of functionalised LCAT-OEGs and diluents (**4**) on the surface were directly proportional to the ratios of these molecules in the applied solutions (Figure 1B).

Electrochemical impedance spectroscopy showed minimum phase angles, at 0.1 Hz, of –88° to –83° for SAMs of **4a:6** and –88° to –87° for SAMs of **4a**:**7a**, corresponding to well-packed, insulating monolayers that are almost free of pinholes and collapsed sites effects.

To demonstrate the potential suitability of MB-functionalised LCAT-OEGs for molecular electronics applications, we assessed the redox behaviour of surface-bound MB by cyclic voltammetry (CV). CV measurements on SAMs of **8** showed clear oxidation and reduction peaks associated with the MB moiety around –130 mV vs. Ag/AgCl. The peak anodic and cathodic current was found to increase linearly with scan rate, characteristic of a surface-tethered redox-active group. From the gradient of the straight line fit to peak current vs. scan rate we calculated a surface coverage, $\Gamma = 8.8 \times 10^{13}$ molecules/cm^2.

Finally, we demonstrated that SAMs of our LCAT-OEGs allow

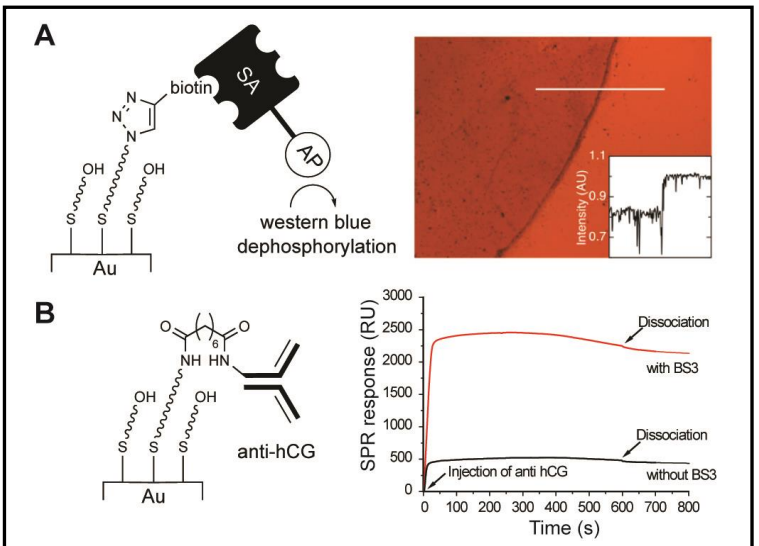

Figure 2: SAM functionalisation: A) Biotin immobilised through SAMs of **4a**:**5** (1:1; left) was detected as purple spots (right), upon incubation of the gold slide with streptavidin-alkaline phosphatase and western blue. B) Immobilisation of anti-hCG on a BS3-activated amine SAM (**4a**:**6**, 1:1; left) was detected by SPR (right).

(bio)molecule immobilisation by Copper-catalysed azide-alkyne cycloaddition (CuAAC) and bis(sulfosuccinimidyl) suberate (BS3)-mediated amide coupling. We 'clicked' propargyl biotin onto a SAM of **4a**:**5** (1:1) and tested for the presence of biotin covalently attached to the surface using a colorimetric assay with streptavidin-alkaline phosphatase and western blue as a stain (Figure 2A). We tested the suitability of SAMs containing amine **6** for immobilisation of the clinically relevant human chorionic gonadotropin antibody (anti-hCG). A SAM of **4a**:**6** (1:1) was formed and activated using the bis-succinimide crosslinker BS3 on a Biacore SPR chip. Injection of anti-hCG gave a much stronger signal in the channel pre-treated with BS3 than in the control channel (no BS3), indicating successful covalent immobilisation of anti-hCG (Figure 2B).

Funding
We thank the Biomedical and Health Research Centre, WELMEC and EPSRC for funding.

Collaborators
External: R. Azhar and S. Johnson (Department of Electronics, University of York).

Unravelling mechano-allostery using the atomic force microscope

Oliver Farrance, Sheena Radford and David Brockwell

Introduction

Protein-protein interactions are integral to diverse cellular processes such as catalysis, transport and signalling. For complexes of low affinity, changes in the relative concentrations of one (or more) binding partners, or alterations in the environment, are sufficient to trigger complex dissociation, allowing spatial and temporal control of the processes in question. More stable complexes require the input of chemical energy for their dissociation. For complexes that are remodelled on the outer membrane of Gram negative bacteria (where there is no direct access to an energy source) it remains unclear how dissociation can be induced on a biologically relevant timescale. It has been hypothesised that energetically unfavourable processes on the outer membrane may be driven by the proton motive force (pmf) across the inner membrane. Such inside-out energy transduction mechanisms require the two membranes to be linked by a series of protein-protein interactions and are exemplified by the Ton and Tol systems of *E. coli*.

While widely accepted, there is no direct evidence for the inside-out energy transduction model. To both test this model and understand the role that force plays in modulating protein:protein interactions at a fundamental level, we are investigating both Tol and Ton systems. Here we focus on the Tol system which is parasitized by colicin antibiotics.

Colicin E9 is nuclease protein antibiotic synthesised by *E.coli* strains to target and kill related bacteria during environmental stress. To prevent host suicide, E9 is expressed alongside a specific immunity protein (Im9) which inactivates E9 activity by binding to an

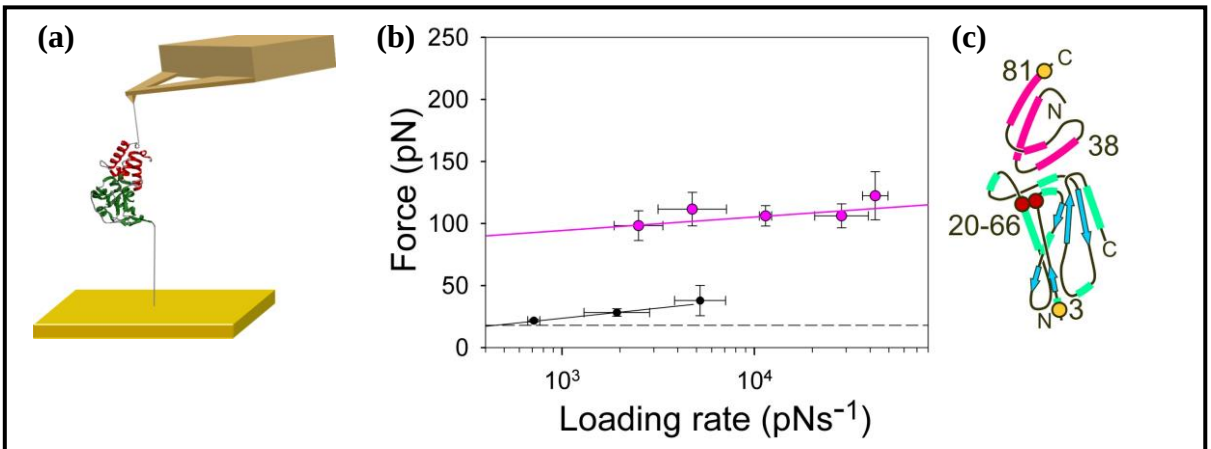

Figure 1: (a) measuring the strength of protein-protein interactions using an AFM. Im9 and E9 are immobilsed onto a derivatised AFM tip and silicon substrate at a defined site (via unique cysteine residues) using heterobifunctional polyethylene glycol linkers. After complex formation, the tip is moved away from the substrate and the force at which the complex breaks apart is quantified. **(b)** DFS of E9:Im9 (black) and $E9_{ds}$:Im9 (pink). The former complex is exceedingly force labile (dissociates at <20 pN) while the latter is mechanically strong. Accordingly, the extrapolated intrinsic off-rate of the former is a million-fold faster than the latter (5 and 5×10^{-6} s^{-1}, respectively). **(c)** a simplified topology diagram showing how formation of a disulfide bond on E9 (residues 20-66) insulates the binding interface from force induced remodelling when extended from residues 3 and 81 on E9 and Im9 respectively.

exo-site adjacent to the active site with high affinity ($K_d \sim 10^{-14}$ M). The affinity between E9:Im9 is highly avid with an off-rate of the order of days. This avidity poses a biological paradox in that tight binding is required to prevent host cell death, yet rapid release is required for cell invasion and intoxication.

Results

To investigate how force affects the dissociation rate of E9:Im9 we used an atomic force microscope (AFM) to form and then break apart the E9:Im9 complex. This is depicted schematically in Figure 1(a). Upon complex formation, retraction of the tip will load the complex with force until it breaks apart at a characteristic force. This force is dependent upon the intrinsic off-rate of the complex (measured by ensemble methods) and the speed at which the tip is retracted. By measuring the unbinding force many times at many different speeds it is possible to calculate the off-rate in the absence of force. This technique is called dynamic force spectroscopy (DFS).

Measuring the rupture forces between E9 and Im9 by DFS revealed that this very strong interaction is surprisingly labile to the application of force. Under application of only 20 pN force (at most) the rate of complex dissociation was found to be a million-fold faster than that measured by ensemble methods (Figure 1(b)). Consequently under low levels of force, Im9 is jettisoned on a timescale of seconds, commensurate with the timescale of colicin intoxication. By analyzing the effect of mutations and the effect of changing the pulling points on E9 and Im9 we identified partial unfolding of the N-terminal region as a position-specific force-triggered, allosteric activator of immunity protein release (Figure 1(c)). We term this novel, catastrophic force-triggered increase in off-rate as a 'trip bond'. Importantly, controls in which the trigger cannot be pulled, created by disulfide bond engineering yielded a mechanically strong complex ($E9_{ds}$:Im9) that dissociated at high force and gave k_{off} values that equate precisely with those measured using ensemble methods (Figure 1(b)).

For colicin function, a trip bond allows bipartite complex affinity whereby force induces a switch from a highly stable complex that is necessary to protect the host cell, to a rapidly dissociating, unstable complex able to trigger colicin intoxication. More generally, trip bonds allow an all-or-none mechano-transduction of a specific signal, adding to the emerging richness of the response of biomolecules and their complexes to force.

Publications

Farrance, O., Hann, E., Kaminska, R., Housden, N., Derrington, S., Kleanthous, C., Radford, S. & Brockwell, D. (2013) A force-activated trip switch triggers rapid dissociation of a colicin from its immunity protein. *PLoS Biol.* **11**: e1001489.

Funding

We thank Nasir Khan for technical support and the BBSRC for funding.

Collaborators

Leeds: Lorna Dougan
External: C. Kleanthous (University of Oxford).

The involvement of β-amyloid precursor protein in neuronal iron homeostasis in dementia

Andrew Tsatsanis and James Duce

Introduction

Iron is an essential element required as a cofactor in metabolic processes throughout the body and specifically in tissues of high oxygen consumption, such as the central nervous system. High levels of unbound iron are detrimental as this may catalyze the production of toxic reactive oxygen species. It is clear that increased cellular susceptibility to oxidative stress associated with iron accumulation leads to neurodegeneration. Age-related increases in neuronal iron, altered iron-related protein expression and increased susceptibility to oxidative stress have all been documented in neuropathological regions from patients with Alzheimer's disease (AD), Parkinson's disease and tauopathies.

One regulatory route in regulating cellular iron homeostasis is through proteins required to facilitate the efflux of iron from the cell. β-Amyloid precursor protein (APP), Ceruloplasmin and Hephaestin are all able to facilitate the movement of iron across the plasma membrane, partly through their ability to complex with the iron exporter ferroportin and promoting its retention on the cell surface.

APP is a type 1 transmembrane protein more commonly known as the precursor to the toxic ß-amyloid peptide that accumulates in the AD brain. However, regulation of APP expression by iron regulatory protein implies an interaction with iron status. Our group strengthened this iron relationship through the discovery of the requirement for APP in promoting the efflux of iron via ferroportin in cells such as neurons. Prior to our discovery no mechanism was known for neuronal iron export as within the brain a membrane-associated form of Ceruloplasmin is only expressed on astrocytes and Hephaestin is only expressed in oligodendrocytes.

Results

Biological evidence of a role for APP in iron efflux via ferroportin continues to be strengthened both by our own work and research from independent groups. While concerns have recently arisen as to some of the original findings on the ability of APP to oxidize Fe^{2+} to Fe^{3+}, we have revisited our original data to establish in more detail the causes of such variability in APP ferroxidase activity. During the course of these studies we have now established that the ability of APP to oxidize iron originate from phosphate. We suggest that the presence of this physiologically abundant anion raises the possibility that APP facilitates the efflux of intraneuronal iron through an alternative mechanism; potentially either using the high anion, or soluble Ceruloplasmin, content within the surrounding extraneuronal environment.

Despite the modification to the original hypothesis proposed on how APP was able to efflux neuronal

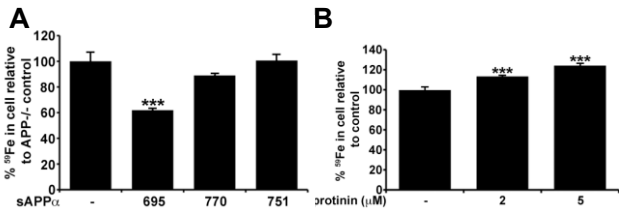

Figure 1: the KPI domain is responsible for larger APP isoforms differentially affect neuronal iron response. **(a)** APP-/- primary neuronal cultures preincubated with Fe^{59} before the administration of each isoform of sAPP illustrate that only $sAPP_{695}$ was able to reduce the intracellular accumulation of iron after 6hrs. **(b)** Retention of Fe^{59} within the cell is dose dependently increased upon the addition of the KPI homologous peptide Aprotinin. Data are means ± SEM, N=3, *=p<0.05, **=p<0.01, ***=p<0.001 compared to control by 2-tailed Ttest.

iron, a significant understanding for the necessity of APP in neuronal iron homeostasis is now provided. This is in part through a substantially greater understanding of the effect each of the 3 major APP isoforms (i.e. APP_{695}, APP_{751} and APP_{770}) has on neuronal iron regulation. Supporting our previous primary publication on the iron homeostatic role of APP and independent validation by other researchers, the increased presence of APP_{695} appears to lower the intracellular labile iron pool (Fig. 1A). However, intriguingly, a similar pattern does not appear to be evident in the presence of the APP_{751} and APP_{770} isoforms (Fig. 1A). The inhibitory role in cellular iron efflux of both APP_{751} and APP_{770} suggests the Kunitz Protease Inhibitor (KPI) domain present in both to be responsible and similar results with the KPI homologous peptide Aprotinin support this theory (Fig. 1B). Altering the proteolytic processing of neuronal APP_{695} has also been recently identified to modify neuronal iron. By either utilizing mutations within the β-secretase cleavage site of APP, or suppression of α- and β-secretase activity by chemical inhibition (Fig. 2), promotion of the amyloidogenic pathway has been identified to increase intracellular iron whereas the non-amyloidogenic processing of APP negates this response. These findings have implications for all AD associated pathogenic mutations of APP and their potential to compound upon neuronal vulnerability to increased iron levels and oxidative stress within the disease.

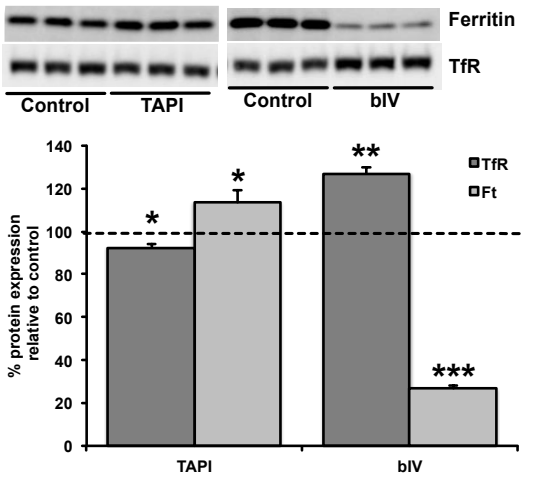

Figure 2: inhibition of α-secretase or β-secretase activity alters neuronal iron homeostasis. SH-SY5Y neuroblastomas incubated with the α-secretase inhibitor TAPI, previously reported (and confirmed by ourselves) to reduce α-cleavage of APP, have decreased TfR and increased ferritin expression representing an increased intracellular labile iron pool. Inversely, β-secretase inhibition by bIV dramatically increases TfR and reduces ferritin expression in SH-SY5Ys signifying an increased labile iron pool. Data are means ± SEM, N=3, *=p<0.05, **=p<0.01, ***=p<0.001 compared to control by 2-tailed Ttest.

Outlook.

By continuing to support a novel candidate function for APP we now begin to explain the diverse trophic and morphoregulatory activities of the protein and elucidate the vulnerability of the body to age-associated iron accumulation. Restoring or replacing the ability of APP to control neuronal iron homeostasis may be a novel mechanism of action for new therapeutics targeting a range of neurodegenerative diseases. Since investigating the therapeutic value of metal chelating compounds in a range of transgenic models of AD and PD pathology it has become gradually clearer that the therapeutic capability of these compounds may not only be through their ability to isolate small amounts of labile iron but also partially through their ability to use the brain's own iron regulatory system to rebalance iron tissue levels.

Publications

Chen, J., Marks, E., Lai, B., Zhang, Z., Duce, J., Lam, L., Volitakis, I., Bush, A., Hersch, S., & Fox, J. (2013) Iron accumulates in Huntington's disease neurons: protection by Deferoxamine. *PLoS One.* **8:** e77023.

Duce, J., Ayton, S., Miller, A., Tsatsanis, A., Lam, L., Leone, L., Corbin, J., Butzkueven, H., Kilpatrick, T., Rogers, J., Barnham, K., Finkelstein, D. & Bush, A. (2013) Amine oxidase

activity of β-amyloid precursor protein modulates systemic and local catecholamine levels. *Mol. Psych*. **18:**245-54.

Funding
This work was supported in the UK by a Senior Research Fellowship from Alzhiemer's Research UK, a Marie Curie Integration Grant from the European Commission and a Translational Project grant from Parkinson's UK. International support is also provided by the NHMRC, Australia.

Collaborators
External: A. Bush (University of Melbourne, Australia), R. Cherny and D. Finkelstein (The Florey Institute, Australia), R. Evans (Brunel University, London), D. Tetard and F. Lewis (Northumbria University, Newcastle upon Tyne) and D. Smith (Sheffield Hallam University).

Nucleocapsid protein structures from orthobunyaviruses reveal insight into ribonucleoprotein architecture and RNA polymerization

Antonio Ariza, Sian Tanner, Cheryl Walter, Dale Shepherd, Alison Ashcroft, Nicola Stonehouse, Neil Ranson, John Barr and Tom Edwards

Introduction

All orthobunyaviruses possess three genome segments of single-stranded negative sense RNA that are encapsidated with the virus-encoded nucleocapsid (N) protein to form a ribonucleoprotein (RNP) complex, which is uncharacterized at high resolution, and this association is critical for gene expression by the viral polymerase. RNP formation is also required for segment packaging during assembly of new virus particles, mediated through direct interaction between N and the viral glycoproteins. Many fundamental aspects of RNP function are poorly understood, including the mechanism of RNA binding, its assembly pathway and quaternary structure and the mechanism by which the RdRp copies the N protein-protected RNA genome.

Results

We report the crystal structure of both the Bunyamwera virus N–RNA complex and the unbound Schmallenberg virus N protein, at resolutions of 3.20 and 2.75 Å, respectively.

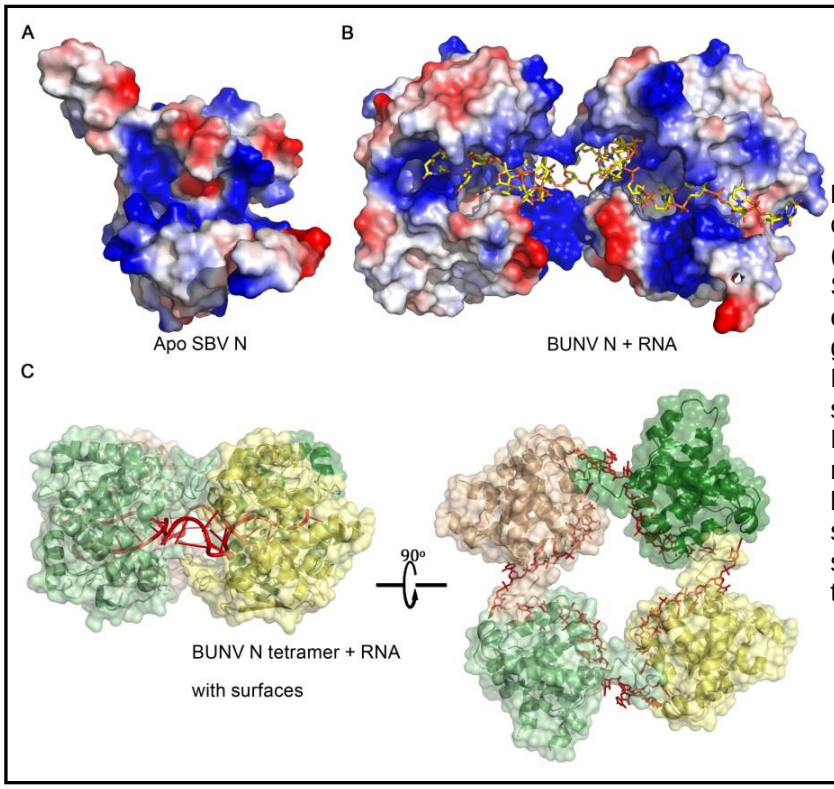

Figure 1: RNA binding by orthobunyavirus N proteins. (**A**) Electrostatic surface of a SBV N protomer reveals the electropositive RNA-binding groove. (**B**) Two molecules of BUNV N bound to RNA (as seen from inside the tetramer; RNA is yellow sticks representation). (**C**) BUNV N bound to RNA (red) with solvent accessible surface shown (yellow/greens, transparent).

N proteins crystallized as ring-like tetramers and exhibit a high degree of structural similarity despite classification into different orthobunyavirus serogroups. The structures represent a new RNA binding protein fold. BUNV N possesses a positively charged groove into which RNA is deeply sequestered, with the bases facing away from the solvent. This location is highly inaccessible, implying that RNA polymerization and other critical base pairing events in the virus life cycle requireRNPdisassembly. Mutational analysis of N protein supports a correlation between structure and function. Comparison between these crystal structures and electron microscopy images of both soluble tetramers and authentic RNPs suggests the N protein does not bind RNA as a repeating monomer; thus, it represents a newly described

architecture for bunyavirus RNP assembly, with implications for many other segmented negative-strand RNA viruses.

N protein structures offer important insight into the mechanism of orthobunyavirus RNA recognition, N–N multimerization and assembly of the RNP complex across the entire genus, with potential implications for all segmented negativestranded RNA viruses. They will provide a critical resource for further analysis of many diverse aspects of the orthobunyavirus life cycle, as well as providing a possible target for structure-based drug design to interfere with critical RNP functions.

Publications

Ariza, A., Tanner, S., Walter, C., Dent, K., Shepherd, D., Wu, W., Matthews, S., Hiscox, J., Green, T. , Luo, M., Elliott, R., Fooks, A., Ashcroft, A., Stonehouse, N., Ranson, N., Barr, J. & Edwards, T. (2013) Nucleocapsid protein structures from orthobunyaviruses reveal insight into ribonucleoprotein architecture and RNA polymerization. *Nucleic Acids Res.* **41**: 5912-5926.

Funding

This work was supported by the Wellcome Trust and BBSRC.

Collaborators

External: J. Hiscox (University of Liverpool), R. Elliott (University of Glasgow), T. Fooks (Animal Health and Veterinary Laboratories Agency), T. Green and M. Luo (University of Birmingham, Alabama).

Optimising inhibitors for *Toxoplasma gondii* enoyl reductase

Martin McPhillie, Stephen Muench and Colin Fishwick

Introduction

Toxoplasmosis is an infectious disease caused by the parasite *Toxoplasma gondii*. Current treatments are antimalarial drugs which are teratogenic and have many unwanted side-effects, and therefore there is an urgent need for specific medicines to treat toxoplasmosis. The fatty acid type II biosynthesis pathway in *T. gondii* is distinct from the type I pathway in humans, where each stage of the synthesis is carried out by a discrete enzyme. The significant differences between the type I and type II pathways have made this biosynthesis pathway a very attractive target for drug development. In particular, enoyl acyl-carrier protein reductase (ENR), which carries out the final stage of FAS II, has gained the most attention with a range of potent drugs developed against it (Figure 1). Our current work includes the design and synthesis of i) analogues of triclosan; ii) scaffolds derived from a Syngenta high-throughput screen (HTS) campaign against a plant homologue of ENR. Both projects utilised in-house crystal structures of *T. gondii* ENR (*Tg*ENR).

Results

Triclosan is an antibacterial agent widely used in household goods such as toothpastes, soaps and plastics due to its activity against a broad spectrum of bacteria. It is unsuitable for oral administration due to its poor pharmacokinetics properties, especially low water solubility. We have shown that triclosan is a very potent inhibitor of *Tg*ENR which binds at the NADH/substrate site, making π-stacking interactions with the reduced NAD+ cofactor and hydrogen bonding to the catalytic tyrosine residue. Chemical modification of both the A- and B-rings of triclosan, designed to improve its PK properties, has led to >40 new analogues. A-ring derivatives have revealed new insights into ligand binding since Phe243 can move to accommodate the increased bulk of the new derivatives, since the A-ring is buried deep

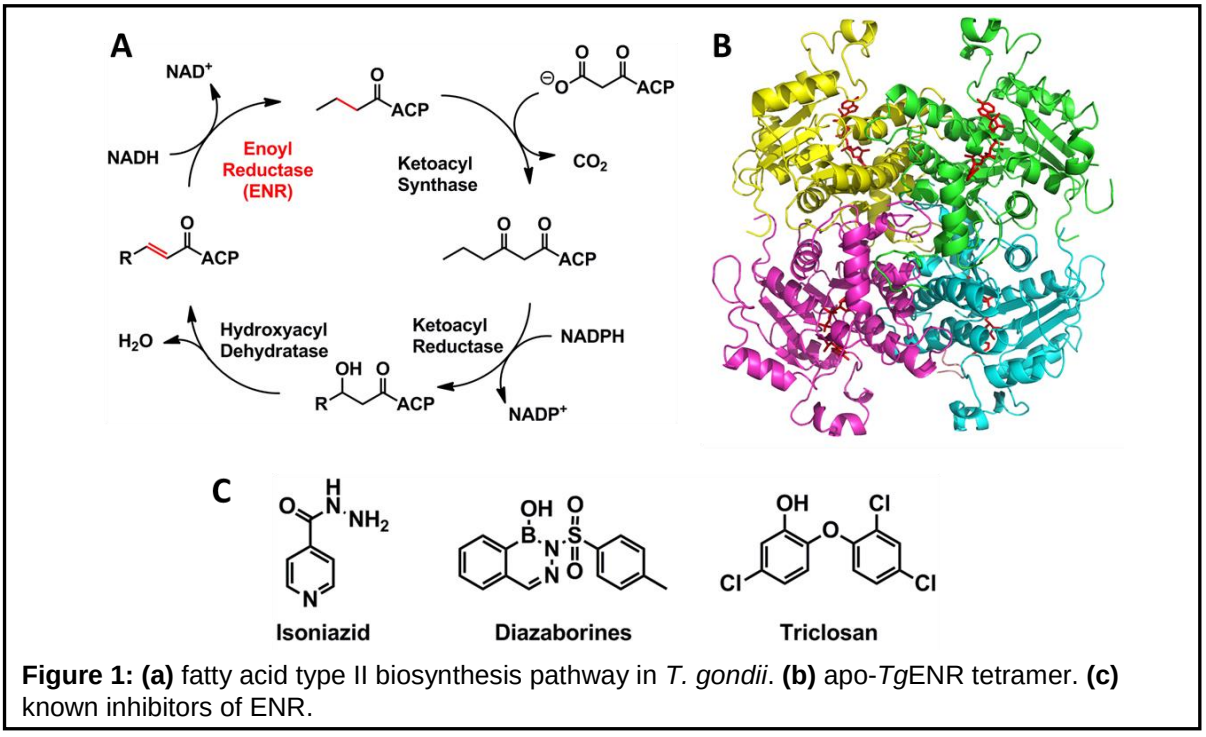

Figure 1: (a) fatty acid type II biosynthesis pathway in *T. gondii*. **(b)** apo-*Tg*ENR tetramer. **(c)** known inhibitors of ENR.

within a hydrophobic pocket. This movement opens up the base of the binding pocket to the solvent. B-ring modifications have led to derivatives with MIC_{50} values of 250 nM against *T.*

gondii tachyzoites without apparent toxicity to the host cells. Derivatives with A+B ring modifications have rings exposed to solvent which opens up the possibility of drug delivery via cationic peptides (Figure 2).

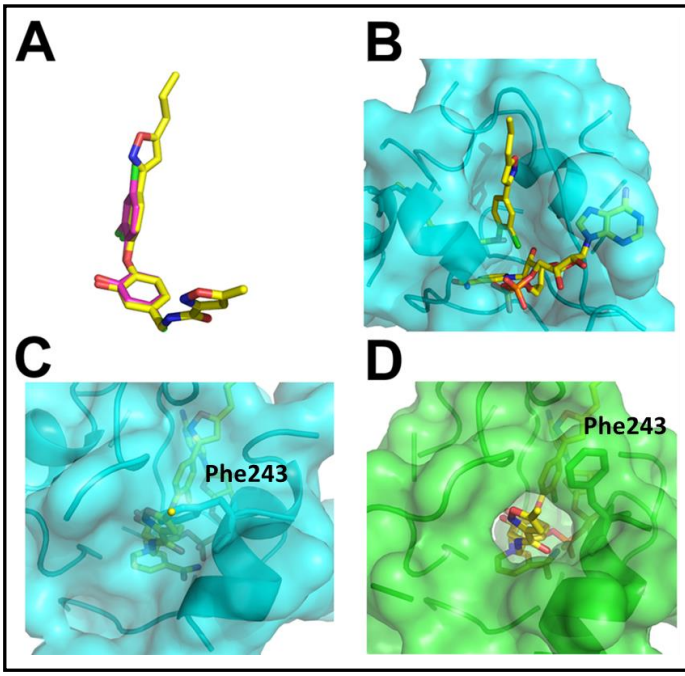

Figure 2: (a) overlap of A+B derivative (yellow) with triclosan (pink). **(b)** A+B derivative (yellow) protruding into the solvent. **(c)** and **(d)** Modelling the movement of Phe243 in the 'closed' position (c) and 'open' position (d).

Publications

Afanador, G., Muench, S., Mcphillie, M., Fomovska, A., Schoen, A., Zhou, Y., Cheng, G., Stec, J., Freundlich, J., Shieh, H.-M., Anderson, J., Jacobus, D. , Fidock, D., Kozikowski, A. P., Fishwick, C. W., Rice, D., Freire, E., Mcleod, R. & Prigge, S. (2013) Discrimination of potent inhibitors of *Toxoplasma gondii* enoyl-acyl carrier protein reductase by a thermal shift assay. *Biochemistry* **52**: 9155-9166.

Muench, S., Stec, J., Zhou, Y., Afanador, G., Mcphillie, M., Hickman, M., Lee, P., Leed, S., Auschwitz, J., Prigge, S., Rice, D. & Mcleod, R. (2013) Development of a triclosan scaffold which allows for adaptations on both the a- and b-ring for transport peptides. *Bioorg. Med. Chem. Lett.* **23**: 3551-3555.

Funding

This work was supported by NIH grant 1R01 AI 111552-01.

Collaborators

External: R. MCleod (University of Chicago) and D. Rice (University of Sheffield).

Identification and optimisation of small molecule as chemical probes or as therapeutics

Ian Yule, Jeff Plante, Rachael Tennant, Jayakanth Kankanala, Rachel Trowbridge, Charlotte Revill, Joseph Thompson, Adam Nelson, Colin Fishwick and Richard Foster

Introduction

Our group is interested in the design, synthesis and optimisation of small molecules for therapeutic application or their use in the elucidation of biological function. By combining tools and techniques in medicinal chemistry, computer-aided drug design and chemical genetics (Figure 1) we aim to identify and optimise targeted small molecules as key modulators of specific biological function to support both basic target validation of proteins implicated in disease and as potential starting points for future drug discovery.

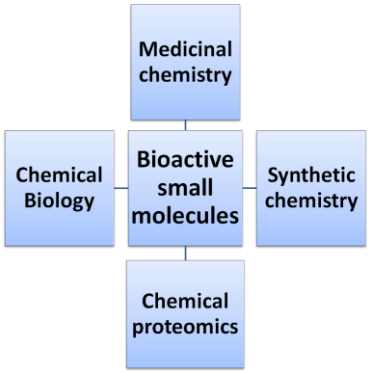

Figure 1: overview of the group's activities

The group has capabilities in a number of areas for which bioactive molecules may be identified, optimised and/or targeted, including:

Medicinal chemistry, probe synthesis and chemical genetics:

- Bio-targeted small molecules
- Targeted imaging agents
- Small molecule microarrays

Computational-aided drug design:

- Ligand- and structure-based design
- Virtual screening

High-throughput screening:

- 30k member diverse lead-like small molecule library
- Fragment library
- Assay transfer/assay development expertise

The activities are managed through the Medicinal Chemistry and Chemical Biology (MCCB) Technology Group as part of the Biomedical Health Research Centre (BHRC) at Leeds. Several new projects have been initiated during 2013.

***Small molecule therapeutics*:**

Development of a novel anticoagulant with minimal bleeding risk

We have identified potent, novel small molecule inhibitors of a key enzyme involved in regulation of the coagulation cascade with exceptional *in vivo* efficacy. The inhibitors have

been identified by a number of parallel approaches incorporating virtual drug design, chemical synthesis and HTS of drug-like small molecule libraries and fragments. Presently, we are optimising the inhibitors for target potency, specificity and drug-like physicochemical properties using iterative rounds of medicinal chemistry development and screening using a panel of orthogonal bioassays.

Identification of novel inhibitors of TRP ion channel function as potential therapeutics
We have identified a series of novel inhibitors of a TRP ion channel implicated in cardioprotection. The compounds have been developed as agents to support detailed understanding of the role of the protein target and its relevance in disease as well for future development of small molecule-based therapeutics. These dual aims are being achieved through iterations of directed chemical synthesis aided by pharmacophore-based design and screening *via* a panel of orthogonal assays.

Funding
Our work was funded by the MRC, EPSRC, Parkinson's UK, BBSRC, AICR, CRUK, BHF and BHRC.

Collaborators
Leeds: R. Ariens, D. Beech, C. Fishwick, H. L.- Jiang, H. Philippou and R.Sivaprasadarao

The mechanism of a unique protozoan parasite primary ion pump

Robert Kolodziejczyk and Adrian Goldman

Introduction

Primary ion pumps interconvert an ion motive force into the free energy in a phosphoanhydride bond. The primordial ion pumps are probably the integral membrane pyrophosphatases (mPPases) because their substrate pyrophosphate (PP_i) is chemically simple. mPPases occur in occur in (archae)bacteria, plants and protozoan parasites and are important under low-energy stress conditions, such as when protozoan parasites enter the bloodstream or during drought in plants. The protozoan parasites include *P. falciparum* (malaria), *L. major* (visceral leishmaniasis) and *T. cruzi*.

In 2012, we solved the first example of a Na^+-activated mPPase, from the hyperthermophile *T. maritima* at 2.6 Å resolution. It revealed a completely new protein fold (Figure 1) and provides a convincing explanation for the *known* mechanistic properties of the enzyme. This structure, in conjunction with the structure of the related mung bean H^+-pumping mPPase also published in 2012, reveals that the hydrolytic centre is located about 20 Å from the membrane surface and that a coupling funnel extends from the active site to the (closed) ionic gate, which in *T. maritima* PPase is formed by an D243-K707-E246 ion triple.

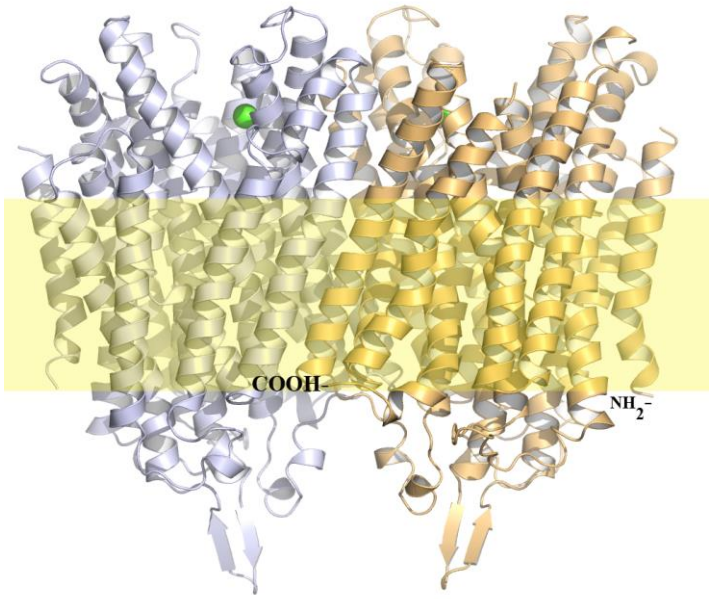

Figure 1: structure of *T. maritima* PPase at 2.6 Å resolution, showing that it is an obligate dimer. The position of one of the active sites is shown by the green sphere, which marks a Mg^{2+}-ion bound in the active site (the second active site is obscured in this view. The active site, about 10 Å above the plane of the membrane is about 20 Å from the ionic gate, which is about halfway into the lipid bilayer.

Results

The work described here focusses on the structure and mechanism of *Thermotoga maritima* pyrophosphatase, and trying to understand the structural basis for the the pumping event. There are three different families of inorganic pyrophosphatases, two soluble ones (type I and type II) and the mPPases. They have remarkably different rate constants, active site structures, and inhibition profiles (Figure 2). Type I and type II PPases are diffusion-controlled enzymes with k_{cat} in the $200s^{-1}$ (type I) to $3000s^{-1}$ (type II) (Table). These values are consistent with strong activation of the water nucleophile, as can be seen (Figure 2) from the fact that the water nucleophile is coordinated by two (type I) or three (type II) metal ions. Furthermore, both enzymes are inhibited by fluoride ion at μM concentrations. In comparison, mPPases are slow enzymes (k_{cat} 10-fold slower than type I) and poorly inhibited by fluoride, which inhibits at millimolar concentrations. This is consistent with the fact that

the active site contains two aspartates (D731 and D287, Figure 2) that coordinate the water molecule.

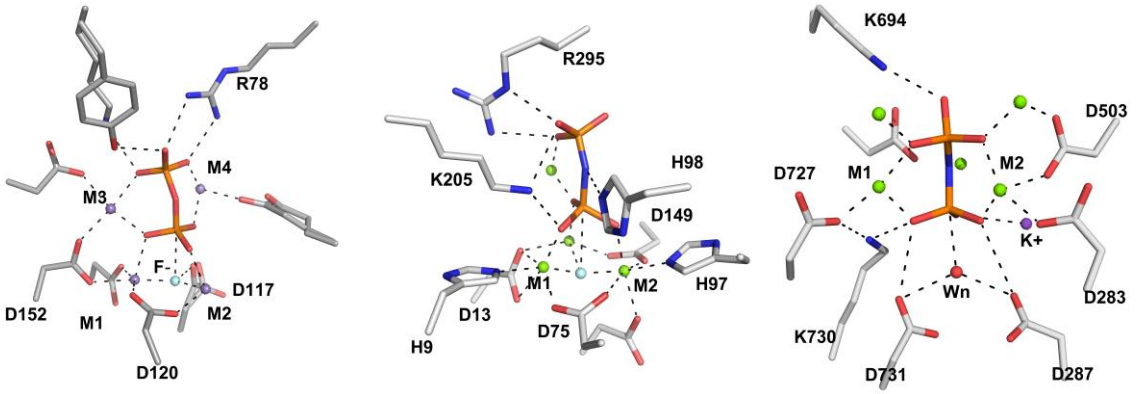

	Mg^{2+}	Mn^{2+}	K_i for AMDP (μM)	K_i for F^- (μM)*	k_{cat} (s^{-1})
Type I	Req.		11 – 150	≤11 – 90	200-400
Type II	Req.	Activates	1000	6*	1700-3000
mPPase	Req.		1.2 – 1.8	3000 – 4800	3.5-20

Figure 2: Type I (left), Type II (middle) and mPPase (right) active sites, emphasizing the difference in active site geometry. The scissile bond is vertical, with the nucleophile directly underneath. Key side chains are shown in atom colours, as are Mg^{2+} (green), F^- (cyan), the Mn^{2+} (type II) light purple, and the K^+ (mPPase) purple. **Table** showing metal ion requirement, K_i for different inhibitors and k_{cat}. Key is that mPPases bind F^- poorly and are slow enzymes.

We therefore suggested that mPPases operate through a mechanism where a positive charge is pumped *before* hydrolysis (*i.e.* 'binding change') and that this change, which inreases the negative charage at D731 and D287 leads to hydrolysis. Such insights into mechanism and how inhibitors bind are essential for drug discovery efforts aimed at the protozon mPPases. Other studies of pathogenesis related proteins have led to papers in PLoS Pathogens on the mechanisms of complement resistance.

Publications

Meri, T., Amdahl, H., Lehtinen, M., Hyvärinen, S., McDowell, J., Bhattacharjee, A., Meri, S., Marconi, R., Goldman, A. & Jokiranta, T. (2013) Microbes bind complement inhibitor factor H via a common site. *PLoS Pathog.* **9**:e1003308.

Bhattacharjee, A., Oeemig, J. S., Kolodziejczyk, R., Meri, T., Kajander, T., Lehtinen, M. J., Iwai, H., Jokiranta, T. & Goldman, A. (2013). Structural basis for complement evasion by Lyme disease pathogen *Borrelia burgdorferi*. *J. Biol. Chem.* **288**:18685-18695.

Kajander, T., Kellosalo, J. & Goldman, A. (2013). Inorganic pyrophosphatases: one substrate, three mechanisms. *FEBS Lett.* **587**:1863-1869.

Funding

This work was supported by the Royal Socieity (Wolfson merit award), by the Academy of Finland, by the European Union and by the Finnish Ministry of Education.

Collaborators

External: R. Lahti (University of Turku), A. Baykov (Moscow State University), R. Docampo (University of Georgia), P. Nissen (University of Aarhus), S. Meri and T. Jokiranta (University of Helsinki).

Structure-guided drug design targeting the release of hepatitis C virus particles

Toshana Foster, Gary Thompson, Arnout Kalverda, Jayakanth Kankanala, Elizabeth Atkins, Joseph Thompson, Amy Barker, Dean Clarke, Marko Noerenberg, Arwen Pearson, David Rowlands, Steven Homans, Mark Harris, Richard Foster and Stephen Griffin

Introduction

Hepatitis C virus (HCV) infects over 170 million individuals, causing severe liver disease, and is the leading cause of liver cancer in the developed world. Current interferon-based therapy for HCV is inadequate and a new era of combination therapy with direct-acting antivirals (DAA) is fast approaching. However, significant concerns regarding availability, cost and viral resistance to DAAs exist, necessitating an ongoing programme of drug development. In particular, current DAA target only three HCV proteins, making the addition of alternative targets a priority.

We discovered that the HCV p7 protein functions as a virus-coded ion channel, or "viroporin". p7 is an essential HCV protein and blocking its channel activity with prototype small molecule inhibitors prevents infectious particles production. However, prototypes lack potency and are in need of significant improvement for drug development.

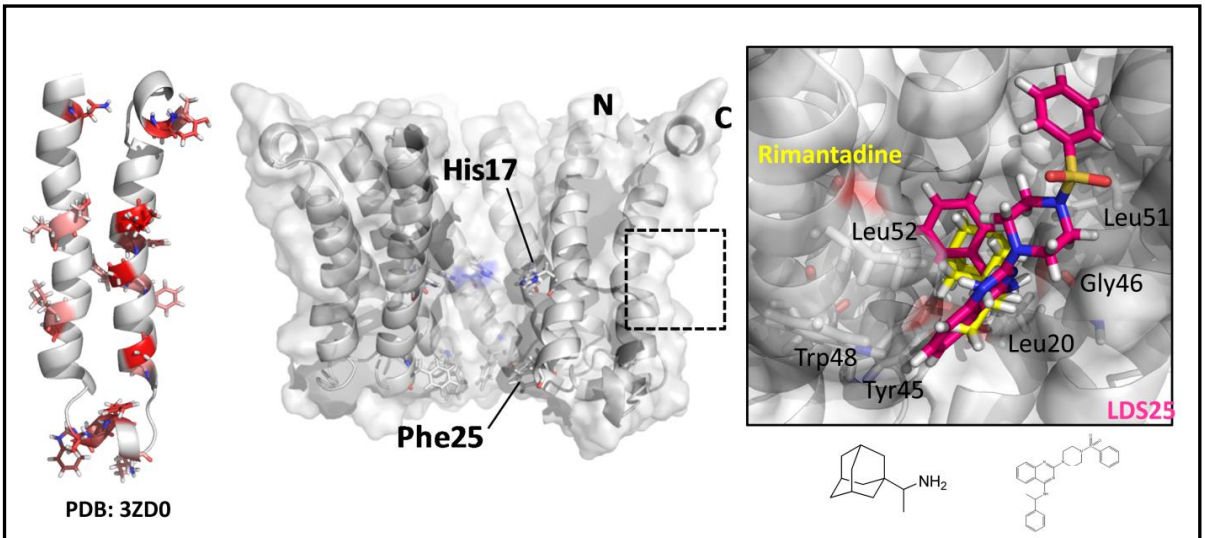

Figure 1: Left: solution structure of HCV p7 monomer (PDB 3ZD0); **Middle**: Structure-guided model of heptameric p7 channel complex, cutaway showing His17 proton sensor and Phe25 gate residue; **Right**: Expanded view of peripheral binding site showing prototype inhibitor, rimantadine (bottom left structure) and a novel molecule LDS25 (bottom right structure).

Results

We have solved the solution structure of monomeric p7 and validated a drug binding site located on the membrane-exposed surface of the channel complex that was predicted by previous drug resistance and molecular modelling studies. This drug binding site, defined by an L20F resistance polymorphism, is the only rationally defined target for p7 in the literature to date.

In silico screening selected a series of candidate inhibitors targeting the peripheral "L20F site" with dramatically improved characteristics compared with prototypes; IC_{50} values were reduced from tens of micromolar to ~100 nM in culture. Expansion of lead chemical series identified several potent molecules with activity against multiple HCV

genotypes. In each case, the L20F mutation modulated compound binding, thus confirming drug targeting to the peripheral site. However, novel inhibitors overcame L20F resistance at sub-micromolar concentrations, illustrating a potentially high genetic barrier to resistance *in vivo*. Combined with excellent drug-like properties and specificity, class leads represent a genuine opportunity for antiviral development.

In addition, we have continued to characterise the role of p7 during the virus life cycle. We have determined that p7 channel activity likely acts at a post-assembly stage of virion production, both mediating secretion and conferring an infectious phenotype to HCV particles. Furthermore, p7 also plays a critical role in "maturing" HCV particles as they become acid-resistant upon release from the cell. Both of these functions point to the potential presence of p7 channel complexes within virions, providing a second target for p7 inhibitors via blockade of virus entry.

Publications

Bentham, M., Foster, T., McCormick, C., Griffin, S. (2013) Mutations in hepatitis C virus p7 reduce both the egress and infectivity of assembled particles via impaired proton channel function. *J. Gen. Virol*. **94:** 2236-2248.

Funding

We are grateful to the Wellcome Trust, Yorkshire Cancer Research, The Royal Society, The MRC, The LTHT Charitable Trustees, The Leeds CRUK Clinical Centre, and the University of Leeds Biomedical Health Research Centre (BHRC).

Studies on hepatitis C virus replication and pathogenesis

Hazel Stewart, Zsofia Igloi, Cheryl Walter, Doug Ross, Joe Shaw, Chris Bartlett, Joe Lattimer, Lorna Kelly, Carsten Zothner and Mark Harris

Overview

Hepatitis C virus (HCV) infects 170 million individuals and is a major cause of chronic liver disease, including fibrosis, cirrhosis and hepatocellular carcinoma. The virus has a single stranded positive sense RNA genome of 9.5kb that contains a long open reading frame encoding a single polyprotein of 3000 amino acids which is cleaved into 10 individual polypeptides by a combination of host cell and virus specific proteases. We are interested in understanding the molecular mechanisms of viral genome replication and assembly, with a particular focus on the virus-host interactions that underpin these processes. The ultimate goal of this research is to identify new targets for the development of novel antivirals.

A major focus of work is NS5A, a pleiotropic phosphoprotein with multiple roles in the virus lifecycle. We are investigating the role of NS5A in virus replication and assembly (4), as well as its interactions with cellular factors (3). For example, recently we have used a mass spectrometric approach to identify sites of phosphorylation within the protein and generated mutants of these phosphorylation sites to characterise the role of this post-translational modification in NS5A function (1).

Other studies are investigating the interactions of NS5A with RNA, both *in vitro* and *in vivo,* using the techniques of SELEX and CLIP. Similar studies are ongoing with the Core (capsid) protein with a view to dissecting the mechanism by which new virus particles are assembled.

In separate studies we are using both proteomic and imaging techniques to probe the multiprotein complex that replicates the viral genome. For example, purifying nascent RNA from infected cells and identifying associated proteins by mass spectrometry, and genetically tagging the virus to enable either high resolution EM or fluorescent imaging. These imaging studies are in collaboration with Michelle Peckham and Jamel Mankouri (Leeds) - we are utilising both super-resolution and confocal microscopy, the latter located within a category III containment facility – a unique resource within the UK for the study of HCV.

In collaboration with Colin Fishwick (Leeds) we are applying structure-based drug design methodology to the NS2 protein, a key protease involved in the cleavage of the viral polyprotein. We have established a robust cell-based assay to identify small molecules with the ability to block NS2 mediated cleavage. We hope that these may form the basis for a novel future therapeutic approach.

Recently, homologues of HCV have been identified in other species, the closest relative is the non-primate hepacivirus (NPHV) identified in both dogs and horses. We have begun a programme of work on this virus (2), both as a model system to study HCV but also for comparative studies – although closely genetically related to HCV, NPHV does not appear to cause disease and this difference may shed light on some of the pathogenic mechanisms specific to HCV.

Publications

Amako, Y., Igloi, Z., Mankouri, J., Kazlauskas, A., Saksela, K., Dallas, M., Peers, C. & Harris, M. (2013) Hepatitis c virus ns5a inhibits mixed lineage kinase 3 to block apoptosis. *J. Biol. Chem.* **288**: 24753-24763.

Ross-Thriepland, D., Amako, Y. & Harris, M. (2013) The C terminus of NS5A domain II is a key determinant of hepatitis C virus genome replication, but is not required for virion assembly and release. *J. Gen. Virol.* **94**: 1009-1018.

Stewart, H., Walter, C., Jones, D., Lyons, S., Simmonds, P. & Harris, M. (2013) The non-primate hepacivirus 5 ' untranslated region possesses internal ribosomal entry site activity. *J. Gen. Virol.* **94**: 2657-2663.

Funding
Joe Shaw and Chris Bartlett are students on the Wellcome Trust programme 'The Molecular Basis of Biological Mechanisms'. This work is funded by a Wellcome Trust project grant and a Wellcome Trust Senior Investigator Award.

Collaborators
Leeds: C. Fishwick, J. Mankouri, M. Peckham and C. Peers.
External: S. Griffin (Leeds Institute for Cancer and Pathology), T. Mbisa (Public Health England, Colindale), P. Simmonds (Roslin Institute, Edinburgh), J. McLauchlan (Centre for Virology Research, Glasgow), K. Saksela (University of Helsinki).

Ligand binding to a novel drug resistance protein measured using circular dichroism

Scott Jackson, Simon Patching, David Sharples and Peter Henderson

Introduction

Drug resistance is an increasing problem in clinical settings with some bacterial pathogens now resistant to virtually all available drugs. Chlorhexidine is a bisbiguanide antimicrobial agent that is extensively used in antiseptics ranging from skin washes, soaps, mouthwashes and preservatives. Increasing resistance to chlorhexidine is seen in some pathogens such as *Acinetobacter baumannii*, in which a novel efflux resistance was associated with a gene designated *aceI* (for Acinetobacer chlorhexidine efflux I). We demonstrate how circular dichroism measurements in both the far-UV and near-UV can illuminate the binding of hydrophobic drugs like chlorhexidine to a membrane protein involved in resistance.

Results

The *A. baumannii aceI* gene was transferred to the pTTQ18 plasmid vector, and transformed into *Escherichia coli* BL21(DE3) host cells, where the expression of *aceI* was amplified. Next, the protein was purified in mg quantities by IMAC. The protein had retained structural integrity since a far-UV CD spectrum clearly demonstrated a high content of alpha-helical and tertiary structure (Figure 1A).

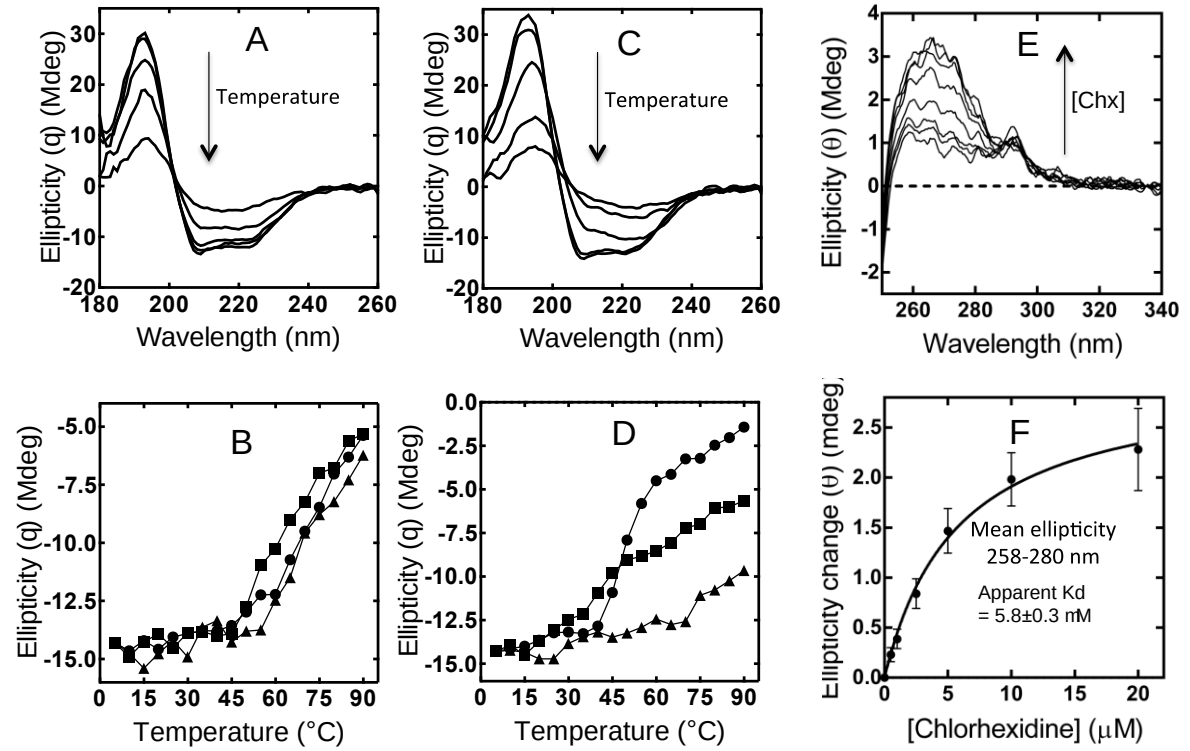

Figure 1: CD spectra and stability of wild-type and E15Q mutant AceI proteins. Far UV CD spectra of AceI proteins at temperatures of 10, 30, 50 70, 90 ^{o}C were determined for 33 μM wild-type **(a, b)** and E15Q mutant **(c, d)** using the DLS beamline B23 CD instrument. The ellipticity at 209nm is shown for protein only (●), protein plus 100 μM chlorhexidine (■; 1:3 molar ratio) and protein plus 500μM chlorhexidine (▲; 1:15 molar ratio) at increasing temperatures. Near-UV CD spectra **(e, f)** of 20 μM purified wild-type AceI protein titrated with 0.0, 0.5, 1.0, 2.5, 5.0, 10.0, 15.0 and 20.0 μM chlorhexidine from low to high (vertical arrow). (e) Complete spectra of AceI protein in the near-UV. (f) Average change in ellipticity (θ, mdeg) (258–280nm) during titration by chlorhexidine.

The far-UV spectrum was not significantly altered by chlorhexidine, so left open the question of whether AceI would bind this putative substrate. Protein melting curves were undertaken by ramping the temperature from 5-90^{o}C while monitoring the far-UV CD spectrum, particularly at 209 or 222nm The wild-type protein was stable at temperatures below 60°C (Figure 1A, B). However, for a mutant protein, E15Q AceI, known to be impaired for resistance to chlorhexidine, denaturation was apparent at 40°C (Figure 1 C,D); chlorhexidine greatly increased the thermal stability of the E15Q protein in a dose-dependent manner (Figure 1D). These experiments yielded indirect evidence that the AceI protein was itself involved in binding chlorhexidine as an integral feature of the resistance mechanism.

More direct evidence was sought by exploring the influence of chlorhexidine on the near-UV spectrum of AceI. Control experiments were done to correct for any contributions of the buffer, the ligand, the solvent, and any instability of the protein over the period of the experiment at 20^{o}C. A titration was then performed with increasing concentrations of chlorhexidine that clearly showed changes in the spectral regions associated with phenylalanine and tyrosine, reflecting the binding of chlorhexidine to the AceI protein (Figure 1E). Estimates of the binding affinity of AceI for chorhexidine were found to lie within the low micromolar range, typical of ligand binding to drug transport proteins (Figure 1F).

The experiments with AceI not only illuminate the function of this protein, but illustrate a general strategy in which CD measurements help elucidate the binding of less tractable ligands to challenging proteins.

Publications

Bettaney, K., Sukumar, P., Hussain, R., Siligardi, G., Henderson, P. & Patching, S. (2013) A systematic approach to the amplified expression, functional characterization and purification of inositol transporters from *Bacillus subtilis*. *Mol. Membr. Biol.* **30**: 3-14.

Henderson, P. & Baldwin, S. (2013). This is about the in and the out. *Nat. Struct. Mol. Biol.* **20**: 654-655.

Hassan, K., Jackson, S, Penesyan, A., Patching, S., Tetu, S., Eijkelkamp, B., Brown, M., Henderson P. & Paulsen, I. (2013) Transcriptomic and biochemical analyses identify a novel family of chlorhexidine efflux proteins. *Proc. Natl. Acad. Sci. USA.* **110:** 20254-20259.

Patching, S., Henderson, P., Sharples, D. & Middleton, D. (2013) Probing the contacts of a low-affinity substrate with a membrane-embedded transport protein using H^{1}-C^{13} cross-polarisation magic-angle spinning solid-state NMR. *Mol. Membr. Biol.* **30**: 129-137.

Funding

Work in the PJFH lab was funded by the EU European Drug Initiative for Channels and Transporters Grant 201924, and in the beamline B23 by grants from the DLS. Work in the ITP and KAH lab was supported by NHMRC (Australia) Project Grant 535053 and ARC Discovery Grant DP110102680. The collaboration is funded by an EU IRSES BacMT 247634 (with Prof. A-B Kolstø, University of Oslo).

Collaborators

External: I. Paulsen and K. Hassan (Macquarie University, Sydney, Australia), G. Siligardi and R. Hussain (Diamond Light Source, Didcot, UK).

Protein-protein interaction regulates the direction of catalysis and electron transfer in a redox enzyme complex

Duncan McMillan and Lars Jeuken

Introduction

Protein-protein interactions are well known to regulate enzyme activity in cell signalling and metabolism. In this report period, we have shown that protein-protein interactions also regulate the activity of a respiratory-chain enzyme, CymA, by changing the direction or 'bias' of catalysis. CymA, a member of the widespread NapC/NirT superfamily, is a menaquinol-7 (MQ-7) dehydrogenase that donates electrons to several distinct terminal reductases in the respiratory network of *Shewanella oneidensis*. Using experimental techniques previously developed in our lab, an inner membrane architecture was engineered on solid supports (Figure 1) in which complex formation with one of CymA's redox partners, flavocytochrome c3 (Fcc_3) fumarate reductase, was studied.

Results

The QCM-D facility at Leeds was used to monitor the association of Fcc_3 with CymA-containing inner membrane architectures assembled on silicon-oxide surfaces. The formation of the so-called 'solid-supported membrane' (SSM) was confirmed by a drop in frequency of ~26-27 Hz and a small change in dissipation (Figure 2A; for clarity the formation of the bilayer itself is not shown and the trace starts after the bilayer is formed). Exposure of these CymA-containing SSMs to Fcc_3 results in a further decrease in frequency to ~-35 Hz (after washing). The shift in frequency (~9 Hz) due to tightly-bound Fcc_3 is equivalent to the adsorption of approximately 0.16 μg Fcc_3/cm^2 and so approximately 2 pmol Fcc_3/cm^2. Control experiments with SSMs that did not contain CymA revealed that no Fcc_3 remained bound to the membrane after washing.

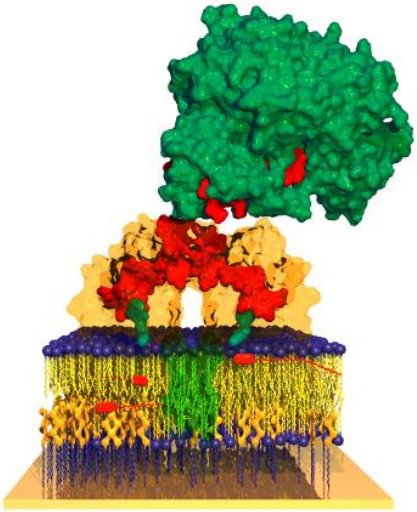

Figure 1: an artistic impression of CymA imbedded in an gold-support membrane mimicking the inner membrane architecture. The single transmembrane helix (transparent green) and the head domain (transparent orange) of CymA are shown. The hemes of CymA are shown in red and a menaquinone bound in CymA is shown in cyan. The binding partner, fcc_3, is shown in green with its hemes, exposed to the proteins surface, in red. This illustration indicates how an electron transfer pathway is possible from the gold surface to menaquinones in the membranes and then, via the hemes in CymA to Fcc_3, where the electrons are used to reduce fumarate.

SSMs were also formed from CymA proteoliposomes by self-assembly on ultra-smooth gold electrodes that had been modified with sub-monolayers of cholesterol tethers. Formation of planar SSMs was confirmed by electrochemical impedance spectroscopy. Cyclic voltammograms (CVs) of the SSMs containing CymA and MQ-7 showed little change after exposure to Fcc_3 (Figure 2B). However, addition of fumarate had a large effect on the appearance of the CV that was converted to a waveshape typical for catalytic reduction reactions, thus indicating fumarate reduction by Fcc_3. To exclude the possibility that Fcc_3

received electrons directly from the electrode, rather than from CymA, an inhibitor of CymA's quinol-dehydrogenase activity was added, HQNO. The addition of HQNO inhibited

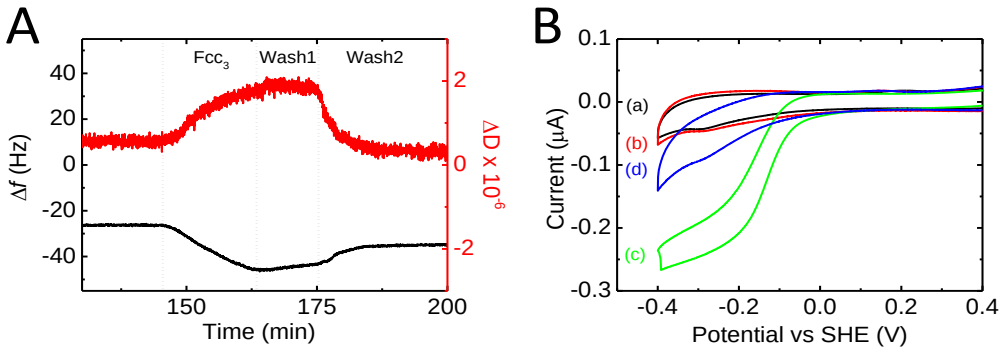

Figure 2: The assembly and catalytic activities of $CymA_{(sol)}$ containing SSMs. **(A)** QCM-D results of a SiO_2 surface in buffer, plotting (black line, left axis) frequency and (red line, right axis) dissipation against time. For clarity, only the results after formation of the SSM are shown. Changes in the solution composition flowing over the SSM are indicated: (Fcc_3) 5μM Fcc_3/1mM fumarate; (Wash 1) 1mM fumarate; (Wash 2) buffer only. SSM was formed with CymA proteoliposomes (90:10 POPC:Cardiolipin; 2% (w/w) CymA; 1% (w/w) MQ-7). The plot shown is representative of triplicate experiments. **(B)** CVs (10 mV/s) of a SSM on a gold electrode modified with cholesterol tethers. The SSM was formed with CymA proteoliposomes (90:10 POPC:Cardiolipin; 1% (w/w) CymA; 1% (w/w) MQ-7). CVs are shown (a) before and after addition of (b) 5μM Fcc_3, (c) 1mM fumarate (after rinsing unbound Fcc_3 from solution) and (d) 1mM fumarate/10μM HQNO.

catalytic fumarate reduction (Figure 2B) demonstrating that the electrons for fumarate reduction are indeed supplied to Fcc_3 from MQ-7 oxidation by CymA (see Figure 1).

The experiments described above reveal that the CymA-Fcc_3 complex is able to oxidize MQ-7 in SSMs. This is in stark contrast to our previous studies of CymA, where only MQ-7 reduction was observed (Astbury report, 2012) In order to establish whether Fcc_3 is responsible for the change in the catalytic bias of CymA, the activity of CymA in the membrane-modified electrodes was measured in the absence of Fcc_3 using chemical reductants and oxidants (Figure 3). Addition of oxidant ferricyanide had almost no effect on the voltammogram (Figure 3A). When, instead of ferricyanide, the reductant dithionite is added to the SSM, a catalytic oxidation signal appears that is inhibited by addition of HQNO (Figure 3B). This confirms our previous findings, namely, that CymA is only able to reduce MQ-7 in the absence of Fcc_3.

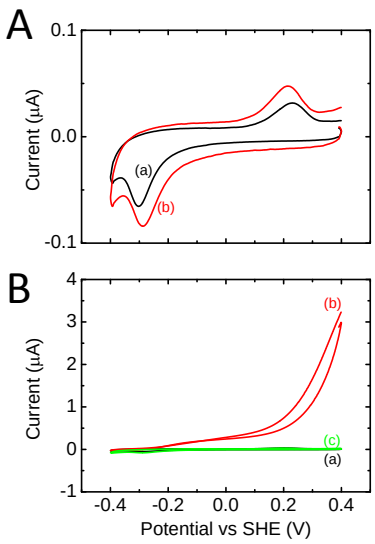

Figure 3: CVs (10 mV/s) of a SSM on a gold electrode modified with cholesterol tethers. The SSM was formed with CymA proteoliposomes (90:10 POPC:Cardiolipin; 1% (w/w) CymA; 1% (w/w) MQ-7). **(A)** CVs (a) before and (b) after addition of 1mM potassium ferricyanide **(B)** CVs (a) before and (b, c) after addition of (b) 1 mM sodium dithionite and (c) 1mM sodium dithionite/10 μM HQNO.

Conclusion

In conclusion, we find that inner membrane architectures can be constructed on planar surfaces and that this provides a powerful approach to resolve protein complex formation and quinone oxidoreductase activity of membrane enzymes. Our finding that protein-protein interactions modulate the catalytic bias of CymA

reveals a new mechanism by which the magnitude and direction of electron flux through respiratory ET networks can be regulated.

Publications

Mcmillan, D., Marritt, S., Firer-Sherwood, M., Shi, L., Richardson, D., Evans, S., Elliott, S., Butt, J. & Jeuken, L. (2013) Protein-protein interaction regulates the direction of catalysis and electron transfer in a redox enzyme complex. *J. Am. Chem. Soc.* **135**: 10550-10556.

Funding

This work was funded by the BBSRC.

Collaborators

External: S. Marritt and J. Butt (University of East Anglia, UK) and S. Elliott (Boston University, USA).

Understanding complex dynamics at atomistic resolution

Polina Banushkina and Sergei Krivov

Introduction

Computational experiments became a vital component of researches arsenal, as was highlighted by the recent Nobel prize awarded to three computational chemists. Advances in computer hardware and simulation algorithms made it possible to obtain detailed dynamical picture of real-life biological processes on a computer. The complex nature of the simulated processes and the large size of data sets generated by such simulations make the development of automated analysis tools very important, practically and conceptually. In particular, their use is indispensable for rigorous quantitative comparison with experiment. One such analysis framework was pioneered and is under active development in our group. Here we report on 1) an analysis of state of the art simulation of folding of an alpha-helical protein and comparison with state of the art experiments; 2) a new methodological development of the framework.

Results: How an all-helical protein folds – a computational perspective.

Recently, Shaw and co-workers have reported the results of "brute-force" atomistic simulations of 12 fast-folding proteins using a custom build supercomputer (Lindorff-Larsen K. *et al*. (2011) *Science*, **334**, 517). All-helical protein HP35 was chosen for the analysis (recently we completed such an analysis for all beta WW protein). The optimal reaction coordinate and the associated free energy profile (FEP) which provide quantitative description of the folding dynamics were determined.

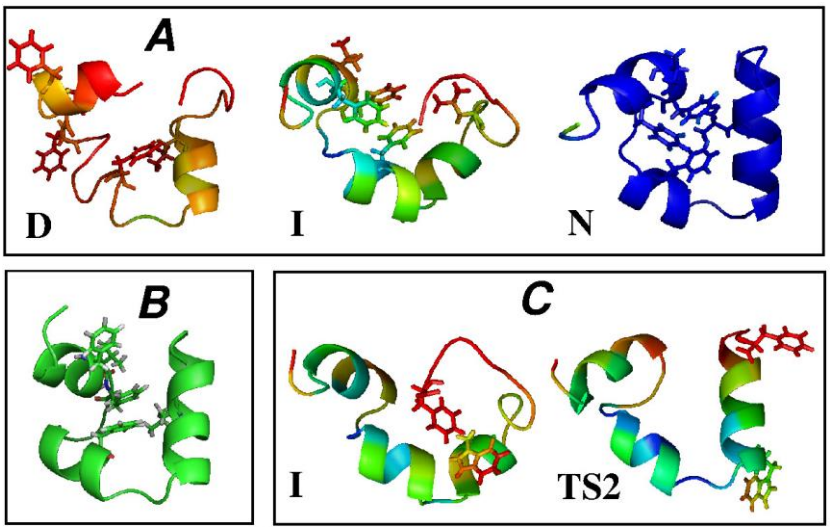

Figure 1: (A) Hydrophobic core formation during HP35 folding: denatured (D) state with fully disordered tertiary structure; intermediate (I) state with the first and second helices formed but still incomplete hydrophobic core; native (N) state with tightly packed phenylalanine core. **(B)** A native-like structure with unpacked phenylalanine core from I state (single snapshot). **(C)** Contact formation between side-chains Trp64 and Phe76: I state with contact between Trp64 and Phe76; TS2 state without the contact. Colors code for the root-mean-square fluctuations of atomic positions around the average structure from 1.5 A (blue) to 7A (red).

A solid state NMR experiment by Tycko and co-worker presented (an indirect) evidence that HP35 folds through an intermediate state with nearly native secondary structure but disordered tertiary structure (Hu K.-N. *et al*. (2010) *J. Am. Chem. Soc*., 132, 24). Our analysis shows that HP35 folds through the intermediates. Figure 1A explores the formation of the hydrophobic core (residues Phe47, Val50, Phe51, Phe58 and Leu69) during the folding process. The snapshots show that formation of native topology and secondary structure begins early during the folding process while the stabilization of the hydrophobic core residues happens later. The denatured state shows some helical content and fully disordered tertiary structure. The intermediate state is characterized by the first and second helices

formed but an incomplete hydrophobic core. The red and yellow colours of side-chains Val50 and Leu69 indicate large fluctuations of these residues. In the native state the tightly packed hydrophobic core is fully formed.

The presence of an intermediate at the native side of the major folding/unfolding barrier in HP35 was suggested by an experiment using TTET to monitor conformational fluctuations (Reiner A. *et al*. (2010) *PNAS*, 107, 4955). In the intermediate state the partially unfolded third helix is flexible enough to allow contact between side-chains Trp64 and Phe76, which is very unlikely in the native state. The experiment detected the presence of conformations without contact (I) and with contact (I*) in the intermediate state. Our analysis confirms that the intermediate state contains both types of conformations, while the second transition state predominantly contains structures without Trp-Phe contact (Figure 1C).

The pre-exponential factor was estimated in four different ways all giving the same order of about k_0^{-1}~20-50 ns in agreement with the previous study of a WW protein. We have highlighted hidden assumptions used by other approaches, which are likely to be violated.
In summary, our analysis provided detailed atomistic picture of the folding process in complete agreement with experimental data.

Optimal coordinates for the description of dynamics in general.
The committor probability (the often employed optimal coordinate) is optimal only for one type of dynamics – a reaction dynamics between two states. Dynamics of such practically important systems as molecular motors, enzymes, stochastic pumps, biochemical networks cannot be analysed. Recently, we have introduced a class of optimal coordinates that can be used to describe the stochastic dynamics in general [4]. The optimal coordinates are *additive eigenvectors* (W_i) which are transformed by a stochastic matrix (P_{ji}) in a simple way by adding an *additive eigenvalue* λ to every component

$$\sum P_{ji} W_j = \lambda + W_i$$

Such solutions have very peculiar properties. For example, an optimal coordinate for stochastic dynamics with detailed balance is a multivalued function. An optimal coordinate for a random walk on a line corresponds to the (phase of) conventional eigenvector of the one-dimensional Dirac equation. The equation for the optimal coordinate in a slowly varying potential reduces to the Hamilton-Jacobi equation for the action function.

The introduced additive eigenvectors solve two other related problems. They can be used for the reconstruction of time from an ensemble of stochastic trajectories and for the decomposition of stationary stochastic dynamics into eigenmodes which do not decay exponentially with time.

Publications
Banushkina, P. & Krivov, S. (2013) High-resolution free-energy landscape analysis of alpha-helical protein folding: Hp35 and its double mutant. *J. Chem. Theory Comput.* **9**: 5257-5266.

Krivov, S. (2013) Method to describe stochastic dynamics using an optimal coordinate. *Phys. Rev. E* **88**: 062131.

Funding
This work was supported in part by an RCUK fellowship and a BBSRC grant.

Studies of small DNA tumour viruses that cause disease in humans

Christopher Wasson, Marietta Muller, Hussein Abdul-Sada, Emma Prescott, Rajni Bhardwaj, Eric Blair, Adrian Whitehouse, Stephen Griffin, Richard Foster and Andrew Macdonald

Introduction

Members of the *Papovaviridae*, which includes the Papillomaviruses and Polyomaviruses, are the causative agents of a number of severe diseases in humans. Notable examples include cervical cancer, which is exclusively associated with infection with human papillomaviruses, and polyomavirus-associated nephropathy (PVAN) and *progressive multifocal leukoencephalopathy* (PML) caused by the BK and JC polyomaviruses, respectively. Current therapeutic strategies to treat these virus-associated maladies are lacking. We have established a multi-disciplinary research group to undertake a broad ranging analysis of these viruses in an effort to identify new targets for therapeutic intervention. These studies have revealed novel information about these viruses.

Results

Human papillomavirus: We have focussed our analysis on the least understood of the three transforming proteins encoded by this virus. The E5 protein is a small membrane protein expressed by all carcinogenic papillomaviruses. Little is understood of the role of E5 in the virus life cycle or its mechanisms of pathogenesis. We discovered that E5 functions as a virus-encoded ion channel or "viroporin" (Wetherill *et al*., 2012). We utilised *de novo* models of an E5 channel complex to identify small molecule inhibitors of E5 channel function and are currently using these models to reveal the functional determinants of E5 channel function *in vitro*. In addition we have established organotypic raft culture systems that mimic the natural three-dimensional nature of human skin. These model systems allow us to grow HPV in the laboratory and provide an ideal opportunity to test our *in vitro* findings in a physiologically relevant system.

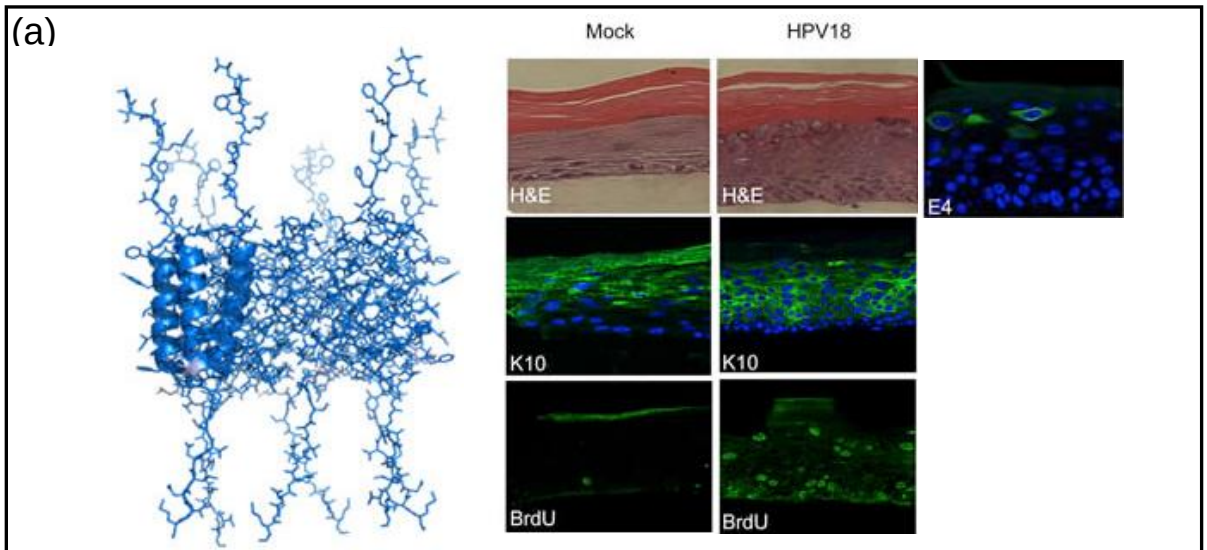

Figure 1: (a) *In silico* molecular modelling of an E5 channel complex (Wetherill et al., 2012). Molecular predictions, based on energy minimisation, suggest that the E5 channel is composed of a hexamer, with a hydrophilic region protruding from the membrane and a luminal pore lined with residues that mediate ion flow. **(b)** Immunohistochemistry of an organotypic raft culture section from control and HPV containing primary keratinocytes. Cells are stained with haematoxylin and eosin to show general morphology and keratin 10 as a marker of keratinocyte differentiation. BrdU staining highlights the increased host cell DNA replication occurring in cells containing HPV. Probing for a HPV late protein, E4 highlights a productive HPV life cycle in the raft culture model.

Human polyomaviruses: Our analysis currently covers three major polyomaviruses associated with disease in humans. These are the JC, BK and Merkel polyomaviruses. In collaboration with Prof. Adrian Whitehouse (UoL), we are dissecting the role of the Small T antigen of Merkel polyomavirus in transformation. Our studies have shown that this virus protein is an efficient and powerful inhibitor of the host innate immune response and is capable of preventing an inflammatory response. This may have profound implications for the persistent nature of virus infection and allow Merkel to persist in the host despite the presence of an immune response. In parallel studies we are beginning to understand more about the enigmatic agnoproteins that are encoded by BK and JC viruses. Our preliminary biochemical characterisation of these proteins suggests that they are ideal targets for antiviral therapeutics and work in 2013 will continue to target these proteins for study.

Publications

Griffiths, D., Abdul-Sada, H., Knight, L., Jackson, B., Richards, K., Prescott, E., Peach, A., Blair, G., Macdonald, A. & Whitehouse, A. (2013) Merkel cell polyomavirus small t antigen targets the nemo adaptor protein to disrupt inflammatory signaling. *J. Virol.* **87**: 13853-13867.

Remenyi, J., Van Den Bosch, M., Palygin, O., Mistry, R., Mckenzie, C., Macdonald, A., Hutvagner, G., Arthur, J., Frenguelli, B. & Pankratov, Y. (2013) Mir-132/212 knockout mice reveal roles for these miRNAs in regulating cortical synaptic transmission and plasticity. *PLoS One* **8:** e62509.

Funding

This work was supported by Cancer Research UK, Yorkshire Cancer Research, Yorkshire Kidney Research Fund and the MRC.

Collaborators

Leeds: R. Foster, B. Turnbull, M. Webb, D. Tomlinson and M. McPherson.
External: S. Griffin (LIMM), S. Roberts (Birmingham), N. Coleman (Cambridge), S. Graham (Glasgow), S. Arthur (Dundee) and M. Imperiale (University of Michigan, USA).

Identification of host cell ion channel modulators as new anti-viral targets

Hessa Taqi, David Hughes, Jon Barr, Adrian Whitehouse, Mark Harris and Jamel Mankouri

Introduction

For any virus to replicate and persist, they must change the environment of the cells they infect. Newly identified factors shown to be important in leading virus entry, survival and release are cellular ion channels, proteins that act as a pore in the membranes of all cells within the body, permitting the selective passage of ions (such as potassium ions, sodium ions, and calcium ions). Through controlling ion passage, these channels serve many critically important cellular functions including chemical signalling, the regulation of pH, and the regulation of cell volume.

We have gained insight into the interactions between clinically important human viruses and cellular ion channels. These studies continue to highlight the importance of ion channel function in the lifecycle of infectious human viruses and enhance our understanding of the host cell processes that viruses require in order to survive.

Results

We have identified the critical role of an ion channel in the pathogenesis of the Kaposi's sarcoma-associated herpesvirus (KSHV). KSHV is one of seven currently known human oncoviruses, and a major cause of Kaposi's sarcoma, as well as primary effusion lymphoma. The channel identified is a voltage gated K^+ channel; which the virus must activate to enter its lytic replicative cycle. We are currently performing experiments to determine the mechanism of virus-channel modulation and the viral proteins involved. Completing this study not only represents the first involvement of K^+ channels in the lifecycle of a DNA virus, it also paves the way to impede the ability of the virus to manipulate K^+ channels, providing a new therapeutic angle to develop anti-KSHV drugs that block lytic replication. Indeed as K^+ channel inhibitors are already commercially available, this may pave the way for investigations in animal/human studies to assess if this effect in required *in vivo*. In addition, as K^+ channel function has been linked to the regulation of cancer cell growth, this study will allow us to investigate if K^+ channel function is linked to the cancer causing ability of KSHV.

Using similar approaches we have identified specific ion channel modulators that impede the lifecycle of human respiratory syncytial virus, hepatitis C virus and zoonotic viruses including buyamwera virus. Current approaches aim of characterise the anti-viral effects of these ion channel modulators and the ability of these viruses to manipulate cellular ion channel function.

Publications

Amako, Y., Igloi, Z., Mankouri, J., Kazlauskas, A., Saksela, K., Dallas, M., Peers, C. & Harris, M. (2013) Hepatitis c virus ns5a inhibits mixed lineage kinase 3 to block apoptosis. *J. Biol. Chem.* **288**: 24753-24763.

Funding

We gratefully thank the Royal Society for funding these studies.

Collaborators

Leeds: A. Whitehouse, J. Barr, M. Harris, A. Macdonald, C. Peers and J. Lippiat.
External: M. Reeves (UCL), A. Kohl (Glasgow), M. Dallas (Reading), C. Crump (Cambridge).

Breaking dogmas: direct entry by RNase E and pervasive transcription

Justin Clarke, Louise Kime, Yu-fei Lin, David Romero and Kenneth McDowall

Introduction

The RNase E family is renowned for being central to the processing and decay of all types of RNA in many species of bacteria, as well as providing the first examples of endonucleases that can recognise 5'-monophosphorylated ends, thereby increasing the efficiency of cleavage. However, we have shown that some transcripts can be cleaved efficiently by *Escherichia coli* RNase E via direct entry, *i.e.* in the absence of the recognition of a 5'-monophosphorylated end.

In the last year, we have used a differential RNA sequencing approach and a 5'-end sensing mutant of the N-terminal half (NTH) of RNase E (T170V) to identify sites of direct entry cleavage in *E. coli*. We have also analysed the requirements for direct entry cleavage of a tRNA precursor *in vitro*. We have extended our RNA-seq analysis to other bacteria and have found evidence for pervasive transcription, abundant small RNAs and leaderless mRNAs.

Results

We have shown that the processing of tRNA in *E. coli*, one of the core functions of RNase E, makes extensive use of direct entry. Moreover, we have shown that, as we predicted, direct entry is facilitated by the recognition of specific unpaired regions that are adjacent, but not contiguous to segments cleaved by RNase E (Figure 1).

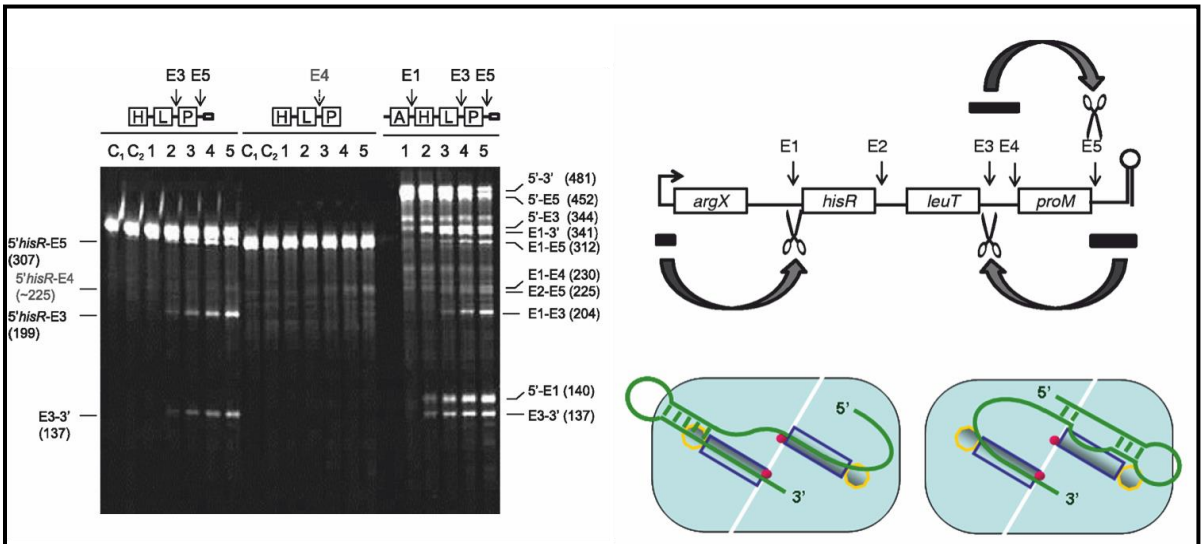

Figure 1: Top – 5'-triphosphorylated *in vitro* transcribed substrates corresponding to full length *argX* precursor or truncations are indicated at the top of each panel. RNase E-NTH T170V and initial substrate concentration at the start of the reaction were 7 nM and 250 nM, respectively. Lanes 1-5 contain samples taken 0, 5, 15, 30 and 60 min after mixing enzyme and substrate. Lanes C1 and C2 correspond to substrate incubated without enzyme for 0 and 60 min, respectively. The identities and sizes of the species produced by cleavage of the precursor starting at the 5' end of *hisR* tRNA are indicated on the left of the panel. The identities and sizes of the products of cleaving full-length transcript are indicated on the right of the panel. **Middle** – Schematic of the *argX-hisR-leuT-proM* precursor showing RNase E cleavage sites E1 to E5, indicated with small arrows. Closed rectangles represent regions required for cooperative binding that mediate direct entry cleavage; grey arrows indicate the site where cooperative binding allows efficient cleavage (indicated as scissors). **Bottom** - A schematic representing the possible contributions of secondary structure to direct entry. RNA is shown in green, the RNase E principal dimer is shown in light blue, the RNA binding channel is shown as a rectangle (outline dark blue), the active site is shown as a red circle and the 5' sensor is shown as a circle (outline yellow).

More recently, we have shown using RNA sequencing approaches that, contrary to current models, direct entry is likely to pervade in the rapid turnover of mRNA, a key aspect of gene regulation. Our RNA-seq approach, which provides insight into virtually every step in gene expression, has been extended to other bacteria including *Propionibacterium acnes* (Figure 2).

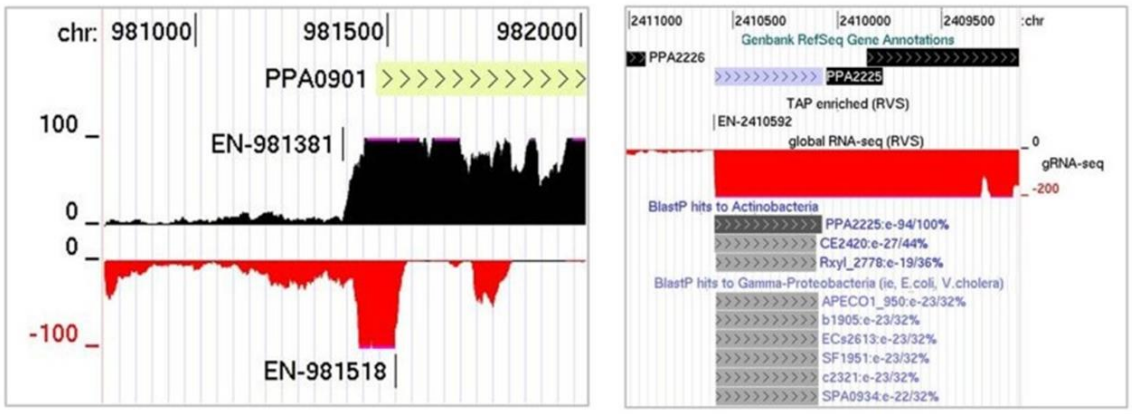

Figure 2: global RNA sequencing data is displayed as tracks in black (positive) and red (negative) for forward and reverse strands, respectively. **Left** – An example of a potential antisense RNA that binds the 5′ RBS of the gene PPA0901, which encodes the GTP-binding protein, LepA. EN-981381 and EN-981518 represent sites of enrichment identified in a separate differential RNA-seq experiment and correspond to transcriptional start sites on the equivalent strand. **Right** – An example of a leaderless mRNA mapped to the gene PPA2225, which encodes ferritin. EN-2410592 represents a site of enrichment associated with transcription rather than processing. BlastP hits are shown in grey below the gRNA-seq data.

The study of this species, which is a major contributor to wide-spread human disease, revealed strong evidence for 'pervasive' transcription and showed that contrary to initial indications it is not biased towards the production of antisense RNAs. Additionally, several examples of leaderless mRNAs, which lack an obvious 5'UTR and hence Ribosome Binding Site (RBS), were found to be the result of transcription initiation, rather than just processing (Figure 2). These findings challenge the dogma that transcription starts and ends just before and after the coding region of a gene. Similar findings were obtained for the transcriptomes of *E. coli* and *S. coelicolor* using the same approach.

Publications

Lin, Y.-F., Romero, D., Guan, S., Mamanova, L. & McDowall, K. (2013) A combination of improved differential and global RNA-seq reveals pervasive transcription initiation and events in all stages of the life-cycle of functional RNAs in propionibacterium acnes, a major contributor to wide-spread human disease. *BMC Genomics* **14**: 620.

Funding

This work was supported by the Leeds Foundation for Dermatological Research, the White Rose University Consortium and BBSRC.

Collaborators

External: Global RNA-sequencing was performed at the Welcome Trust Sanger Institute.

Understanding the mechanism and regulation of the Vacuolar ATPase

Kostas Papachristos, Emanuele Paci, John Trinick and Stephen Muench

Introduction

The vacuolar ATPase (V-ATPase) is a large (1MDa), transmembrane, ATP driven proton pump, essential to eukaryotic cell homeostasis. It contains ~30 subunits of up to 14 different types separated into an ATP hydrolysing V_1 domain and proton translocating V_o domain. Previous work by the group revealed the subunit organisation within the complex (Figure 1A). The AB subunits within V_1 are responsible for ATP hydrolysis which drives the rotation of a central axle and c-ring relative to the *a* subunit, transporting protons over the membrane. The V-ATPase is regulated through the controlled dissociation of V_1 from V_o which renders V_o impermeable to protons and V_1 unable to hydrolyse ATP. The structural changes which bring about the inactivation of V_1 are currently unresolved. Despite the progress which has been made with regards to understanding the structural arrangement of the V-ATPase and other members of the rotary ATPase family, we are only just starting to understand the mechanical properties which allow these complex rotary machines to work at close to 100% efficiency. The remarkable efficiency of this molecular motor is hypothesised to be due in part to the intrinsic flexibility in the stator connections and central rotor axle which links the two motors.

Results

The structure of the V_1 domain was solved by single particle cryo electron microscopy (Figure 1B,C). The isolated V_1 structure has revealed the changes that bring about dissociation and silence ATP turnover, allowing us to propose a mechanism for V_1 dissociation. Understanding the mode of dissociation has important implications for the development of novel therapeutics which can silence the V-ATPase in disease states. Previous work on understanding the mechanism of the V-ATPase has focused on calculating the dynamic properties of individual subunits and extrapolating this to understand the flexibility of the whole system. We have used both negative stain and single particle cryo electron microscopy to show the intrinsic flexibility available to both the *Manduca sexta* and *Saccharomyces cerevisiae* V-ATPase (Figure 1D). This has been successfully combined with molecular dynamic simulations to explore the conformational landscape available to the system (Figure 1E).

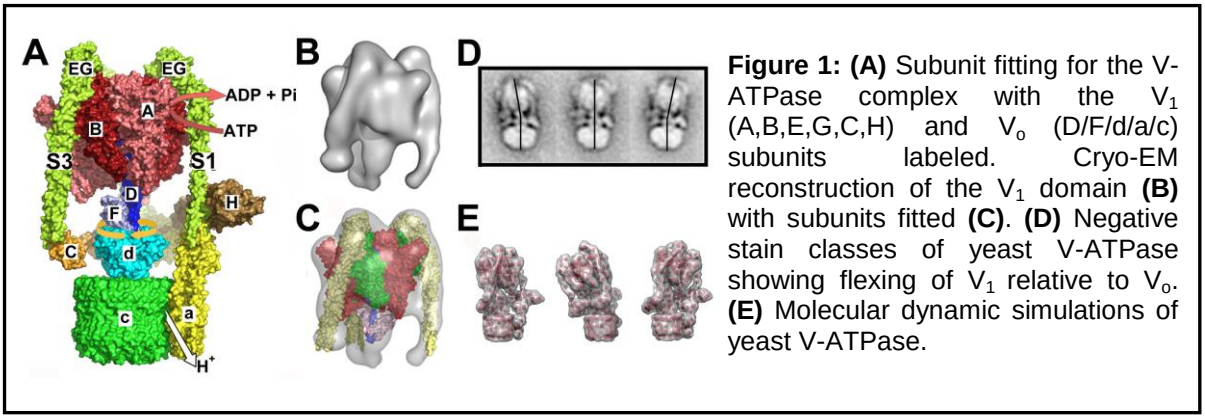

Figure 1: (A) Subunit fitting for the V-ATPase complex with the V_1 (A,B,E,G,C,H) and V_o (D/F/d/a/c) subunits labeled. Cryo-EM reconstruction of the V_1 domain **(B)** with subunits fitted **(C)**. **(D)** Negative stain classes of yeast V-ATPase showing flexing of V_1 relative to V_o. **(E)** Molecular dynamic simulations of yeast V-ATPase.

In particular we show that flexing of the catalytic V_1 domain relative to the proton translocating V_o domain is apparent to a maximum of 30°. This study has provided valuable insights into the rapidly expanding field of rotary ATPase motor dynamics which is crucial in understanding how these complex systems can operate with close to 100% efficiency.

Publications

Afanador, G., Muench, S., Mcphillie, M., Fomovska, A., Schoen, A., Zhou, Y., Cheng, G., Stec, J., Freundlich, J., Shieh, H.-M., Anderson, J., Jacobus, D. , Fidock, D., Kozikowski, A. P., Fishwick, C. W., Rice, D., Freire, E., Mcleod, R. & Prigge, S. (2013) Discrimination of potent inhibitors of *Toxoplasma gondii* enoyl-acyl carrier protein reductase by a thermal shift assay. *Biochemistry* **52**: 9155-9166.

Cheng, G., Muench, S., Zhou, Y., Afanador, G., Mui, E., Fomovska, A., Lai, B., Prigge, S., Woods, S., Roberts, C., Hickman, M., Lee, P., Leed, S., Auschwitz, J. M., Rice, D. & Mcleod, R. (2013) Design, synthesis, and biological activity of diaryl ether inhibitors of *Toxoplasma gondii* enoyl reductase. *Bioorg. Med. Chem. Lett.* **23**: 2035-2043.

Muench, S., Stec, J., Zhou, Y., Afanador, G., Mcphillie, M., Hickman, M., Lee, P., Leed, S., Auschwitz, J., Prigge, S., Rice, D. & Mcleod, R. (2013) Development of a triclosan scaffold which allows for adaptations on both the a- and b-ring for transport peptides. *Bioorg. Med. Chem. Lett.* **23**: 3551-3555.

Song, C., Papachristos, K., Rawson, S., Huss, M., Wieczorek, H., Paci, E., Trinick, J., Harrison, M. A. & Muench, S. (2013) Flexibility within the rotor and stators of the vacuolar H^+-ATPase. *PLoS One* **8:** e82207.

Stec, J., Fomovska, A., Afanador, G., Muench, S., Zhou, Y., Lai, B.-S., El Bissati, K., Hickman, M., Lee, P., Leed, S., Auschwitz, J., Sommervile, C., Woods, S., Roberts, C., Rice, D., Prigge, S., Mcleod, R. & Kozikowski, A. (2013) Modification of triclosan scaffold in search of improved inhibitors for enoyl-acyl carrier protein (acp) reductase in *Toxoplasma gondii*. *ChemMedChem* **8**: 1138-1160.

Funding

This work was supported by the MRC and NIH

Collaborators

Leeds: M. Harrison
External: H. Wieczorek (University of Osnabrueck), S. Scheres (MRC-LMB) and R. McLeod (University of Chicago).

Development of tools and approaches to facilitate more systematic exploration of lead-like chemical space

Ramakrishnan Basak, Richard Doveston, Mark Dow, Martin Fisher, Colin Fishwick, Daniel Foley, Thomas James, Arnout Kalverda, Steven Kane, Paul MacLellan, Sushi Maurya, Bruce Turnbull, Stuart Warriner and Adam Nelson

Introduction

Chemists have explored chemical space in an uneven and unsystematic manner. An analysis of the scaffolds of the 25 million known cyclic small molecules (in 2008) revealed that one sixth of the compounds are based on just 30 (out of the 2.5 million) known molecular scaffolds! To address this historic uneven exploration, we have developed a vibrant research programme focusing on the identification and development of synthetic methods that have potential to facilitate more systematic exploration of chemical space.

Extension to lead-like chemical space

A strongly developed theme within the Nelson group has been to develop diversity-oriented synthetic approaches that map onto the requirements of drug discovery programmes. Established diversity-oriented approaches have tended to focus on small molecules that lie well outside drug-like space. It is now generally accepted that attrition rates in drug discovery are strongly linked to molecular properties such including molecular weight and lipophilicity. Optimisation almost always leads to increases in both molecular weight and lipophilicity, so it is important to control the properties of initial lead molecules. We are thus continuing to develop a robust and growing toolkit of synthetic reactions that address the challenges raised in the nascent field of lead-oriented synthesis. This research programme is now feeding into the €196M European Lead Factory in which Leeds is a partner.

Integration of computation tools and diversity-oriented synthesis in bioactive ligand discovery

We have developed an approach for designing bioactive small molecules in which *de novo* structure-based ligand design was focused on regions of chemical space accessible using a diversity-oriented synthetic approach. The approach was exploited in the design and synthesis of potential ligands for FabF, an enzyme that catalyses the chain elongation in the bacterial (FAS II) fatty acid biosynthetic pathway, and that may have potential as an antimicrobial target. Accordingly, analogues of the natural product platensimycin were prepared in which the complex bridged ring system was simplified. A range of compounds was discovered that had significantly improved affinity for the protein relative to a reference ligand. The integration of synthetic accessibility with ligand design enabled focus to be placed on synthetically-accessible regions of chemical space that were relevant to

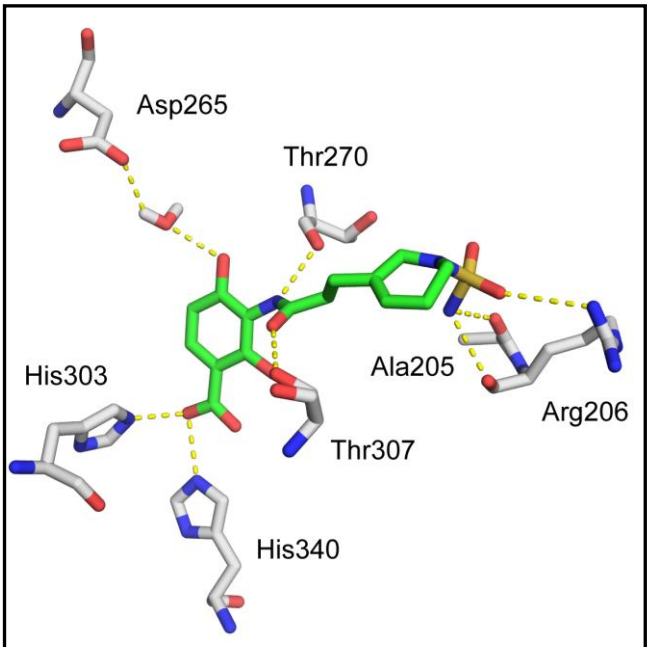

Figure 1: active site of FabF.

the target protein under investigation.

Publications

Doveston, R., Marsden, S. & Nelson, A. (2013), "Towards the realisation of lead-oriented synthesis", *Drug Discov. Today* 2013, doi: 10.1016/j.drudis.2013.11.006.

James, T., Simpson, I., Grant, J., Sridharan, V. & Nelson, A. (2013) Modular, gold-catalyzed approach to the synthesis of lead-like piperazine scaffolds. *Org. Lett.* **15**: 6094-6097.

Maclellan, P. & Nelson, A. (2013) A conceptual framework for analysing and planning synthetic approaches to diverse lead-like scaffolds. *Chem. Commun.* **49**: 2383-2393.

Maurya, S., Dow, M., Warriner, S. & Nelson, A. (2013) Synthesis of skeletally diverse alkaloid-like molecules: Exploitation of metathesis substrates assembled from triplets of building blocks. *Beilstein J. Org. Chem.* **9**: 775-785.

Timms, N., Windle, C., Polyakova, A., Ault, J., Trinh, C., Pearson, A., Nelson, A. & Berry, A. (2013) Structural insights into the recovery of aldolase activity in N-acetylneuraminic acid lyase by replacement of the catalytically active lysine with gamma-thialysine by using a chemical mutagenesis strategy. *ChemBioChem* **14**: 474-481.

Funding

We thank EPSRC, the Wellcome Trust, the EU, GSK and AstraZeneca for support.

Collaborators

Leeds: S. Marsden and S. Sridharan,
External: I. Churcher (GSK) and I. Simpson and A. Grant (AstraZeneca). We also acknowledge other scientific collaborators from who have also contributed strongly to this on-going programme.

Structural and mechanistic insights into the FusB family of fusidic acid resistance proteins

Jennifer Tomlinson, Gary Thompson, Arnout Kalverda, Anastasia Zhuravleva, Steve Homans and Alex O'Neill

Introduction.

A major focus in the O'Neill laboratory is on understanding the mechanisms by which bacteria resist the effects of the antibiotics that are used to treat the infections they cause. The antibiotic fusidic acid inhibits bacterial protein synthesis in the bacterial pathogen *Staphylococcus aureus* by blocking release of the translocase, elongation factor G (EF-G), from the ribosome. Resistance to fusidic acid is most commonly mediated by proteins of the FusB family, which bind to elongation factor G and protect it from the inhibitory effect of fusidic acid. The mechanism by which the FusB-type proteins interact with EF-G to mediate resistance to fusidic acid is not fully understood, and recent efforts have therefore focused on gaining a detailed understanding of this protein-protein interaction (PPI).

Mapping of the binding interface between FusB and EF-G by mutagenesis

Previous studies using NMR chemical shift perturbations have determined the binding site for FusB-type proteins in domain IV of EF-G_{C3}, a fragment of EF-G composed of domains III-V. To more precisely delineate the FusB binding site within this region, alanine-scanning mutagenesis was employed to systematically substitute surface exposed residues of EF-G that lie within the predicted binding site. 11 alanine substitution mutations were generated but none resulted in proteins that were unable to bind to FusB, potentially suggesting that this PPI involves numerous contact points on EF-G, none of which are alone essential for binding.

Determining a model of the FusB-EF-G interaction by NMR

To understand the interaction between FusB-type proteins and EF-G_{C3}, NMR experiments are underway to refine our current *in silico* docked model, shown in Figure 1, and thereby facilitate a better understanding of this unusual antibiotic resistance mechanism. NMR residual dipolar couplings have been measured to refine the relative orientations of the two proteins while PRE distance restraints are being used to provide distance information across the protein-protein interface. Preliminary data suggest some internal domain reorientation occurs in EF-G_{C3} upon binding to FusB. Spectra of the side chain methyl groups in full length EF-G are also

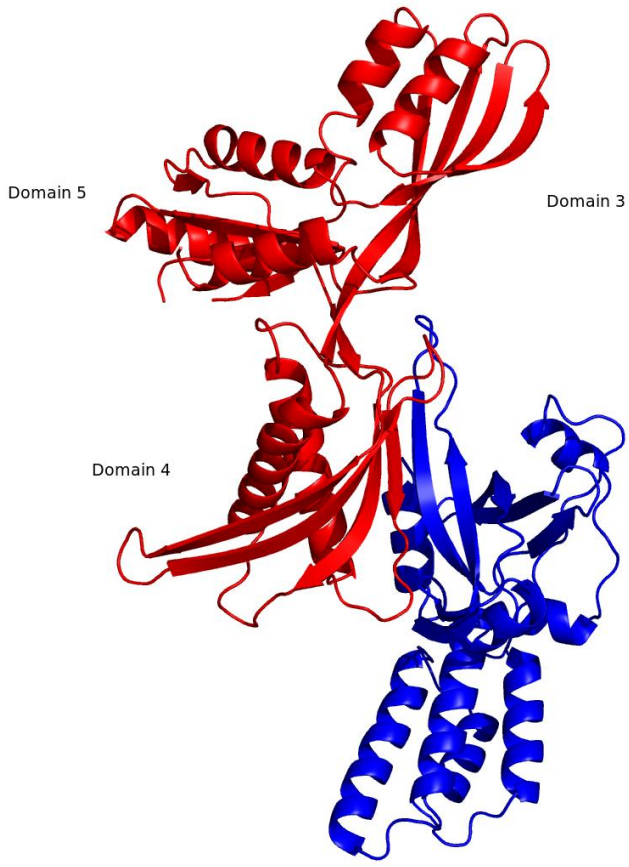

Figure 1: proposed model of the interaction between EF-G and FusB from initial docking of the crystal structures of the two proteins (PDB IDs 2XEX and 4ADN, respectively). Domains 3-5 of EF-G are shown in red, and FusB is shown in blue.

being acquired to determine whether the interaction between EF-G_{C3} and FusB transmits conformational changes into domains I and II.

Publications

Cox, G., Edwards, T. & O'Neill, A. (2013) Mutagenesis mapping of the protein-protein interaction underlying fusb-type fusidic acid resistance. *Antimicrob. Agents Chemother.* **57**: 4640-4644.

Funding

This work is funded by the BBSRC.

Developing new tools for time-resolved structural biology

Briony Yorke, Anna Polyakova, Diana Monteiro, James Gowdy,
Stuart Warriner, Michael Webb and Arwen Pearson

Introduction

When considering the macromolecules that comprise our cells and organelles, we must remember that these molecules are not static and that their structure changes as they function. Without being able to observe these dynamic structural changes, we cannot hope to truly understand how biological macromolecules work. The design and creation of new materials, catalysts and therapeutics therefore currently relies on empirical rule-based approaches as well as a fair degree of serendipity. It is therefore vitally important that we are able to determine detailed structures of macromolecular systems of interest in multiple functional states. The gold-standard experiment is one that yields atomic resolution structural information in real-time. Although many experimental approaches are available that are able to probe functionally related dynamics in real-time (e.g. ultrafast spectroscopic techniques) the majority of these are indirect probes that report on the local change, but do not provide an overall atomic description of how the structure of the system is changing with time. There is currently only one method, time-resolved pump-probe Laue X-ray diffraction, that enables the direct visualisation of macromolecular structure in real-time during function. Unfortunately, its applicability to structure-function studies is limited by stringent requirements for specific sample properties.

We are developing a suite of complementary methodologies that together will allow us to obtain detailed, time-resolved descriptions of macromolecular function.

Results

We are approaching the challenge of generating a genuinely broadly applicable time-resolved X-ray diffraction experiment in several ways. The first, is to bring a serial crystallographic approach to a synchrotron beamline, taking advantage of the new microfocus beamlines, humidified sample environments and the on-axis laser excitation and spectroscopy geometries we have previously helped develop. On a standard insertion device beamline this should enable 100s of microsecond to millisecond time-resolutions. The second is a novel data collection multiplexing strategy which, in principle, should enable us to access nano-second to microsecond time scales on a standard monochromatic beamline. We have recently demonstrated, for the first time, the application of this method to study X-radiation damage processes during diffraction data collection (Figure 1) and a manuscript describing this work is currently under consideration for publication.

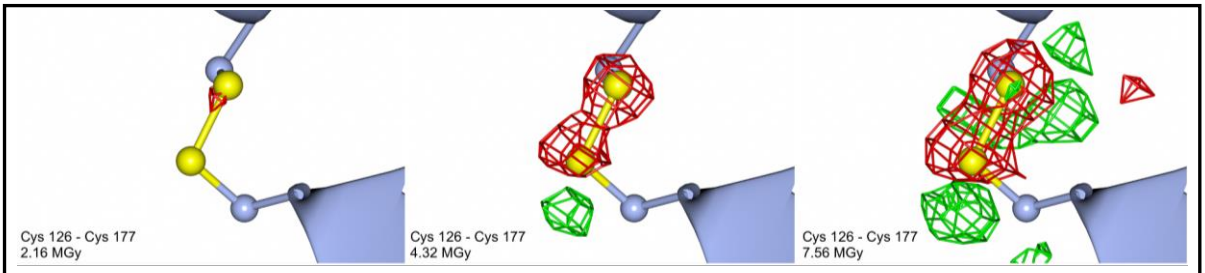

Figure 1: dose dependent changes in electron density at the Cys126-Cys177 disulfide bond of thaumatin measured in a millisecond multiplexing experiment. Fo-Fc electron density is contoured at 3 (green) and -3 (red) r.m.s.d.

To enable time-resolved structure determination the reaction of interest must be triggered simultaneously throughout the sample. For fast time-resolution (sub millisecond) this requires activation by light. However, the majority of biological systems are not photoactivated. We are developing a library of photocages that can be incorporated into proteins using a number of strategies. These include directly caging the active site by caging either the substrate or an active site residue, or using photocleavable crosslinkers that can be used to confirmationally lock the protein into a ligand binding but catalytically incompetent state. For slower reactions (millisecond to second) rapid mixing techniques can be used to trigger the reaction. We are developing a beamline mounted rapid mixing and flow cell device. Such a flow device can be used both to trigger slow reactions in microcrystals but also, and perhaps more importantly, can be used for solution phase experiments. Many biological processes cannot be probed by X-ray crystallography as they are not compatible with the confines of a crystal lattice. These include viral capsid assembly and disassembly as well as the large scale conformational changes associated with membrane protein pumps. To study these we have recently begun to explore small angle X-ray scattering (SAXS). SAXS yields a low resolution molecular envelope that can reveal gross structural rearrangements. By combining the SAXS envelopes, and crystal structures a detailed model of the structural rearrangements associated with function can be obtained.

Publications

Burnett, A., Kendrick, J., Russell, C., Christensen, J., Cunningham, J., Pearson, A., Linfield, E. & Davies, A. (2013) The effect of molecular size and particle shape on the terahertz absorption of a homologous series of tetraalkylammonium salts. *Anal. Chem.* **85**: 7926-2934.

Ford, R., Barker, A., Bakker, S., Coutts, R., Ranson, N., Phillips, S., Pearson, A. & Stockley, P. (2013) Sequence-specific, RNA-protein interactions overcome electrostatic barriers preventing assembly of satellite tobacco necrosis virus coat protein. *J. Mol. Biol.* **425**: 1050-1064.

Foster, T., Thompson, G., Kalverda, A., Kankanala, J., Bentham, M., Wetherill, L., Thompson, J., Barker, A., Clarke, D., Norenberg, M., Pearson, A., Rowlands, D., Homans, S., Harris, M., Foster, R. & Griffin, S. (2013) Structure-guided design affirms inhibitors of Hepatitis C Virus p7 as a viable class of antivirals targeting virion release. *Hepatology* **59**: 408-422.

Stockley, P., Twarock, R., Bakker, S., Barker, A., Borodavka, A., Dykeman, E., Ford, R., Pearson, A., Phillips, S., Ranson, N. & Tuma, R. (2013) Packaging signals in single-stranded RNA viruses: Nature's alternative to a purely electrostatic assembly mechanism. *J. Biol. Phys.* **39**: 277-287.

Timms, N., Windle, C., Polyakova, A., Ault, J., Trinh, C., Pearson, A., Nelson, A. & Berry, A. (2013) Structural insights into the recovery of aldolase activity in N-acetylneuraminic acid lyase by replacement of the catalytically active lysine with gamma-thialysine by using a chemical mutagenesis strategy. *ChemBioChem* **14**: 474-481.

Yuzugullu, Y., Trinh, C., Fairhurst, L., Ogel, Z., McPherson, M. & Pearson, A. (2013) Investigating the active centre of the *Scytalidium thermophilum* catalase. *Acta Crystallogr. F Struct. Biol. Commun.* **69**: 369-375.

Yuzugullu, Y., Trinh, C.H., Smith, M.A., Pearson, A.R., Phillips, S.E.V., Sutay Kocabas, D., Bakir, U., Ogel, Z.B., & McPherson, M.J. (2013) Crystal structure, recombinant expression

and mutagenesis studies of the bifunctional catalase-phenol oxidase from *Scytalidium thermophilum*. *Acta Crystallogr. D Biol. Crystallogr.* **69**: 398-408.

Funding
This work was supported by the Wellcome Trust PhD Programme "The Molecular Basis of Biological Mechanisms", the EPSRC Dynamic Structural Science Consortium and the BBSRC.

Collaborators
Leeds: G. Beddard
External: R. Owen (Diamond Light Source), P. Raithby (University of Bath), J. Evans (University of Southhampton), E. Snell (Hauptmann Woodward Medical Research Institute and SUNY Buffalo), D. Miller (Max Planck Research Department at the University of Hamburg).

Investigating how mutations in cardiac myosin cause heart and skeletal muscle disease

Kathryn White, Katarzyna Makowska, Marcin Wolny, Matthew Batchelor, Francine Parker, Adriana Klyszejko, Ruth Hughes and Michelle Peckham

Introduction

In skeletal and cardiac muscles, myosin is organised into thick filaments in muscle sarcomeres in a highly precise fashion. Each thick filament is 1.6μm long and contains exactly 296 molecules of myosin. Building the almost crystalline structure of a muscle sarcomere is key to ensure that each sarcomere generates the same amount of force, and that the forces sum along the muscle to generate contraction. Once the sarcomere is built, the turnover rate of sarcomeric proteins is quite slow. The half-life of myosin in the heart is about 15 days. This raises the intriguing question as to how new myosin molecules are exchanged into thick filaments while the heart is beating.

The myosin molecule (Figure 1, top) consists of two heavy chains, two essential light chains and two regulatory light chains. The heavy chain forms a coiled coil and this C-terminal portion both dimerises the molecule, and is the part of the molecule that assembles into filaments. Of the 400 or so different mutations have been described for β-cardiac myosin heavy chain that cause heart disease, 60% are in the motor domain (Figure 1, bottom) and it is likely that these mutations affect the ability of the myosin to generate force during contraction, resulting in heart failure. However, 20% of the mutations are in the coiled-coiled tail and it is unclear how these mutations might result in heart disease.

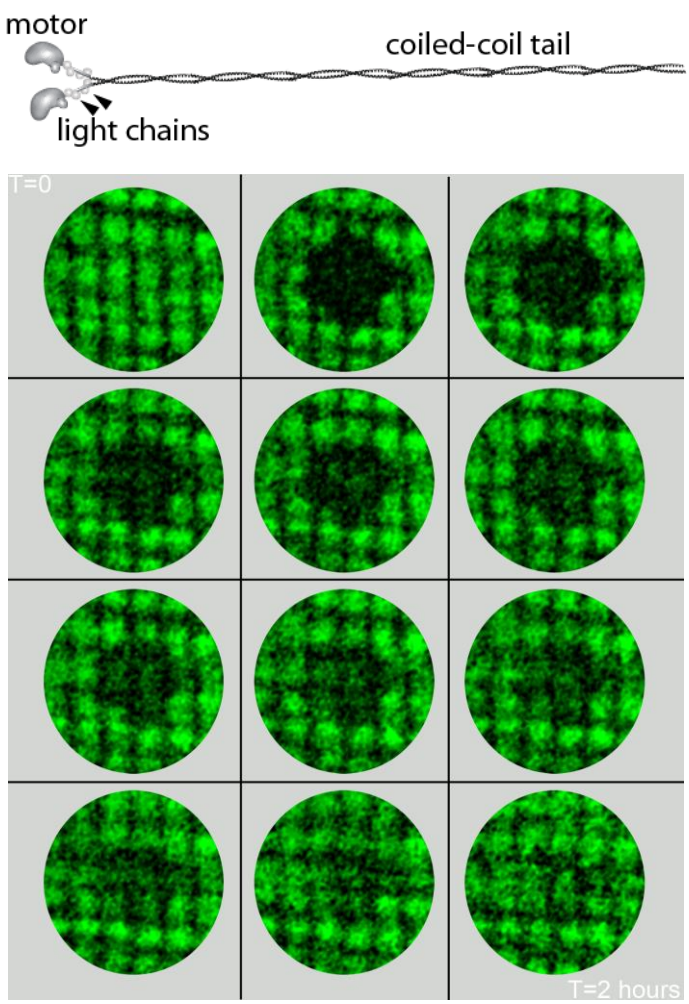

Figure 1: (top) the myosin molecule. **(bottom)** the FRAP experiments to investigate the rate of myosin exchange into the thick filaments in muscle sarcomeres, showing that fluorescence takes about 2 hours to recover.

Results

To try to understand why mutations in the coiled-coil tail cause heart disease, we investigated several of these mutations using both cellular and in vitro approaches. We found that these mutations have effects on the local coiled-coil structure by investigating the secondary structure of peptides with, and without the mutations, using circular dichroism. We expressed eGFP-tagged β-cardiac myosin heavy chain in adult rat cardiomyocytes, and found that the

mutations that had the strongest effects on secondary structure resulted in higher levels of myosin aggregation in cells, suggesting that effects on secondary structure lead to defects in myosin incorporation into thick filaments. We also used fluorescence recovery after photobleaching (FRAP) to find out how quickly myosin exchanges into thick filaments, and discovered that this is quite slow, with a half time of 30 minutes. The most severe mutation, N1327K had a significantly higher rate of exchange.

Altogether then, our results provided some new insight into how mutations in the filament forming tail result in heart disease, suggesting that these mutations affect the structure of the tail of the molecule, and thereby influence its ability to incorporate into thick filaments, which would in turn compromise the force output of the cardiomyocytes.

Other projects:

We are following up on this work to investigate why mutations in the tail of myosins lead to skeletal muscle disease (MRC funded). We are additionally continuing to investigate myosin regulation (Wellcome Trust funded), the roles of myosins in metastasis (CRUK funded), the structure and function of single alpha helical domains found in myosins and other proteins (BBSRC funded), Tuba8 (Wellcome Trust funded) and developing our super-resolution microscopy (MRC Next Generation funded).

Publications

Riches, K., Franklin, L., Maqbool, A., Peckham, M., Adams, M., Bond, J. Warburton, P., Feric, N., Koschinsky, M., O'Regan, D., Ball, S., Turner, N. & Porter, K. (2013) Apolipoprotein(a) acts as a chemorepellent to human vascular smooth muscle cells via integrin alphabeta3 and RhoA/ROCK-mediated mechanisms. *Int. J. Biochem. Cell Biol.* **45**: 1776-83

Sevdali, M., Kumar, V., Peckham, M. & Sparrow, J. (2013) Human congenital myopathy actin mutants cause myopathy and alter Z-disc structure in drosophila flight muscle. *Neuromuscul. Disord.* **23**: 243-255.

Stones, R., Benoist, D., Peckham, M. & White, E. (2013) Microtubule proliferation in right ventricular myocytes of rats with monocrotaline-induced pulmonary hypertension. *J. Mol. Cell. Cardiol.* **56**: 91-96.

Wolny, M., Colegrave, M., Colman, L., White, E., Knight, P. & Peckham, M. (2013) Cardiomyopathy mutations in the tail of beta-cardiac myosin modify the coiled-coil structure and affect integration into thick filaments in muscle sarcomeres in adult cardiomyocytes. *J. Biol. Chem.* **288**: 31952-31962.

Funding

This work was funded by the YCR, CRUK, BBSRC, the Wellcome Trust and MRC.

In vitro studies of outer membrane protein assembly

Bob Schiffrin, Lindsay McMorran, David Brockwell and Sheena Radford

Introduction

The outer membranes (OM) of Gram negative bacteria perform numerous essential and diverse functions. These functions are mediated by β-barrel outer membrane proteins (OMPs) which are found exclusively in the OM of bacteria, mitochondria and chloroplasts. In bacteria, OMP biogenesis begins with their synthesis on cytosolic ribosomes. These hydrophobic, aggregation-prone proteins must then be translocated across the inner membrane and chaperoned across the periplasm, before their final folding and insertion into the OM. While OMPs can fold spontaneously into lipid membranes, this process is too slow to be biologically relevant so a dedicated folding catalyst is required at the OM. This role is carried out by the β-barrel Assembly Machinery (BAM) complex, a large heterooligomeric complex. BAM is an excellent potential antibiotic target given that it is essential, surface located and widely conserved across Gram negative species. Our work aims to gain insight into OMP assembly by recapitulating aspects of the pathway using purified components. Here, building on previous work examining the folding and stability of the model OMP PagP, data are presented on the interactions of PagP with the periplasmic chaperones Skp and SurA.

Results

We developed an *in vitro* assay to study the kinetics of chaperone-mediated folding of the model OMP PagP. From an unfolded state in 10 M urea PagP can be diluted rapidly into folding conditions in the presence of synthetic liposomes, and the folding rate measured spectroscopically by monitoring changes in the intrinsic fluorescence of PagP (Figure 1).

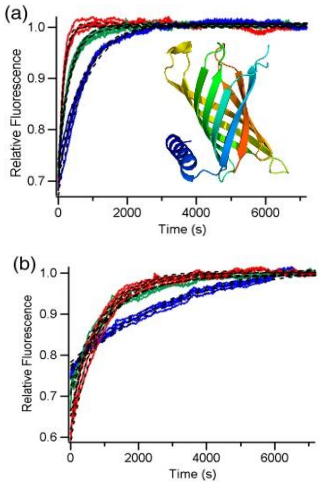

Figure 1: spectroscopic measurement of PagP folding into zwitterionic and negatively charged liposomes. PagP folding monitored by intrinsic fluorescence in the presence of 2, 3 and 4 M urea (blue, green and red traces respectively) (a) *di*$C_{12:0}$PC zwitterionic liposomes. (b) 80:20 *di*$C_{12:0}$PC:*di*$C_{12:0}$PG negatively charged liposomes. Traces are normalised to their maximum fluorescence signal and fits to a single exponential are shown by black dashed lines. All measurements carried out in 50 mM glycine-NaOH, pH 9.5 at 37 °C. Insert: crystal structure of PagP (PDB: 36P6).

The kinetics of PagP folding into both zwitterionic *di*$C_{12:0}$PC (1,2-dilauroyl-sn-glycero-3-phosphocholine) liposomes and negatively charged 80:20 *di*$C_{12:0}$PC: *di*$C_{12:0}$PG[1,2-dilauroyl-sn-glycero-3-phospho-(1′-rac-glycerol)] liposomes were investigated, both with and without pre-incubation with the periplasmic chaperones, SurA and Skp. The results show that pre-incubation of PagP with a three-fold molar excess of SurA made no difference to the rate constant of PagP folding into either neutral or negatively charged liposomes. Further, SDS-PAGE analysis of PagP samples allowed to fold overnight in the presence of a six-fold molar excess of SurA showed no change in final folding yield, and a PagP-SurA complex was not observed by analytical gel filtration. Therefore, despite the proposed role of SurA as the major periplasmic chaperone, under the conditions employed, no evidence of a SurA-PagP interaction could be detected.

In contrast, Skp was found to affect the observed rate of PagP folding dramatically, in a manner dependent on the composition of the membrane and the ionic strength of the buffer (Fig 2). After pre-incubation with a two-fold molar excess of Skp trimers, PagP folding into zwitterionic liposomes was slowed so as to be undetectable in a 2h time course. However, a ~9-fold increase in the folding rate was observed when Skp-PagP was added to negatively charged liposomes. Addition of NaCl to the folding reactions ablated the inhibition of folding in neutral liposomes, and reduced 3-fold the increase in folding rate into negatively charged liposomes. These data suggest that electrostatic interactions play an important role in Skp-assisted substrate delivery to the membrane. Skp is a very basic protein with a jellyfish-like architecture around a central hydrophobic cavity. The tips of the 'tentacles' are rich in basic residues which likely assist in vitro PagP delivery to negatively charged liposomes (Fig 2). Additionally, Pag-Skp complexes could be detected by analytical gel filtration, and Skp was able to prevent the aggregation of the aggregation-prone His-tagged PagP. Taken together the data support the hypothesis that Skp acts as a holdase, and that electrostatic interactions are important for its function. The contrasting results for Skp and SurA are consistent with the view that these chaperones act by distinct mechanisms in partially redundant parallel chaperone pathways.

Current work is now continuing to examine the role and interactions of folding factors involved in OMP assembly with additional model OMPs. We are expanding the range of folding factors examined to include members of the BAM complex. We hope to provide new insights into the molecular mechanism of the BAM complex, chacterise its interactions with OMPs and periplasmic chaperones, and assess how BAM modulates the OMP folding pathway.

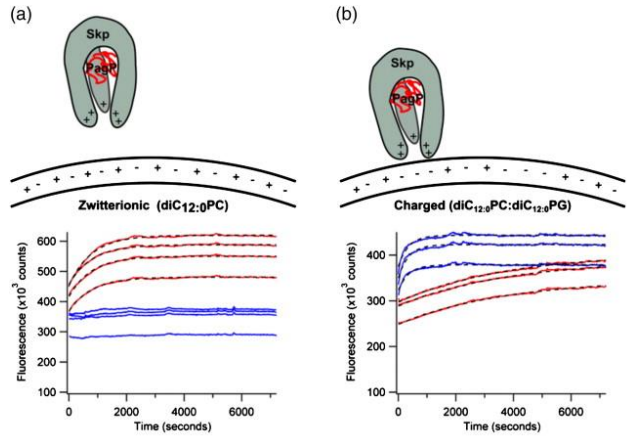

Figure 2: electrostatic interactions are important for *in vitro* Skp-mediated PagP folding. Kinetic traces of PagP folding into (a) *di*$C_{12:0}$PC and (b) 80:20 *di*$C_{12:0}$PC:*di*$C_{12:0}$PG liposomes in the presence (blue lines) or absence (red lines) of a two-fold molar excess of Skp trimers. Fits of the data to a single exponential function are shown as black dashed lines.

Publications

McMorran, L., Bartlett, A., Huysmans, G., Radford, S. & Brockwell, D. (2013) Dissecting the effects of periplasmic chaperones on the *in vitro* folding of the outer membrane protein PagP. *J. Mol. Biol.* **425**: 3178-3191.

Funding

This work was funded by the BBSRC.

Mechanistic insights into the material and cytotoxic properties of amyloid fibril polymorphs

Claire Sarell, Tania Sheynis, Lucy Woods, Kevin Tipping, Sophia Goodchild, Eric Hewitt, Peter Stockley, Alison Ashcroft and Sheena Radford

Introduction

Amyloid disorders represent a class of protein misfolding diseases characterized by the formation and deposition of structurally defined, filamentous aggregates at the site of tissue degeneration. Amyloid fibrils are associated with a wide variety of human diseases, including the neurodegenerative disorders Alzheimer's and Parkinson's disease, and systemic amyloidoses, such as familial amyloid neuropathy. Despite their prevalence, the mechanisms of toxicity associated with this breadth of diseases remain to be elucidated.

We aim to shed light on aspects of amyloid diseases using the well-characterised model protein β_2m and the N-terminally truncated variant β_2m ΔN6. These proteins aggregate into amyloid fibrils in patients undergoing long-term haemodialysis treatment and are also associated with familial forms of amyloidosis. This report details our attempts to understand the mechanisms that underlie amyloid fibril-mediated membrane disruption, to investigate the biophysical properties of hetero-polymeric fibril assemblies and elucidate the mechanism of amyloid fibril fragmentation.

Expanding the repertoire of amyloid polymorphs by co-aggregation of related precursor proteins

Polymeric amyloid assemblies are becoming of increasing interest within the amyloid field, most notably due to *in vivo* fibrils being readily composed of an ensemble of related precursor sequences as opposed to a single polypeptide chain. In this study, the biophysical properties of homopolymeric β_2m and ΔN6 fibrils were compared with fibrils composed of both proteins. Comparison of the two homopolymeric fibril structures using MAS-NMR reveals significant differences in the amino acid side-chain packing within the fibrillar cores, suggesting a reduction in side-chain dynamics within ΔN6 fibrils (Figure 1). In addition, analysis of proteolytic fragments using ESI-MS reveals that fibrils formed of *wt* β_2m exhibit an extended fibril core as compared with ΔN6 fibrils. Analysis of heteropolymeric fibrils revealed a digest pattern most similar to that of the ΔN6 homopolymer. Nonetheless, spectroscopic analysis indicated distinct tryptophan fluorescence signatures, surface hydrophobicity patterns and thermodynamic stabilities for the heteropolymeric fibrils, highlighting how co-aggregation of related precursors can result in a polymorphic assembly with properties distinct from both of their homopolymeric counterparts.

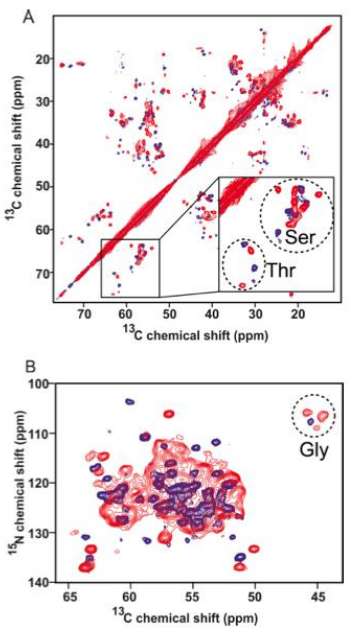

Figure 1: MAS-NMR spectra of uniformly ^{13}C,^{15}N-labelled β_2m (blue) and ΔN6 (red) fibrils. A, shown are one-bond ^{13}C-^{13}C correlations from a RFDR experiment. B, shown are backbone N_α-C_α correlations obtained with ZF TEDOR.

Predicting amyloid behavior using an imaging and systems modelling approach

Understanding the complex dynamics and nano-scale properties of amyloid fibrils are key prerequisites for the design of therapeutic strategies for amyloid disease

intervention and for developing technological applications aimed at utilizing their favourable material properties. By combining a generic mathematical framework and a single particle image analysis method derived from atomic force microscopy imaging, we developed an approach capable of resolving fragmentation time dependent fibril concentrations and length distributions. Being able to calculate these parameters enables one to predict fibril elongation rates, post-extension fibril concentrations and length distributions, as well as the length and position dependent fibril fragmentation rate from complex polymeric solutions. These predictions were validated to a high degree of accuracy from experimental data derived from β_2m amyloid fibrils. The approach developed can be applied to any amyloidogenic system and should provide a useful tool to characterize the nano-mechanical properties of a multitude of fibrillar assemblies.

Small molecule modulators of amyloid assembly interfere with fibril - membrane interactions

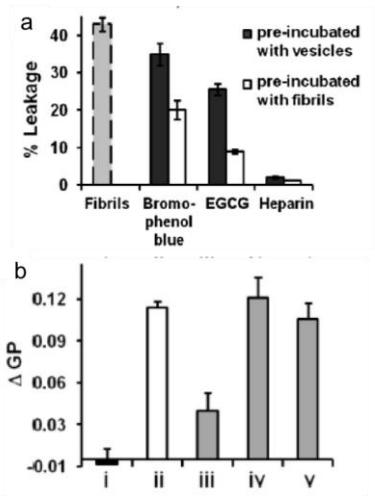

Figure 2: the effect of polyphenols and GAGs on fibril mediated membrane disruption and bilayer fluidity. A The amplitude of dye release in the presence and absence of aggregation modulators. B Laurdan emission shift within vesicles in the presence of β_2m monomer(i), fibrils (ii) and fibrils with bromophenol blue (iii), full length heparin (iv) and LMW heparin (v).

Therapeutic strategies targeted towards amyloid disease have focused on ameliorating the aggregation of protein into oligomeric species that are most commonly accepted as the major cytotoxic entity. However, accumulating evidence suggests that amyloid fibrils may also exhibit an innate cytotoxic capacity. In this study, the effect of glycosaminoglycans (GAGs) and polyphenols on fibril-mediated membrane disruption were investigated using a range of biophysical and imaging techniques. Of the polyphenols and GAGs tested, all showed a reduction in the amplitude of dye released from synthetic vesicles upon pre-incubation with fibrils. The most potent inhibitor of β_2m fibril-mediated membrane disruption was low molecular weight heparin, which reduced dye release by 95%. Interestingly, a reduction in membrane disruption was achieved by modulating rather than eliminating fibril-membrane association. Although the generic nature of the impact of small molecules upon the cytotoxic potential of fibrils remains to be tested, these findings suggest that an important consideration for the development of therapeutics should include an analysis of the effect of small molecule inhibitors on fibril-mediated toxicity mechanisms.

Publications

Sarell, C., Woods, L., Su, Y., Debelouchina, G., Ashcroft, A., Griffin, R., Stockley, P. & Radford, S. (2013) Expanding the repertoire of amyloid polymorphs by co-polymerization of related protein precursors. *J. Biol. Chem.* **288**: 7327-7337.

Sheynis, T., Friediger, A., Xue, W.-F., Hellewell, A., Tipping, K., Hewitt, E., Radford, S. & Jelinek, R. (2013) Aggregation modulators interfere with membrane interactions of beta(2)-microglobulin fibrils. *Biophys. J.* **105**: 745-755.

Xue, W.-F. & Radford, S. (2013) An imaging and systems modeling approach to fibril breakage enables prediction of amyloid behavior. *Biophys. J.* **105**: 2811-2819.

Funding

This work was funded by a Marie Curie Intra-European Fellowship, The Wellcome Trust, BBSRC, the British Council, MRC and NIH.

Collaborators

External: R. Jelenik (Ben-Gurion University), R. Griffin (Massachusetts Institute of Technology) and W.-F. Xue (University of Kent).

Alteration of the metal ion binding site of RepSTK1

Paola Cruz Flores and Christopher Thomas

Introduction

Rolling-circle replication of small plasmids is initiated by plasmid-encoded Rep proteins. These enzymes have sequence-specific topoisomerase-like nicking-closing activity *in vitro*, with a divalent metal ion such as Mg^{2+} being essential for DNA cleavage and religation. Our studies of the *rep_trans* family of initiator proteins previously showed the intermediate form to have a covalent link between the conserved catalytic tyrosine at one active centre of the dimeric protein and the 5' end of the DNA at the double-stranded origin nick site. Recent successful crystallisation and X-ray diffraction studies have also provided structural data for the N-terminal 269 aa fragment of RepSTK1, the initiator protein encoded by the cryptic plasmid pSTK1 of moderate thermophile *Geobacillus stearothermophilus*. This structure presents the Rep dimer in a doughnut-shaped conformation with conserved residues of the active site accessible from the inner face of the hole.

Crystal soaking experiments with manganese ions suggested the presence of a metal ion coordinated via three previously uncharacterised acidic residues conserved at the *rep_trans* active site (Fig. 1). These residues have therefore been subjected to site-directed mutagenesis to assess their relative importance in the nicking-closing reaction.

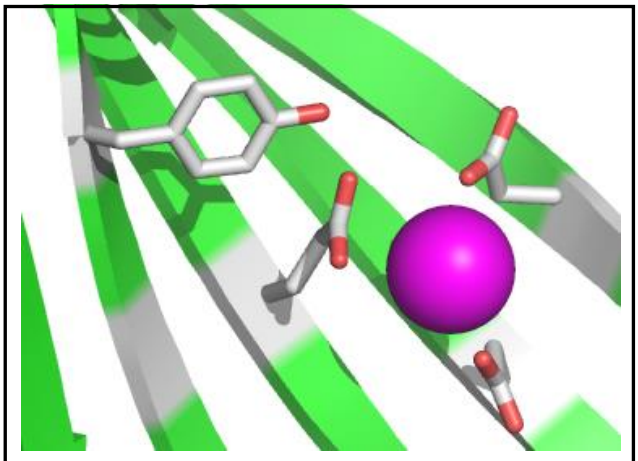

Figure 1: M^{2+} binding location within the active site of RepSTK1. Coordination by the conserved acidic residues adjacent to the catalytic tyrosine is shown.

Results

Substitutions D9A, D116A and E196A have each been constructed in the context of the full (343 aa) RepSTK1, with proteins subsequently purified via affinity tag and heparin sepharose chromatography as normal.

These mutant proteins have been assayed for site-specific topoisomerase activity against a negatively-supercoiled substrate containing the pSTK1 origin of replication, with products being separated by agarose gel electrophoresis in the presence of ethidium bromide (Fig. 2). In comparison with the wild-type protein, mutant D9A is seen to retain partial activity but both D116A and E196A appear inactive. Similar results were obtained in an oligonucleotide cleavage assay (data not shown).

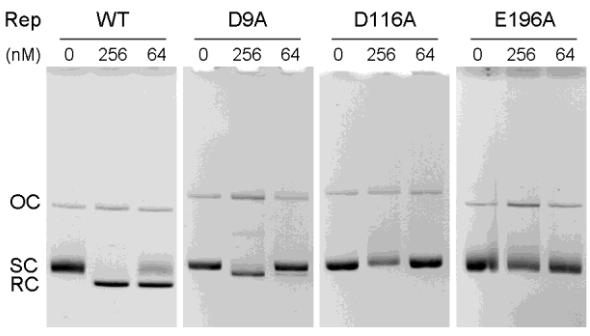

Figure 2: sample topoisomerase data. SC, negatively-supercoiled substrate; OC, nicked open-circled intermediate; RC, relaxed covalently-closed product.

Implications

The *rep_trans* motif is found within both plasmid replication initiator proteins and relaxases responsible for mobilisation of Tn916-like conjugative transposons. It is distinct from the *Hu*

H-family motifs in both sequence and structural organisation, but it appears that the role of both motifs is to present the essential divalent metal ion at the active site adjacent to the catalytic tyrosine, suitably spaced to coordinate the phosphodiester bond at the cleavage site of the incoming DNA substrate. This is an example of the convergent evolution of such sites; it is of note that the TOPRIM domain found within type IA and type II topoisomerases uses a further distinct arrangement of residues to achieve the same result.

Our current goals are now to determine the orientation of DNA at the active site, examine the mechanism by which co-ordination via Mg^{2+} assists catalysis, and investigate how encircling of DNA by the Rep protein through the central hole may assist in the termination of replication.

Publications

Carr, S., Mecia, L., Phillips, S. & Thomas, C. (2013) Identification, characterization and preliminary X-ray diffraction analysis of the rolling-circle replication initiator protein from plasmid pSTK1. *Acta Crystallogr. Sect. F Struct. Biol. Cryst. Commun.* **69**: 1123-1126.

DNA secondary structure imaged by AFM

Sergio Santos, Oliver Chammas, Daniel Billingsley, William Bonass and Neil Thomson

Introduction

The atomic force microscope (AFM) is a high resolution surface profilometer that uses a cantilever probe as a force sensor to feel the top surface of a sample. Since it measures forces, it is versatile and can image all kinds of samples, including biological molecules and materials. The integrated sharp tip at the end of the probe has a radius of curvature on the order of 10 nanometres or less, the absolute size of which affects the ultimate resolution. Probes are made in commercial batch fabrication, micro-machining techniques and in the last decade, the sharpness and reliability of the tips has improved. However, since the AFM operates in near contact or continuous contact with a surface, the tip may change in physical size or chemical state, due to wearing or contamination. Preservation of the sharpness of the tip is required to maximise resolution along with a feedback control mechanism to "feel" the sample surface without damage to sample or tip.

Amplitude modulation AFM

AFM is often run in a dynamic imaging mode, whereby the cantilever is vibrated, typically at kHz to MHz frequencies. The intermittent contact that the tip has with the sample in the normal direction eliminates shearing forces that are particularly damaging for biological specimens. In dynamic AFM, the presence of the surface is detected because changes in the tip-sample potential modulate both the amplitude and frequency of the cantilever oscillation.

In conventional amplitude modulation (AM) AFM, the amplitude of the cantilever is detected and used as the feedback control mechanism to try and fix the amount of energy dissipated by the tip per vibration cycle as the tip taps across the surface. When the tip is periodically entering the repulsive part of the tip-sample potential this technique has become known as tapping mode.

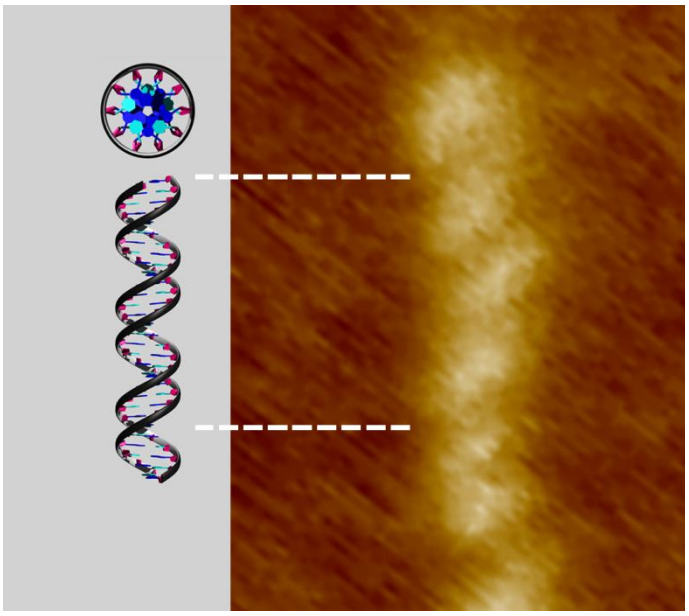

Figure 1: SASS mode topographical image of six helical turns of B-form dsDNA taken in ambient conditions on a mica support surface showing the characteristic right-handed pitch and the major groove.

SASS mode

We recently introduced a new way of operating AM AFM called small amplitude small set-point (SASS) mode. Generally, if the cantilever has a smaller amplitude there is less energy stored in it and so the propensity of the tip to deform or damage the sample is reduced. Tapping mode has been a game changer for elimination of shearing forces, enabling reproducible imaging of biological samples. Typically, however, the sample is addressed with too much energy and the tip becomes blunt through wearing processes. This limits the resolution that is achievable, particularly on individual biomolecules such as DNA.

Conventional tapping mode imaging is operated as follows. First, an appropriate free amplitude of the AFM cantilever off the surface is excited. Secondly, the tip is engaged to the surface with a given reduction in the amplitude (typically 5 to 30%) used to topographically track the surface. Another downside of this approach is that the minimum distance of approach of the AFM tip to the surface is determined by the percent reduction in the free amplitude regardless of the interaction causing this reduction. In AM, the frequency of the cantilever is free to shift in response to the conservative force interactions between tip and surface, which at a set drive frequency of the cantilever, can cause the force sensing cantilever to halt at a position where the imaging tip is on average not close enough to the sample surface to optimise resolution (see Astbury Report, Thomson, 2012). SASS mode overcomes this limitation by first engaging the tip to the surface with the minimal excitation amplitude possible. Second, the excitation of the cantilever is increased until a stable image is formed. By putting the tip in close proximity to the sample surface with an initial small amplitude, means that the tip will be on average closer to the sample surface in SASS than conventional tapping mode.

The right-handed double helix

Using SASS imaging mode we have successfully imaged portions of the double helix of double-stranded DNA. Figure 1 was taken in ambient air conditions and reveals the right-handed DNA double helix with the major groove visible. Linear DNA molecules are deposited on a mica support surface. Mica is a very hydrophilic mineral which under ambient conditions retains nanometre thick water layers on the surface, sufficient to keep the DNA in a hydrated B-form.

Publications

Santos, S., Barcons, V., Christenson, H., Billingsley, D., Bonass, W., Font, J. & Thomson, N. (2013) Stability, resolution, and ultra-low wear amplitude modulation atomic force microscopy of DNA: small amplitude small set-point imaging. *Appl. Phys. Lett.* **103:** 063702.

Funding

This work was funded by the BBSRC Doctoral Training Grant and a CASE award from Asylum Research Corporation and the EPSRC through Doctoral Training Centres.

Studies of the troponin complex in relaxed muscle thin filaments

Shixin Yang, Lucian Barbu-Tudoran, Marek Orzechowski, Roger Craig,
William Lehman and John Trinick

Introduction

Muscle force results from a large shape change in the heads of the myosin whilst attached to actin in thin filaments. In vertebrate striated muscle contraction is regulated by the troponin/tropomyosin complex on thin filaments. Calcium released from the sarcoplasmic reticulum in response to an action potential binds to troponin; this changes shape to move tropomyosin, revealing binding sites for myosin on actin. Relaxation is the reverse of this process. Troponin consists of three subunits, TnT, TnI and TnC, but although there are partial crystal structures of the complex, details of its shape changes during regulation are not known. This is because it tends to detach from thin filaments and because of problems posed for image processing. We have obtained an improved thin filament preparation from heart and studied it by electron microscopy, using a new image processing procedure to make 3D models. Our models reveal troponin on thin filaments with considerably improved detail.

Results

Pig heart thin filaments were studied by negative stain electron microscopy. Single particle processing to make 3D models combines many particles imaged from different angles. Processing of thin filaments to reveal troponin is complicated by there being only one troponin for every seven actin subunits and by troponins located above and below filaments being obscured. A new method developed in Leeds straightens thin filaments and then searches for troponin in Fourier space. Once located, troponin particles, together with associated troponin and actin, were windowed out, classified into homogeneous groups, averaged, and combined in 3D reconstruction. At the 2.5 nm resolution achieved, troponin was considerably better defined than in published reconstructions. Troponin density closely

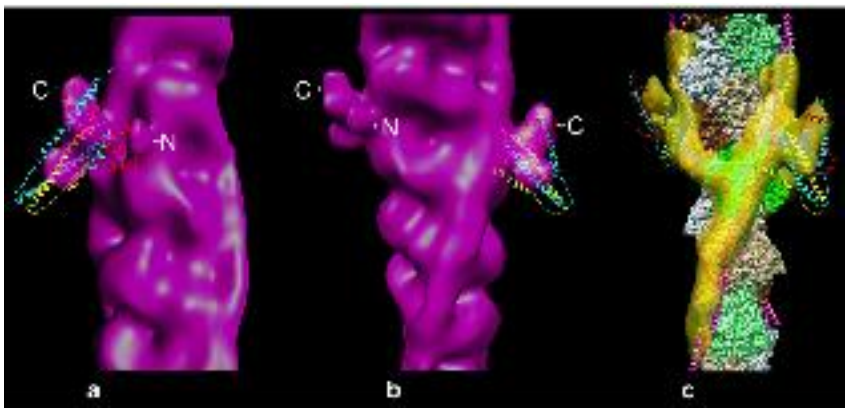

Figure 1: fitting troponin core-domain crystal structures to the 3D reconstruction. (**a** and **b**) Two orthogonal views of the thin filament with the low Ca^{2+} core domain fitted into corresponding densities, showing back and front views of the fitting. The core domain is shown in ribbon view with TnI, cyan, TnT, yellow, and TnC red. Note the ~50° orientation of the TnIT helix of the troponin core domain relative to the filament long axis. **(c)** In addition to the core domain, the atomic model of actin-tropomyosin was fitted to the reconstruction and substituted for corresponding densities shown in (b). Troponin difference densities made translucent are superposed. The tropomyosin structure is shown in ribbon view and actin subunits in space-filling view, with one actin subunit lying under the putative TnI mobile domain.

resembled the shape of partial crystal structures, facilitating detailed interpretation of models. The orientation of TnT and the troponin core domain established polarity. Density attributable to the TnI mobile regulatory domain was positioned where it could hold

tropomyosin in its blocking position on actin, suggesting the basis of thin filament regulation of contraction.

Publications

Song, C., Papachristos, K., Rawson, S., Huss, M., Wieczorek, H., Paci, E., Trinick, J., Harrison, M. & Muench, S. (2013) Flexibility within the rotor and stators of the vacuolar H^+-ATPase. *PLoS One* **8:** e82207.

Muench, S., Scheres, S.,Huss, M., Phillips, C., Vitavska, O., Wieczorek, H., Trinick, J. **&** Harrison, M. (2013) Subunit positioning and stator filament stiffness in regulation and power transmission in the V1 motor of the *Manduca sexta* V-ATPase. *J. Mol. Biol.* **426:** 286-300.

Funding

Supported by the British Heart Foundation and NIH (USA).

Collaborators

External: H. White (Eastern Virginia Medical School, Norfolk, VA., USA) and K. and D. Taylor (Florida State University, Talahassee, USA).

Structure and dynamics of hexameric helicases – from atomic details to single molecule biophysics

Adam Cawte and Roman Tuma

Introduction

A key event in the life-cycle of numerous complex viruses is the packaging of their genome into preformed empty capsids. Double-stranded RNA bacteriophages of the *Cystoviridae* family utilize P4 hexamer to translocate single-stranded RNA genomic precursors into a procapsid at the expense of ATP hydrolysis. While the ring-like hexamer is part of the icosahedral procapsid it retains ATPase and RNA-specific helicase activity in the absence of other viral proteins.

Results

We have determined the crystal structures of three P4 proteins from cystoviruses ϕ6, ϕ8 and ϕ13 and compared them with the previously determined structures of ϕ12 P4. The comparison indicates that these proteins are structurally conserved and constitute a distinct, RNA-specific subfamily of RecA-type helicase superfamily 4. ATPase activity of ϕ8P4 is tightly coupled to RNA translocation and the new structures together with hydrogen-deuterium exchange identified a dynamic C-terminal domain that may mediate RNA loading via ring opening mechanism. (Figure 1A). To further shed light on the mechanism of the tight coupling between the ATPase and RNA translocation we used the crystal structure of ϕ8P4 to label the hexamer with a donor-acceptor pair for Forster resonance energy transfer (FRET). Using single molecule fluorescence a high FRET efficiency between dyes on neighbouring subunits was observed (Figure 1B) and allows us to monitor the ring opening and the conformational changes of the C-terminus.

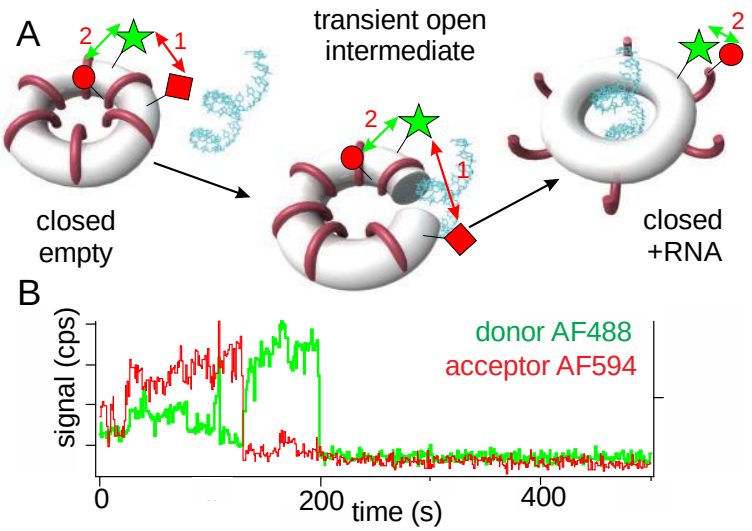

Figure 1: (A) A schematic of ring opening that mediates RNA (cyan) loading into the central channel. The C-termini (magenta) initially occupy the central channel and get expelled during loading. A labelling with donor (AlexaFluor 488, green star) and acceptor (AlexaFluor 594, red dot) dyes on neighbouring subunits is shown. **(B)** A representative single molecule fluorescence trace recorded using Total Internal Reflection Microscopy from surface-immobilised hexamers labelled with the donor-acceptor pair.

Publications

El Omari, K., Meier, C., Kainov, D., Sutton, G., Grimes, J., Poranen, M., Bamford, D., Tuma, R., Stuart, D. & Mancini, E. (2013) Tracking in atomic detail the functional specializations in viral reca helicases that occur during evolution. *Nucleic Acids Res.* **41**: 9396-9410.

Funding
This collaboration was funded by The Royal Society, MRC, Academy of Finland, The Wellcome Trust and European Union.

Collaborators
External: K. El Omari, C. Meier, G. Sutton, J. Grimes, D. Stuart, E. Mancini (University of Oxford) and D. Kainov, M. Poranen and D. Bamford (University of Helsinki).

Methods for re-engineering bacterial toxins

Thomas Branson, Martin Fascione, Tom M^{c}Allister, Darren Machin, James Ross, Daniel Williamson, Michael Webb and Bruce Turnbull

Introduction

Cholera toxin interacts with glycolipids on the surface of the cells lining the intestine, and uses this interaction to enable the toxin to cross the cell membrane and initiate a series of events that lead to potentially fatal diarrhoea. The cholera toxin protein is an AB_5 protein (Fig. 1a) comprising a single toxic A-subunit that is threaded through the middle of a doughnut shaped pentamer of B-subunits (Fig. 1b) that are not themselves toxic. We are pursuing a series of projects aimed at understanding the ways in which the B-subunit interacts with intestinal carbohydrates, and how we might redesign the B-subunit protein to make safe delivery systems for transporting therapeutic biomolecules into cells.

Our research continues to focus on new methods for protein modification. We have extended our chemical and enzymatic modification strategies to allow site-specific modification at the N-terminus (by both oxime ligation and sortase ligation), and also the N-terminus of an AB_5 version of the protein (oxime ligation and sortase ligation). We have extended the range of depsipeptide labelling reagents used in this work to include a range of fluorophores, affinity tags and bioorthogonal reactive groups that will allow us to append macromolecule cargos to the delivery vehicles. We have also appended carbohydrates on to a mutant B-subunit and demonstrated that the neoglycoprotein can be used an effective multivalent inhibitor of cholera toxin.

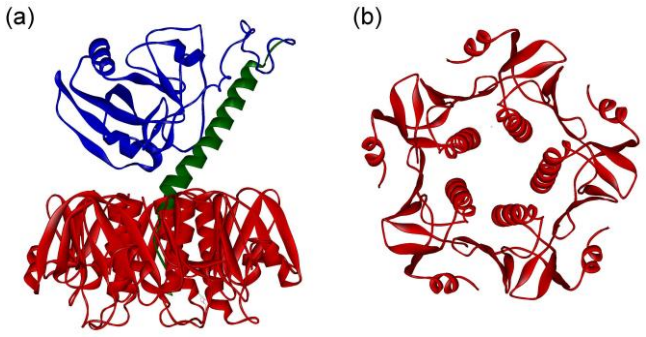

Figure 1: crystal structure of cholera toxin based on 1S5E.pdb: a) holotoxin is an AB_5 protein complex in which a toxic A-subunit (blue) is linked via an extended alpha helix (green) to a pentameric B-subunit (red); b) the doughnut-shaped B-pentamer is responsible for cell adhesion and entry, but is not itself toxic.

Publications

Bernardi, A., Jimenez-Barbero, J., Casnati, A., De Castro, C., Darbre, T., Fieschi, F., Finne, J., Funken, H., Jaeger, K.-E., Lahmann, M., Lindhorst, T., Marradi, M., Messner, P., Molinaro, A., Murphy, P., Nativi, C., Oscarson, S., Penades, S., Peri, F., Pieters, R., Renaudet, O., Reymond, J.-L., Richichi, B., Rojo, J., Sansone, F., Schaeffer, C., Turnbull, W., Velasco-Torrijos, T., Vidal, S., Vincent, S., Wennekes, T., Zuilhof, H. & Imberty, A. (2013) Multivalent glycoconjugates as anti-pathogenic agents. *Chem. Soc.Rev.* **42**: 4709-4727.

Branson, T. & Turnbull, W. (2013) Bacterial toxin inhibitors based on multivalent scaffolds. *Chem. Soc. Rev.* **42**: 4613-4622.

Funding
This work is funded by the Royal Society, EPSRC, the Wellcome Trust, GlaxoSmithKline and the University of Leeds.

Collaborators
External: B. Andrews (GlaxoSmithKline) and A. Daranas and J. Gavín (University of La Laguna, Tenerife).

Identification of the ribonucleoprotein complex required for efficient viral RNA processing in oncogenic herpesviruses

Brian Jackson, Sophie Schumann, Belinda Basquero, Anja Berndt and Adrian Whitehouse

Introduction

Post-transcriptional events which regulate mRNA biogenesis are central to the regulation of gene expression. As a consequence, cells have evolved a 'gene-expression production line' that encompasses the routing of a nascent transcript through multimeric mRNA–protein complexes that mediate its splicing, polyadenylation, nuclear export and translation. Of these events it has become clear that splicing is particularly important for mRNA nuclear export, as recruitment of multiprotein complexes required for mRNA export are bound to mRNA in a splicing dependent manner. Two multiple protein complexes, namely, hTREX and the EJC bind at separate locations on spliced mRNA. hTREX, which comprises Aly, UAP56 and the multiprotein ThoI complex, is recruited exclusively to the 5' end of the first exon, providing 5'-polarity and therefore directionality observed in mRNA export.

However, in contrast to the majority of mammalian genes, analysis of herpesvirus genomes has highlighted that most lytically expressed viral genes lack introns. Herpesviruses replicate in the nucleus of the host mammalian cell, and therefore require their intronless mRNAs to be exported out of the nucleus to allow viral mRNA translation in the cytoplasm. This therefore leads to an intriguing question concerning the mechanism by which the viral intronless mRNAs are exported out of the nucleus in the absence of splicing. To circumvent this problem, and to facilitate viral mRNA export, γ-2 herpes viruses encode the ORF 57 protein. ORF 57 interacts with Aly, binds viral RNA, shuttles between the nucleus and the cytoplasm and promotes the nuclear export of viral mRNA.

Results

We are currently investigating how an intronless viral mRNP is assembled in KSHV and what role ORF57 plays in that process. We have shown that ORF57 interacts with hTREX and is essential for the recruitment of hTREX onto intronless viral mRNA transcripts. Importantly, ORF57 does not recruit the EJC to intronless viral transcripts. Moreover, we are currently determining how ORF 57 recognises the viral mRNA and allows recruitment of hTREX. This is the first system that has distinguished between hTREX and EJC *in vivo* and demonstrates that recruitment of hTREX alone to mRNA transcripts is sufficient for their nuclear export. Therefore, we believe this viral system is an exciting model to further study mRNA export mechanisms. We propose a model for herpesvirus mRNA export, whereby ORF57 mimics splicing in order to recruit the mRNA export machinery to intronless viral mRNAs.

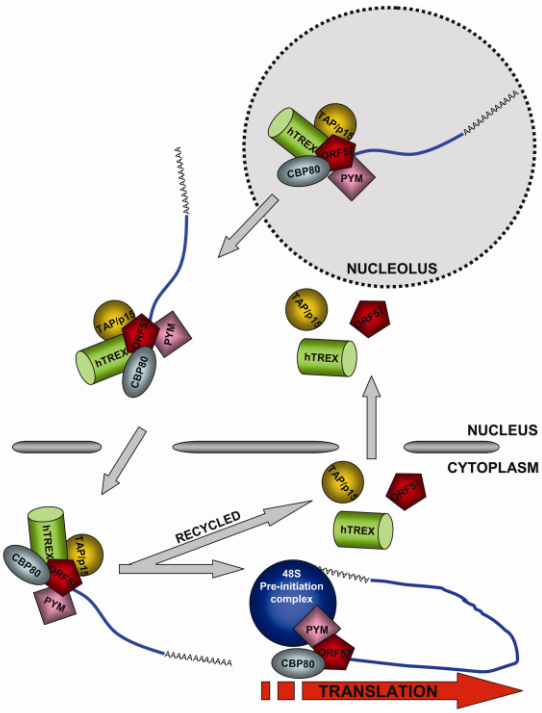

Figure 1: KSHV ORF57 mimics splicing to recruit the necessary nuclear export factors onto viral intronless transcripts and also mimics an EJC to enhance their translation.

We are now determining the structure of the interaction interface at atomic-resolution between ORF57 homologues and the hTREX

proteins, such as Aly, In collaboration with Dr Alexander Golovanov (University of Manchester) and Professor Stuart Wilson (University of Sheffield). This will provide a detailed comparison of the binding interfaces between ORF57 homologues and Aly using solution-state NMR. The regions of HSV ICP27 and HVS ORF57 involved in binding by Aly have been mapped as residues 104-112 and 103-120, respectively. We have identified the pattern of residues critical for Aly recognition, common to both ICP27 and ORF57. The importance of the key amino acid residues within these binding sites was confirmed by site-directed mutagenesis. The functional significance of the ORF57-REF/Aly interaction was also probed using an *ex vivo* cytoplasmic viral mRNA accumulation assay and this revealed that mutants that reduce the protein-protein interaction dramatically decrease the ability of ORF57 to mediate the nuclear export of intronless viral mRNA. Together these data precisely map amino acid residues responsible for the direct interactions between viral adaptors and cellular REF/Aly and provide the first molecular details of how herpes viruses access the cellular mRNA export pathway. Future work will utilise these identified binding interfaces as possible new drug targets, to be used in the future for anti-viral drug design efforts, for the prevention or treatment of KSHV-related malignancies using rational-based drug design approaches.

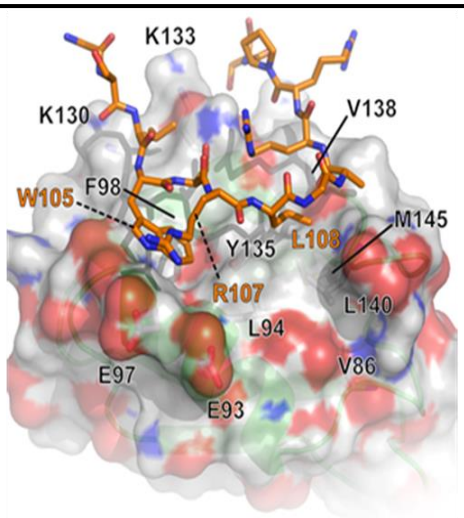

Figure 2: ORF57 homologue (HSV ICP27) recognizes and specifically binds to the surface of the RRM domain of cellular export factor REF/Aly

Publications

Brown, H., Unger, C. & Whitehouse, A. (2013) Potential of herpesvirus saimiri-based vectors to reprogram a somatic Ewing's sarcoma family tumor cell line. *J. Virol.* **87**: 7127-7139.

Emmott, E., Munday, D., Bickerton, E., Britton, P., Rodgers, M., Whitehouse, A., Zhou, E.-M. & Hiscox, J. (2013) The cellular interactome of the coronavirus infectious bronchitis virus nucleocapsid protein and functional implications for virus biology. *J. Virol.* **87**: 9486-9500.

Griffiths, D., Abdul-Sada, H., Knight, L., Jackson, B., Richards, K., Prescott, E., Peach, A., Blair, G., Macdonald, A. & Whitehouse, A. (2013) Merkel cell polyomavirus small t antigen targets the nemo adaptor protein to disrupt inflammatory signaling. *J. Virol.* **87**: 13853-13867.

Funding

Projects in the Whitehouse laboratory are funded by the BBSRC, YCR, AICR, BSF and Wellcome Trust.

Developing inhibitors of protein-protein interactions

Valeria Azzarito, Anna Barnard, George Burslem, Hannah Kyle, Kerya Long, Natasha Murphy, Panchami Prabhakaran, Silvia Rodriguez-Marin, Jennifer Miles, David Yeo, Alison Ashcroft, James Ault, Thomas Edwards, Adam Nelson, Sheena Radford, Stuart Warriner and Andrew Wilson

Introduction

This report summarises our group's efforts to develop inhibitors of protein-protein interactions (PPIs); a key challenge in chemical biology and small molecule drug discovery.

New Methods for the Synthesis of Proteomimetics

α-helices mediate ~ 30% of PPIs; proteomimetics can act as inhibitors of such PPIs by matching the spacial orientation of key binding residues on the native α-helix. Aromatic oligoamides based on two different scaffolds; 3-*O*-alkylated and *N*-alkylated (Figure 1a), have previously been shown to act as inhibitors of the p53/*h*DM2 PPI. To provide rapid access to libraries of these compounds we developed solid-phase syntheses of both the 3-*O*-alkylated and *N*-alkylated helix mimetics (Figure 1b).

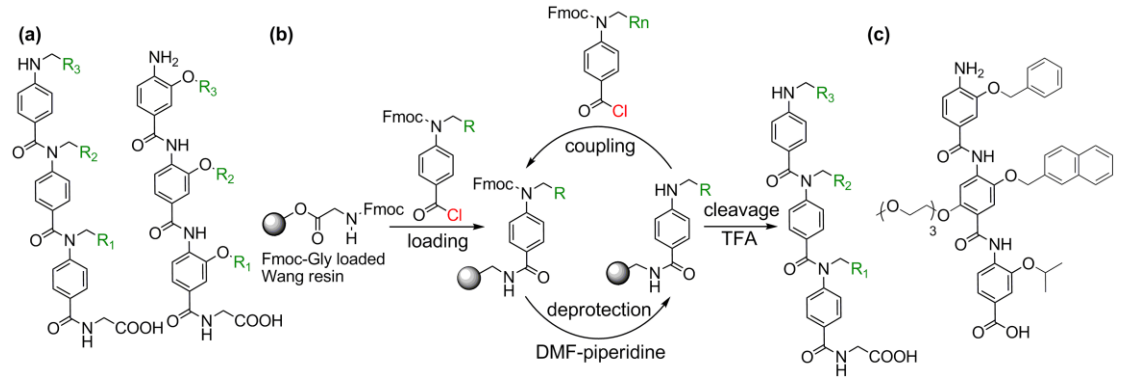

Figure 1: (a) Structures of the *N*- and 3-*O*-alkylated helix-mimetic scaffolds; **(b)** Solid-phase synthesis of the *N*-alkylated scaffold; **(c)** Structure of ethylene glycol functionalised scaffold

Using an automated microwave peptide synthesiser we were able to access over 100 different proteomimetic structures, each produced in around 4 hours. To improve the physical properties of these proteomimetics we also developed a method for introduction of a solubilising group on the non-binding face of the scaffold (Fig 1c). It was found that the ethylene glycol moiety significantly improved aqueous solubility without having any negative impact on the binding affinity of the analogous trimer.

Peptide stapling

Constraining a peptide can promote its biologically active conformation and confer favourable biological properties – this strategy is often termed *"stapling"*. We developed monosubstituted α-alkenyl amino acids as reagents for stapling, which should allow for easier syntheses. Alkenyl amino acid containing peptides based on the BID BH3 sequence were subjected to olefin metathesis to generate stapled peptides (Figure 2) for inhibition of BH3/Bcl-x_L PPIs. The helix stabilising properties were assessed by circular dichroism (Figure 2a), with the stapled peptides exhibiting enhanced helicty. Stapled peptides were shown to inhibit the native PPI in a fluorescence anisotropy competition assay (Figure 2c). This illustrated that monosubstituted alkenylamino acids are a valid replacement for α'α-disubstituted variants commonly used for peptide stapling.

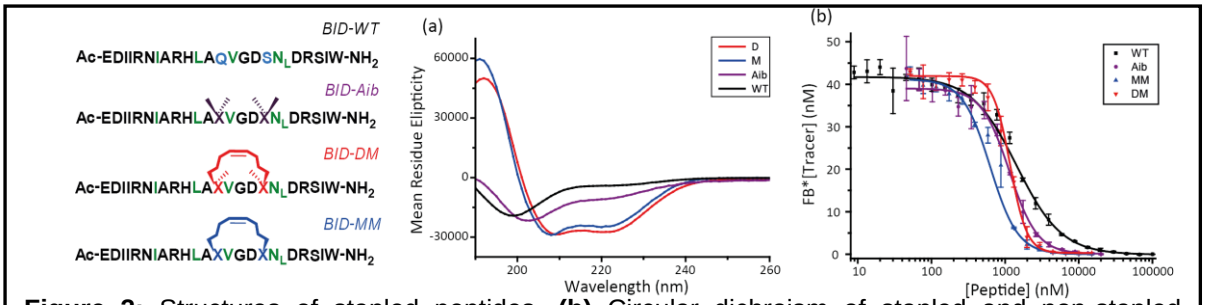

Figure 2: Structures of stapled peptides. **(b)** Circular dichroism of stapled and non-stapled peptides **(c)** Fluorescence anisotropy competition assay of peptides.

Protein Surface Mimetics

We previously illustrated that ruthenium complexes (Figure 3) are capable of selectively binding cytochrome *c* with low nM K_d. One of these complexes significantly and selectively reduces the melting temperature of the protein (as evidenced by CD). IMS-MS demonstrated that **1** alters the distribution of states of cyt *c* at RT. Overall, we were able to show that ruthenium complex **1** changes the conformational properties of the protein through specific binding interactions.

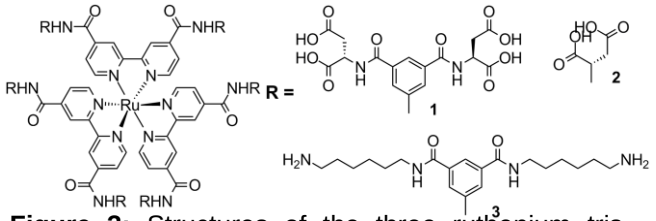

Figure 3: Structures of the three ruthenium tris-bipyridine receptors **1-3**

Publications

Long, K., Edwards, T. & Wilson, A. (2013) Microwave assisted solid phase synthesis of highly functionalized n-alkylated oligobenzamide alpha-helix mimetics. *Bioorg. Med. Chem.* **21**: 4034-4040.

Murphy, N., Prabhakaran, P., Azzarito, V., Plante, J., Hardie, M., Kilner, C., Warriner, S. & Wilson, A. (2013) Solid-phase methodology for synthesis of o-alkylated aromatic oligoamide inhibitors of alpha-helix-mediated proteinprotein interactions. *Chem. Eur. J.* **19**: 5546-5550.

Prabhakaran, P., Barnard, A., Murphy, N., Kilner, C., Edwards, T. & Wilson, A. (2013) Aromatic oligoamide foldamers with a "wet edge" as inhibitors of the -helix-mediated p53-hdm2 protein-protein interaction. *European J. Org. Chem.* 3504-3512.

Wilson, A., Ault, J., Filby, M., Philips, H., Ashcroft, A. & Fletcher, N. (2013) Protein destabilisation by ruthenium(ii) tris-bipyridine based protein-surface mimetics. *Org. Biomol. Chem.* **11**: 2206-2212.

Yeo, D., Warriner, S. & Wilson, A. (2013) Monosubstituted alkenyl amino acids for peptide "stapling". *Chem. Commun.* **49**: 9131-9133.

Funding

This work was funded by the BBSRC, the EPSRC, the Wellcome Trust, Waters UK Ltd., LGC, AZ, GSK, UCB and Medimmune. We thank the BMSS for student travel grants.

Structural analysis of BTB-domain proteins implicated in human cancer

Mark Stead, Simon Connell and Stephanie Wright

Introduction

BTB (*b*ric-a`-brac, *t*ramtrack and *b*road complex) domains are protein-protein interaction domains that are found in transcription factors and in adaptor proteins that recruit substrates for ubiquitination by E3 ligase complexes. Many BTB-domain proteins play roles in development, and several have been implicated in specific human malignancies. Targeting BTB-domain interactions is a potential therapeutic strategy, and our approach is to use X-ray crystal structures as the basis for drug design.

Most BTB domains form highly stable domain-swapped dimers that have been well characterised. The higher-order oligomerisation of several BTB-proteins is important for their biological activity, and understanding the structural basis for these associations has been a focus of our recent work.

Structural basis of high-order oligomerisation of the BTB-domain adaptor, SPOP

SPOP (*s*peckle-type *P*OZ *p*rotein) is a BTB-domain adaptor protein that recruits substrates for ubiquitination by the cullin3-type E3 ligase complex; the high-order oligomerisation of SPOP significantly enhances the efficiency of substrate ubiquitination. SPOP contains a previously characterised N-terminal MATH domain that recruits substrates for ubiquitination, and a central BTB domain that mediates dimerisation and interactions with the cullin3 (Cul3) component of the E3 ligase complex (Figure 1A).

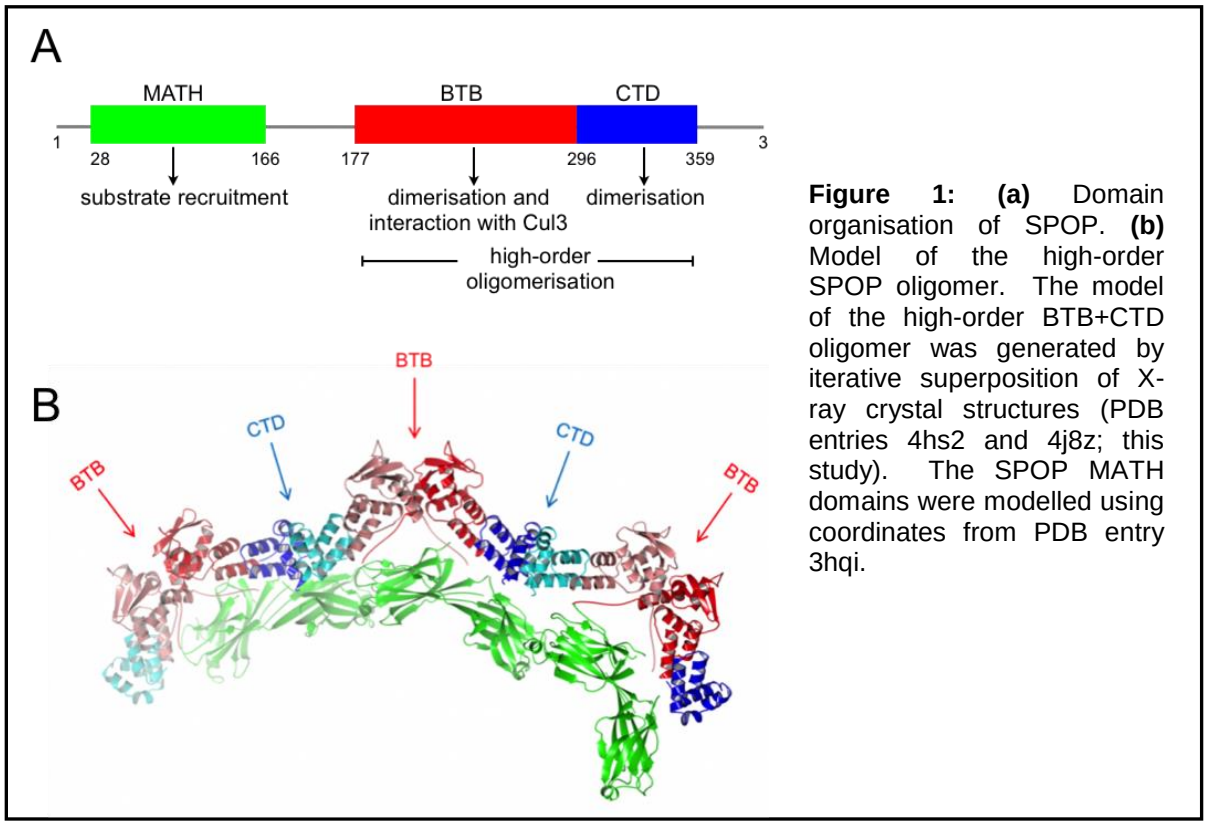

Figure 1: (a) Domain organisation of SPOP. **(b)** Model of the high-order SPOP oligomer. The model of the high-order BTB+CTD oligomer was generated by iterative superposition of X-ray crystal structures (PDB entries 4hs2 and 4j8z; this study). The SPOP MATH domains were modelled using coordinates from PDB entry 3hqi.

We analysed the oligomerisation properties of the SPOP C-terminus and showed that this region contains a previously undescribed dimerisation interface; we termed this region the SPOP C-terminal domain (CTD). We showed that the dimerisation interfaces of the CTD and BTB domains act independently and in tandem to generate high-order SPOP oligomers. We solved the X-ray crystal structure of the SPOP CTD to 1.5Å resolution, and generated a

model of the high-order SPOP; we confirmed this model using atomic force microscopy (Figure 1B). This model provides a mechanistic explanation for the enhancement of substrate ubiquitination by high-order oligomerisation: high-order oligomerisation of SPOP could enhance substrate recruitment by facilitating the cooperative binding of multiple MATH domains to a single substrate molecule, and could also enhance the efficiency of the ubiquitination reaction by bringing multiple E2 conjugating enzymes into proximity of the substrate.

We are currently studying the mechanisms of high-order oligomerisation of other BTB-domain proteins implicated in human cancer with the aim of characterising protein-protein interaction interfaces that would be appropriate for therapeutic targeting.

Publications

Van Geersdaele, L., Stead, M., Harrison, C., Carr, S., Close, H., Rosbrook, G., Connell, S. & Wright, S. (2013) Structural basis of high-order oligomerization of the cullin-3 adaptor Spop. *Acta Crystallogr. D Biol. Crystallogr.* **69**: 1677-1684.

Funding

We thank Yorkshire Cancer Research for funding this work.

A magnetic nanoparticle-enzyme based ultrasensitive diagnostic assay

Yue Zhang, Lei Song, Haiyan Zhang, Yifei Kong, Weili Wang, Oscar Cespedes, Yuan Guo, Philip Quirke and Dejian Zhou

A great healthcare challenge currently facing the society is finding solutions to some of the most devastating diseases, such as cancer, which alone accounts for > 8 million annual deaths worldwide. This requires the development of sensitive, specific and rapid diagnostic tools for earlier cancer diagnosis as well as more effective, targeted anticancer therapeutic strategies. In an attempt to address this challenge, we are developing smart nanoparticles that can offer ultrasensitive biomarker detection for earlier diagnosis, and novel nanomedicine for effective targeted therapeutic treatments.

Results

By combining magnetic nanoparticle (MNP) based rapid homogenous target capture and magnetic separation, together with enzyme-based efficient signal amplification, we have developed a MNP-enzyme based sandwich assay that can be used for ultrasensitive quantitation of unlabelled DNA target down to low fM level. Our assay uses a pair of specific DNA probes, one covalently conjugated to a MNP for target capture and the other linked to an enzyme for signal amplification, to sandwich a DNA target. This forms a MNP-dsDNA-enzyme sandwich that can be easily separated magnetically using an external magnet to convert each bound target into a MNP tagged enzyme. After removing unbound species via washing, enzyme substrate was subsequently added to initiate great signal amplification to achieve high sensitivity. Careful optimization of the MNP surfaces and assay conditions has reduced the background greatly, allowing for sensitive, specific detection of as little as 5 attomole (50 fM in 100 μL) of target DNA. This sensor is robust: it works efficiently in 10% human serum and can discriminate cancer specific single-nucleotide polymorphisms (SNPs) from wild-type non-cancer genes (with a discrimination ratio, DR, of ~3). Furthermore, it can simultaneously quantitate two different DNA targets using two pairs of unique capture-/ signal- DNA probes specific for each DNA target (Figure 1).

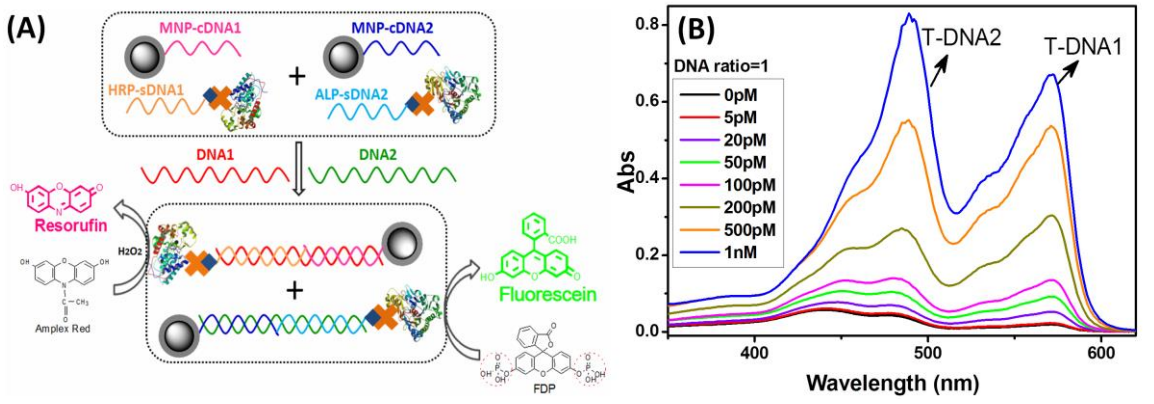

Figure 1: (**a**) Principle of the MNP-enzyme sandwich assay for simultaneous quantitation of two DNA targets. T-DNA1 and T-DNA2 are sandwiched and converted to horseradish peroxidase and alkaline phosphatase catalyzed reactions, respectively. (**b**) The corresponding UV-vis absorption spectra of the assay for simultaneous detection of two different DNA targets.

A SNP DR of ~3 is comparable to most other assays, but may not be suitable for detection of rare cancer mutants in large excess of wild-type targets. To improve the SNP discrimination, we have developed a DNA ligation assay using a pair of biotin and phosphate probes and Tag DNA ligase based specific ligation (Figure 2). When the two probes are fully complementary to the target, they are covalently linked together to produce a biotinylated ligated product, but not those having a single mismatch. After multiple cycles of ligation, the ligated products are

captured with a MNP-cap-DNA for enzymatic signal amplification (Figure 2A). This assay can offer universal greatly improved the DRs between cancer specific SNPs and wild-type target to > 100 fold, and can quantitate rare cancer specific SNPs (KRAS mutations) in large excess of wild-type non-cancer target down to 0.75%, which is significantly more sensitive than current sequencing techniques (~2-20% detection limit).

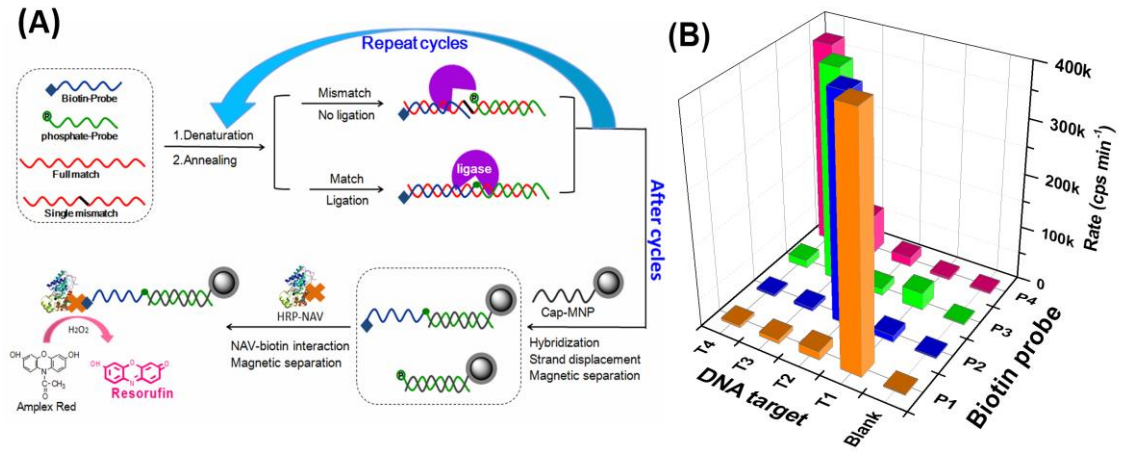

Figure 2: (**a**) Principle of the ligation coupled MNP-enzyme sandwich assay: only when biotin and phosphate probes are fully complementary to the target DNA can lead to covalent ligation, but not single mismatch target, leading to high SNP discrimination. (**b**) General discrimination of perfect match DNAs against all possible SNP mismatches.

Publications

Kong, Y., Chen, J., Gao, F., Brydson, R., Johnson, B., Heath, G., Zhang, Y., Wu, L. & Zhou, D. (2013) Near-infrared fluorescent ribonuclease-a-encapsulated gold nanoclusters: Preparation, characterization, cancer targeting and imaging. *Nanoscale* **5**: 1009-1017.

Song, L., Ho, V., Chen, C., Yang, Z., Liu, D., Chen, R. & Zhou, D. (2013) Efficient, pH-triggered drug delivery using a pH-responsive DNA-conjugated gold nanoparticle. *Adv. Healthc. Mater.* **2**: 275-280.

Zhang, H., Feng, G., Guo, Y. & Zhou, D. (2013) Robust and specific ratiometric biosensing using a copper-free clicked quantum dot-DNA aptamer sensor. *Nanoscale* **5**: 10307-10315.

Zhang, Y., Guo, Y., Quirke, P. & Zhou, D. (2013) Ultrasensitive single-nucleotide polymorphism detection using target-recycled ligation, strand displacement and enzymatic amplification. *Nanoscale* **5**: 5027-5035.

Zhang, Y., Pilapong, C., Guo, Y., Ling, Z., Cespedes, O., Quirke, P. & Zhou, D. (2013) Sensitive, simultaneous quantitation of two unlabeled DNA targets using a magnetic nanoparticle-enzyme sandwich assay. *Anal. Chem.* **85**: 9238-9244.

Funding

This work was supported by the University of Leeds, the Leeds Biomedical Health Research Centre, the Leeds Cancer Research UK Centre and the Wellcome Trust (Grant No: 097354/Z/11/Z).

Collaborators

External: R. Chen (Imperial College London), D. Liu and Z. Yang (Tsinghua University, China).

The relationship between conformational flexibility, landscape roughness, sequence variability and function for Hsp70 molecular chaperones

Anastasia Zhuravleva

Introduction

The family of Hsp70 molecular chaperones is used as a paradigm for allostery in the multidomain protein system: all Hsp70s contain two domains, the N-terminal nucleotide-binding domain (NBD) and the substrate-binding domain (SBD), which is further subdivided into a β-sandwich subdomain (βSBD) and a α-helical domain (αLid). All of Hsp70 functions rely on the ability of the SBD to bind and release protein substrates under the tight nucleotide-dependent control of the NBD. In turn, substrate binding to the SBD regulates the ATP hydrolysis rate of the NBD. Our recent findings (Cell 2012 and PNAS 2011) suggest the detailed structural mechanism of intradomain Hsp70 allostery and identified several allosteric 'hotspots' in Hsp70 that regulates Hsp70 conformation and thus control and find-tune its function (Figure 1).

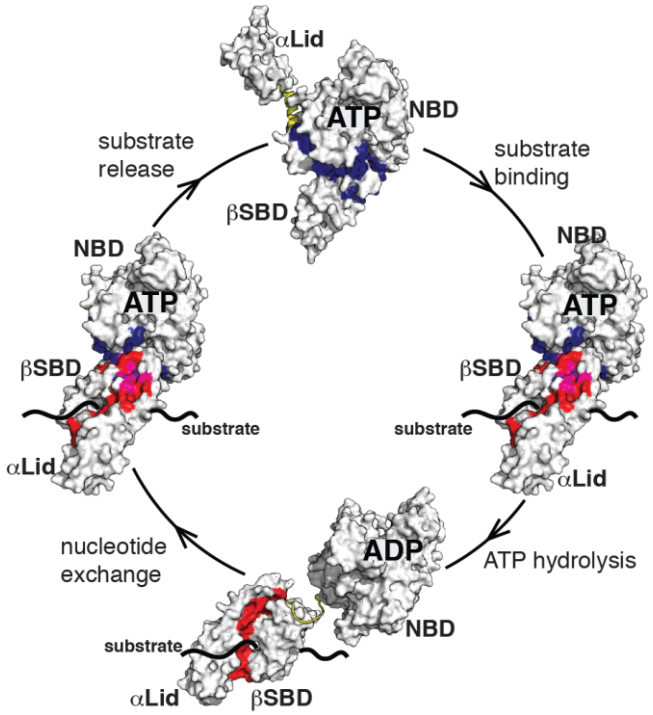

Figure 1: Hsp70 allosteric (functional) cycle. The Hsp70 cycle comprises three distinct conformations; these allosteric changes are reversible, and the resulting cycle of substrate binding/release, nucleotide hydrolysis, which are controlled by nucleotide and substrate binding. The interfaces between the NBD and the β-SBD (blue) and between the β-SBD and the α-helical lid (red; magenta–residues participate in both interfaces) are internal 'tunable' hotspots of the Hsp70 allosteric machine that define the thermodynamics and kinetics of the allosteric cycle and can be modulated by either internal (sequence variations within the Hsp70 family) or external (binding to nucleotide, substrates, co-chaperones, posttranslational modifications) factors.

The main focus of our research is to understand the molecular mechanisms that control and fine-tune function and activity of the Hsp70 chaperones – a fundamental biomedical question that offers new opportunities to intervene in many pathological processes, including neurodegenerative diseases, diabetes and cancers.

Results

This project aims to understand the molecular details on how small sequence variations in different Hsp70s add posttranslational modifications affect the key Hsp70 function: ability to bind and release unfolded substrates under tight control of ATP hydrolysis. Intriguingly, despite the extremely high conservation in the Hsp70 family, different Hsp70s reveal small but significant sequence variations in Hsp70 allosteric hotspots, suggesting that these 'allosteric' amino acid substitutions apparently impact the Hsp70 functional cycle and thus, fine-tune functions for different Hsp70s. To characterize the intriguing relationship between Hsp70 function and sequence, we use a 'divide-and-conquer' approach that combines construct design, state-of-the-art multi-dimensional solution NMR and computational

methods with *in vitro* functional assays. Particularly we aim to understand the unique features of the conformational landscape for E. coli Hsp70 called DnaK and human endoplasmic reticulum Hsp70 called BiP in order to depict differences and similarities between these two Hsp70 members.

To elucidate how sequence variations affect Hsp70 function we employ NMR for characterization of the ER Hsp70 BiP. We have successfully completed the first (essential) step of the NMR analysis – optimizations of NMR sample conditions for different BiP constructs.

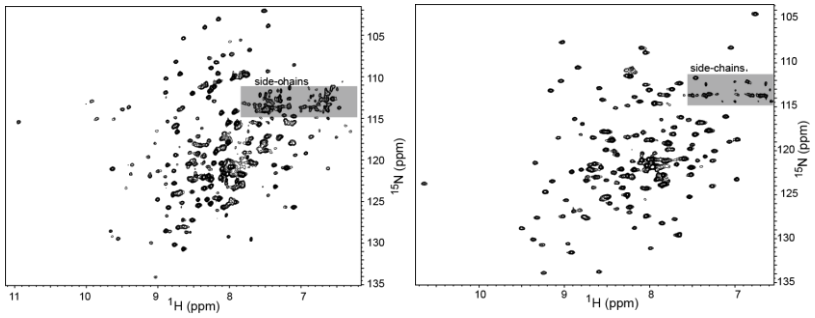

Figure 2: both BiP and SBD are suitable for detailed NMR analysis. Backbone NH spectra of BiP NBD (left) and SBD (right).

To understand how allosteric signal transduced from the NDB domain to the substrate-binding site, we employed molecular dynamics (MD) simulations and NMR chemical shift analysis to characterize dynamic and allosteric features of two X-ray βSBD conformations.

We found that in the domain-undocked state, βSBD adopts 'closed' conformations with high substrate affinity, while domain docking results in opening of two βSBD lobes (red and blue in Figure 3). The resulting 'open' conformation has low substrate affinity but enables proper interactions with the NBD. Intriguingly, the open and closed βSBD conformations have similar structure but drastically different dynamics, suggesting that conformational flexibility play an essential role for transduction of the allosteric signal.

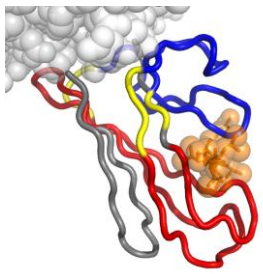

Figure 3: βSBD intradomain allostery relies on conformational rearrangements of two βSBD dynamic lobes. The lobe I and II are shown as red and blue; the hinge/bending regions are highlighted in yellow; the bound substrate and NBD are shown as orange and white spheres, respectively.

Publications

Budyak, I., Zhuravleva, A. & Gierasch, L. (2013). The role of aromatic-aromatic interactions in strand-strand stabilization of β-sheets. *J. Mol. Biol.* **425**: 3522-3535.

Ferrolino, M., Zhuravleva, A., Budyak, I., Krishnan, B. & Gierasch, L. (2013). Delicate balance between functionally required flexibility and aggregation risk in a rich protein. *Biochemistry* **52**: 8843–8854.

Funding

We thank the Faculty of Biological Sciences (University of Leeds) for start-up funding.

Collaborators

External: L. Gierasch (University of Massachusetts, USA) and L. Hendershot (St. Jude Children's Research Hospital, USA.

ASTBURY SEMINARS 2013

17th January
Prof. David Klenerman, University of Cambridge
"Single molecule studies of amyloid beta and alpha synuclein aggregation"

7th February
Dr Ed Tate, Imperial College
"The chemistry of protein modification inside living systems"

7th March
Prof. Johan Neyts, University of Leuven
"Strategies to inhibit the replication of various RNA viruses"

11th April
Dr Clair Baldock, University of Manchester
"Nanostructural studies of extracellular regulators of BMP signalling"

2nd May
Dr Jan Löwe, MRC Laboratory of Molecular Biology
"Structure and function of the bacterial cytoskeleton"

6th June
Prof. Steve Busby, University of Birmingham
"Bacterial transcription: ancient and modern"

1st July
Bragg Centenary Astbury Annual Lecture
Prof. Frances Ashcroft, University of Oxford
"Metabolic regulation of KATP channels: from molecule to disease"

3rd September
Prof. Carol Hall, North Carolina State University, USA
"Spontaneous formation of oligomers and fibrils in large scale molecular dynamics simulations of peptides"

5th September
Prof. Mark Sansom, University of Oxford
"Membrane proteins in context: MD simulations of membrane proteins and their lipid interactions"

3rd October
Dr Jo Parish, University of Birmingham
"Specific recruitment of the genomic insulator CTCF to the HPV genome"

31st October
Dr Jane Dyson, Scripps Research Institute
"Dynamics in biological processes"

7th November
Prof. Dagmar Klostermeier, Westfaelische Wilhelms-Universitaet Muenster
"The role of conformational changes for the function of ATP-driven molecular machines"

14th November
Prof . Rudi Ettrich, Institute of Nanobiology and Structural Biology, Nove Hardy, Czech Republic
"Was binding of free amino acids an early innovation in the evolution of allostery?"

28th November
Prof. Alison Smith, University of Cambridge
"Thiamine pyrophosphate riboswitches in algae - their role in metabolism and biotechnology"

PUBLICATIONS BY ASTBURY CENTRE MEMBERS 2013

Abou-Saleh, R., Peyman, S., Critchley, K., Evans, S. & Thomson, N. (2013) Nanomechanics of lipid encapsulated microbubbles with functional coatings. *Langmuir* **29**: 4096-4103.

Afanador, G., Muench, S., Mcphillie, M., Fomovska, A., Schoen, A., Zhou, Y., Cheng, G., Stec, J., Freundlich, J., Shieh, H.-M., Anderson, J., Jacobus, D. , Fidock, D., Kozikowski, A. P., Fishwick, C. W., Rice, D., Freire, E., Mcleod, R. & Prigge, S. (2013) Discrimination of potent inhibitors of *Toxoplasma gondii* enoyl-acyl carrier protein reductase by a thermal shift assay. *Biochemistry* **52**: 9155-9166.

Alexander, C., Juergens, M., Shepherd, D., Freund, S., Ashcroft, A. & Ferguson, N. (2013) Thermodynamic origins of protein folding, allostery, and capsid formation in the human hepatitis B virus core protein. *Proc. Natl. Acad. Sci. USA* **110**: 2782-2791.

Al-Lawati, Z., Bushby, R. & Evans, S. (2013) Alignment of a columnar hexagonal discotic liquid crystal on self-assembled monolayers. *J. Phys. Chem. C* **117**: 7533-7539.

Amako, Y., Igloi, Z., Mankouri, J., Kazlauskas, A., Saksela, K., Dallas, M., Peers, C. & Harris, M. (2013) Hepatitis c virus ns5a inhibits mixed lineage kinase 3 to block apoptosis. *J. Biol. Chem.* **288**: 24753-24763.

Amer, M., Mckeown, L., Tumova, S., Liu, R., Seymour, V. a. L., Wilson, L., Naylor, J., Greenhalgh, K., Hou, B., Majeed, Y., Turner, P., Sedo, A., O'regan, D., Li, J., Bon, R., Porter, K. & Beech, D. (2013) Inhibition of endothelial cell Ca^{2+} entry and transient receptor potential channels by sigma-1 receptor ligands. *Br. J. Pharmacol.* **168**: 1445-1455.

Ariza, A., Tanner, S., Walter, C., Dent, K., Shepherd, D., Wu, W., Matthews, S., Hiscox, J., Green, T. , Luo, M., Elliott, R., Fooks, A., Ashcroft, A., Stonehouse, N., Ranson, N., Barr, J. & Edwards, T. (2013) Nucleocapsid protein structures from orthobunyaviruses reveal insight into ribonucleoprotein architecture and RNA polymerization. *Nucleic Acids Res.* **41**: 5912-5926.

Azzarito, V., Long, K., Murphy, N. & Wilson, A. (2013) Inhibition of alpha-helix-mediated protein-protein interactions using designed molecules. *Nat. Chem.* **5**: 161-173.

Banushkina, P. & Krivov, S. (2013) High-resolution free-energy landscape analysis of alpha-helical protein folding: Hp35 and its double mutant. *J. Chem. Theory Comput.* **9**: 5257-5266.

Beales, P., Geerts, N., Inampudi, K., Shigematsu, H., Wilson, C. & Vanderlick, T. (2013) Reversible assembly of stacked membrane nanodiscs with reduced dimensionality and variable periodicity. *J. Am. Chem. Soc.* **135**: 3335-3338.

Bellucci, L., Corni, S., Di Felice, R. & Paci, E. (2013) The structure of neuronal calcium sensor-1 in solution revealed by molecular dynamics simulations. *PLoS One* **8**: e74383.

Bentham, M., Foster, T., McCormick, C. & Griffin, S. (2013) Mutations in hepatitis c virus p7 reduce both the egress and infectivity of assembled particles via impaired proton channel function. *J. Gen. Virol.* **94**: 2236-2248.

Bernardi, A., Jimenez-Barbero, J., Casnati, A., De Castro, C., Darbre, T., Fieschi, F., Finne, J., Funken, H., Jaeger, K.-E., Lahmann, M., Lindhorst, T., Marradi, M., Messner, P., Molinaro, A., Murphy, P., Nativi, C., Oscarson, S., Penades, S., Peri, F., Pieters, R., Renaudet, O., Reymond, J.-L., Richichi, B., Rojo, J., Sansone, F., Schaeffer, C., Turnbull, W., Velasco-

Torrijos, T., Vidal, S., Vincent, S., Wennekes, T., Zuilhof, H. & Imberty, A. (2013) Multivalent glycoconjugates as anti-pathogenic agents. *Chem. Soc.Rev.* **42**: 4709-4727.

Bettaney, K., Sukumar, P., Hussain, R., Siligardi, G., Henderson, P. & Patching, S. (2013) A systematic approach to the amplified expression, functional characterization and purification of inositol transporters from *Bacillus subtilis*. *Mol. Membr. Biol.* **30**: 3-14.

Blake, K. & O'Neill, A. (2013) Transposon library screening for identification of genetic loci participating in intrinsic susceptibility and acquired resistance to antistaphylococcal agents. *J. Antimicrob. Chemother.* **68**: 12-16.

Bon, R. & Beech, D. (2013) In pursuit of small molecule chemistry for calcium-permeable non-selective TRPc channels - mirage or pot of gold? *Br. J. Pharmacol* **170**: 459-474.

Booth, M., Peel, R., Partanen, R., Hondow, N., Vasilca, V., Jeuken, L. & Critchley, K. (2013) Amphipol-encapsulated cuins2/zns quantum dots with excellent colloidal stability. *RSC Adv.* **3**: 20559-20566.

Borodavka, A., Tuma, R. & Stockley, P. (2013) A two-stage mechanism of viral rna compaction revealed by single molecule fluorescence. *RNA Biol.* **10**: 481-489.

Branson, T. & Turnbull, W. (2013) Bacterial toxin inhibitors based on multivalent scaffolds. *Chem. Soc. Rev.* **42**: 4613-4622.

Brown, H., Unger, C. & Whitehouse, A. (2013) Potential of herpesvirus saimiri-based vectors to reprogram a somatic Ewing's sarcoma family tumor cell line. *J. Virol.* **87**: 7127-7139.

Brown, L.-A., Larson, T., Graham, I., Hawes, C., Paudyal, R., Warriner, S. & Baker, A. (2013) An inhibitor of oil body mobilization in *Arabidopsis*. *New Phytol.* **200**: 641-649.

Budyak, I., Zhuravleva, A. & Gierasch, L. (2013). The role of aromatic-aromatic interactions in strand-strand stabilization of β-sheets. *J. Mol. Biol.* **425**: 3522-3535.

Burnett, A., Kendrick, J., Russell, C., Christensen, J., Cunningham, J., Pearson, A., Linfield, E. & Davies, A. (2013) The effect of molecular size and particle shape on the terahertz absorption of a homologous series of tetraalkylammonium salts. *Anal. Chem.* **85** 7926-2934.

Care, M., Barrans, S., Worrillow, L., Jack, A., Westhead, D. & Tooze, R. (2013) A microarray platform-independent classification tool for cell of origin class allows comparative analysis of gene expression in diffuse large B-cell lymphoma. *PLoS One* **8**: e55895.

Carr, S., Mecia, L., Phillips, S. & Thomas, C. (2013) Identification, characterization and preliminary X-ray diffraction analysis of the rolling-circle replication initiator protein from plasmid pSTK1. *Acta Crystallogr. Sect. F Struct. Biol. Cryst. Commun.* **69**: 1123-1126.

Chammas, O., Billingsley, D., Bonass, W. & Thomson, N. (2013) Single-stranded DNA loops as fiducial markers for exploring DNA-protein interactions in single molecule imaging. *Methods* **60**: 122-130.

Cheng, G., Muench, S., Zhou, Y., Afanador, G., Mui, E., Fomovska, A., Lai, B., Prigge, S., Woods, S., Roberts, C., Hickman, M., Lee, P., Leed, S., Auschwitz, J. M., Rice, D. & Mcleod, R. (2013) Design, synthesis, and biological activity of diaryl ether inhibitors of *Toxoplasma gondii* enoyl reductase. *Bioorg. Med. Chem. Lett.* **23**: 2035-2043.

Churchman, A., Wallace, R., Milne, S., Brown, A., Brydson, R. & Beales, P. (2013) Serum albumin enhances the membrane activity of zno nanoparticles. *Chem. Commun.* **49**: 4172-4174.

Connell, S., Heath, G., Olmsted, P. & Kisil, A. (2013) Critical point fluctuations in supported lipid membranes. *Faraday Discuss.* **161**: 91-111.

Cox, G., Edwards, T. & O'Neill, A. (2013) Mutagenesis mapping of the protein-protein interaction underlying fusb-type fusidic acid resistance. *Antimicrob. Agents Chemother.* **57**: 4640-4644.

De Marcos Lousa, C., Van Roermund, C., Postis, V., Dietrich, D., Kerr, I., Wanders, R., Baldwin, S., Baker, A. & Theodoulou, F. (2013) Intrinsic acyl-CoA thioesterase activity of a peroxisomal ATP binding cassette transporter is required for transport and metabolism of fatty acids. *Proc. Natl. Acad. Sci. USA* **110**: 1279-1284.

Dent, K., Thompson, R., Barker, A., Hiscox, J., Barr, J., Stockley, P. & Ranson, N. (2013) The asymmetric structure of an icosahedral virus bound to its receptor suggests a mechanism for genome release. *Structure* **21**: 1225-1234.

Duce, J., Lei, P., Tsatsanis, A., Wong, B., Lam, L., Ayton, S., Rogers, J., Finkelstein, D. & Bush, A. (2013) A novel relationship between beta-amyloid protein precursor and tau in Alzheimer's disease related iron disruption. *Am. J. Hematol.* **88**: E34-E35.

Dykeman, E., Stockley, P. & Twarock, R. (2013) Packaging signals in two single-stranded RNA viruses imply a conserved assembly mechanism and geometry of the packaged genome. *J. Mol. Biol.* **425**: 3235-3249.

El Omari, K., Meier, C., Kainov, D., Sutton, G., Grimes, J., Poranen, M., Bamford, D., Tuma, R., Stuart, D. & Mancini, E. (2013) Tracking in atomic detail the functional specializations in viral reca helicases that occur during evolution. *Nucleic Acids Res.* **41**: 9396-9410.

Emmott, E., Munday, D., Bickerton, E., Britton, P., Rodgers, M., Whitehouse, A., Zhou, E.-M. & Hiscox, J. (2013) The cellular interactome of the coronavirus infectious bronchitis virus nucleocapsid protein and functional implications for virus biology. *J. Virol.* **87**: 9486-9500.

Farrance, O., Hann, E., Kaminska, R., Housden, N., Derrington, S., Kleanthous, C., Radford, S. & Brockwell, D. (2013) A force-activated trip switch triggers rapid dissociation of a colicin from its immunity protein. *PLoS Biol.* **11**: e1001489.

Ferrolino, M., Zhuravleva, A., Budyak, I., Krishnan, B. & Gierasch, L. (2013). Delicate balance between functionally required flexibility and aggregation risk in a rich protein. *Biochemistry* **52**: 8843–8854.

Figueiredo, A., Whittaker, S., Knowling, S., Radford, S. & Moore, G. (2013) Conformational dynamics is more important than helical propensity for the folding of the all alpha-helical protein Im7. *Prot. Sci.* **22**: 1722-1738.

Fisher, H., Smith, M. & Ashcroft, A. (2013) De novo sequencing of short interfering ribonucleic acids facilitated by use of tandem mass spectrometry with ion mobility spectrometry. *Rapid Commun. Mass Spectrom.* **27**: 2247-2254.

Ford, R., Barker, A., Bakker, S., Coutts, R., Ranson, N., Phillips, S., Pearson, A. & Stockley, P. (2013) Sequence-specific, RNA-protein interactions overcome electrostatic barriers preventing assembly of satellite tobacco necrosis virus coat protein. *J. Mol. Biol.* **425**: 1050-1064.

Foster, T., Thompson, G., Kalverda, A., Kankanala, J., Bentham, M., Wetherill, L., Thompson, J., Barker, A., Clarke, D., Norenberg, M., Pearson, A., Rowlands, D., Homans, S., Harris, M., Foster, R. & Griffin, S. (2013) Structure-guided design affirms inhibitors of Hepatitis C Virus p7 as a viable class of antivirals targeting virion release. *Hepatology* **59:** 408-422.

Gates, A., Marritt, S., Bradley, J., Shi, L., Mcmillan, D., Jeuken, L., Richardson, D. & Butt, J. (2013) Electrode assemblies composed of redox cascades from microbial respiratory electron transfer chains. *Biochem. Soc. Trans.* **41**: 1249-1253.

Geerts, N., Schreck, C., Beales, P., Shigematsu, H., O'hern, C. & Vanderlick, T. (2013) Using DNA-driven assembled phospholipid nanodiscs as a scaffold for gold nanoparticle patterning. *Langmuir* **29**: 13089-13094.

Glennon, E., Whitehouse, I., Miners, J., Kehoe, P., Love, S., Kellett, K. & Hooper, N. (2013) Bin1 is decreased in sporadic but not familial Alzheimer's disease or in aging. *PLoS One* **8**: e78806.

Gooch, A., Murphy, N., Thomson, N. & Wilson, A. (2013) Side-chain supramolecular polymers employing conformer independent triple hydrogen bonding arrays. *Macromolecules* **46**: 9634-9641.

Griffiths, D., Abdul-Sada, H., Knight, L., Jackson, B., Richards, K., Prescott, E., Peach, A., Blair, G., Macdonald, A. & Whitehouse, A. (2013) Merkel cell polyomavirus small t antigen targets the nemo adaptor protein to disrupt inflammatory signaling. *J. Virol.* **87**: 13853-13867.

Guzik-Lendrum, S., Heissler, S., Billington, N., Takagi, Y., Yang, Y., Knight, P., Homsher, E. & Sellers, J. (2013) Mammalian myosin-18a, a highly divergent myosin. *J. Biol. Chem.* **288**: 9532-9548.

Heath, G., Johnson, B., Olmsted, P., Connell, S. & Evans, S. (2013) Actin assembly at model-supported lipid bilayers. *Biophys. J.* **105**: 2355-2365.

Heidarsson, P., Otazo, M., Bellucci, L., Mossa, A., Imparato, A., Paci, E., Corni, S., Di Felice, R., Kragelund, B. & Cecconi, C. (2013) Single-molecule folding mechanism of an EF-hand neuronal calcium sensor. *Structure* **21**: 1812-1821.

Henderson, P. & Baldwin, S. (2013) This is about the in and the out. *Nat. Struct. Mol. Biol.* **20**: 654-655.

Hoffmann, T., Tych, K., Brockwell, D. & Dougan, L. (2013) Single-molecule force spectroscopy identifies a small cold shock protein as being mechanically robust. *J. Phys. Chem. B* **117**: 1819-1826.

Hoffmann, T., Tych, K., Hughes, M., Brockwell, D. & Dougan, L. (2013) Towards design principles for determining the mechanical stability of proteins. *Phys. Chem. Chem. Phys.* **15**: 15767-15780.

Hrast, M., Turk, S., Sosic, I., Knez, D., Randall, C., Barreteau, H., Contreras-Martel, C., Dessen, A., O'Neill, A., Mengin-Lecreulx, D., Blanot, D. & Gobec, S. (2013) Structure-activity relationships of new cyanothiophene inhibitors of the essential peptidoglycan biosynthesis enzyme murf. *Eur. J. Med. Chem.* **66**: 32-45.

Ingram, N., Macnab, S., Marston, G., Scott, N., Carr, I., Markham, A., Whitehouse, A. & Coletta, P. (2013) The use of high-frequency ultrasound imaging and biofluorescence for *in vivo* evaluation of gene therapy vectors. *BMC Med. Imaging* **13**: 35

James, T., Simpson, I., Grant, J., Sridharan, V. & Nelson, A. (2013) Modular, gold-catalyzed approach to the synthesis of lead-like piperazine scaffolds. *Org. Lett.* **15**: 6094-6097.

Jiang, L.-H., Baldwin, J., Roger, S. & Baldwin, S. (2013) Insights into the molecular mechanisms underlying mammalian p2x7 receptor functions and contributions in diseases, revealed by structural modeling and single nucleotide polymorphisms. *Front. Pharmacol.* **4**: 55-55.

Jin, X., Shah, S., Liu, Y., Zhang, H., Lees, M., Fu, Z., Lippiat, J., Beech, D., Sivaprasadarao, A., Baldwin, S., Zhang, H. & Gamper, N. (2013) Activation of the Cl^- channel Ano1 by localized calcium signals in nociceptive sensory neurons requires coupling with the IP3 receptor. *Sci. Signal.* **6:** ra73.

Juergens, M., Voeroes, J., Rautureau, G., Shepherd, D., Pye, V., Muldoon, J., Johnson, C., Ashcroft, A., Freund, S. & Ferguson, N. (2013) The hepatitis b virus pres1 domain hijacks host trafficking proteins by motif mimicry. *Nat. Chem. Biol.* **9**: 540-547.

Kashchiev, D., Cabriolu, R. & Auer, S. (2013) Confounding the paradigm: peculiarities of amyloid fibril nucleation. *J. Am. Chem. Soc.* **135**: 1531-1539.

Keef, T., Wardman, J., Ranson, N., Stockley, P. & Twarock, R. (2013) Structural constraints on the three-dimensional geometry of simple viruses: Case studies of a new predictive tool. *Acta Crystallogr. A* **69**: 140-150.

Knapman, T., Valette, N., Warriner, S. & Ashcroft, A. (2013) Ion mobility spectrometry-mass spectrometry of intrinsically unfolded proteins: Trying to put order into disorder. *Curr. Anal. Chem.* **9**: 181-191.

Kong, Y., Chen, J., Gao, F., Brydson, R., Johnson, B., Heath, G., Zhang, Y., Wu, L. & Zhou, D. (2013) Near-infrared fluorescent ribonuclease-a-encapsulated gold nanoclusters: Preparation, characterization, cancer targeting and imaging. *Nanoscale* **5**: 1009-1017.

Krivov, S. (2013) Method to describe stochastic dynamics using an optimal coordinate. *Phys. Rev. E* **88**: 062131.

Krivov, S. (2013) On reaction coordinate optimality. *J. Chem. Theory Comput.* **9**: 135-146.

Lewis, M., Arnot, C., Beeston, H., Mccoy, A., Ashcroft, A., Gay, N. & Gangloff, M. (2013) Cytokine spatzle binds to the drosophila immunoreceptor toll with a neurotrophin-like specificity and couples receptor activation. *Proc. Natl. Acad. Sci. USA* **110**: 20461-20466.

Lin, Y.-F., Romero, D., Guan, S., Mamanova, L. & McDowall, K. (2013) A combination of improved differential and global RNA-seq reveals pervasive transcription initiation and events in all stages of the life-cycle of functional RNAs in propionibacterium acnes, a major contributor to wide-spread human disease. *BMC Genomics* **14**: 620.

Lloyd, A., Potter, N., Fishwick, C., Roper, D. & Dowson, C. (2013) Adenosine tetraphosphoadenosine drives a continuous ATP-release assay for aminoacyl-tRNA synthetases and other adenylate-forming enzymes. *ACS Chem. Biol.* **8**: 2157-2163.

Long, K., Edwards, T. & Wilson, A. (2013) Microwave assisted solid phase synthesis of highly functionalized n-alkylated oligobenzamide alpha-helix mimetics. *Bioorg. Med. Chem.* **21**: 4034-4040.

Lousa, C., Van Roermund, C., Postis, V., Dietrich, D., Kerr, I., Wanders, R., Baldwin, S., Baker, A. & Theodoulou, F. (2013) Intrinsic acyl-coa thioesterase activity of a peroxisomal ATP binding cassette transporter is required for transport and metabolism of fatty acids. *Proc. Natl. Acad. Sci. USA* **110**: 1279-1284.

Maclellan, P. & Nelson, A. (2013) A conceptual framework for analysing and planning synthetic approaches to diverse lead-like scaffolds. *Chem. Commun.* **49**: 2383-2393.

Maurya, S., Dow, M., Warriner, S. & Nelson, A. (2013) Synthesis of skeletally diverse alkaloid-like molecules: Exploitation of metathesis substrates assembled from triplets of building blocks. *Beilstein J. Org. Chem.* **9**: 775-785.

McAllister, T., Hollins, J. & Webb, M. (2013) Prospects for stable analogues of phosphohistidine. *Biochem. Soc. Trans.* **41**: 1072-1077.

Mcmillan, D., Marritt, S., Firer-Sherwood, M., Shi, L., Richardson, D., Evans, S., Elliott, S., Butt, J. & Jeuken, L. (2013) Protein-protein interaction regulates the direction of catalysis and electron transfer in a redox enzyme complex. *J. Am. Chem. Soc.* **135**: 10550-10556.

McMillan, D., Marritt, S., Kemp, G., Gordon-Brown, P., Butt, J. & Jeuken, L. (2013) The impact of enzyme orientation and electrode topology on the catalytic activity of adsorbed redox enzymes. *Electrochim. Acta* **110**: 79-85.

McMorran, L., Bartlett, A., Huysmans, G., Radford, S. & Brockwell, D. (2013) Dissecting the effects of periplasmic chaperones on the *in vitro* folding of the outer membrane protein PagP. *J. Mol. Biol.* **425**: 3178-3191.

Mitchell, J. & Harris, S. (2013) Thermodynamics of writhe in DNA minicircles from molecular dynamics simulations. *Phys. Rev. Lett.* 110: 148105.

Monteiro, D., Kamdoum, W. & Paci, E. (2013) Growth kinetics of bacterial pili from pairwise pilin association rates. *PLoS One* **8**: 10.1371.

Meri, T., Amdahl, H., Lehtinen, M., Hyvärinen, S., McDowell, J., Bhattacharjee, A., Meri, S., Marconi, R., Goldman, A. & Jokiranta, T. (2013) Microbes bind complement inhibitor factor H via a common site. *PLoS Pathog.* **9**:e1003308.

Bhattacharjee, A., Oeemig, J., Kolodziejczyk, R., Meri, T., Kajander, T., Lehtinen, M., Iwai, H., Jokiranta, T. & Goldman, A. (2013). Structural basis for complement evasion by Lyme disease pathogen *Borrelia burgdorferi*. *J. Biol. Chem.* **288**:18685-18695.

Kajander, T., Kellosalo, J. & Goldman, A. (2013). Inorganic pyrophosphatases: one substrate, three mechanisms. *FEBS Lett.* **587**:1863-1869.

Muench, S., Scheres, S., Huss, M., Phillips, C., Vitavska, O., Wieczorek, P., Trinick, J. & Harrison, M. (2013) Subunit positioning and stator filament stiffness in regulation and power transmission in the V1 motor of the *Manduca sexta* V-ATPase. *J. Mol. Biol.* **426**: 286-300.

Muench, S., Stec, J., Zhou, Y., Afanador, G., Mcphillie, M., Hickman, M., Lee, P., Leed, S., Auschwitz, J., Prigge, S., Rice, D. & Mcleod, R. (2013) Development of a triclosan scaffold which allows for adaptations on both the a- and b-ring for transport peptides. *Bioorg. Med. Chem. Lett.* **23**: 3551-3555.

Murphy, N., Prabhakaran, P., Azzarito, V., Plante, J., Hardie, M., Kilner, C., Warriner, S. & Wilson, A. (2013) Solid-phase methodology for synthesis of o-alkylated aromatic oligoamide inhibitors of alpha-helix-mediated proteinprotein interactions. *Chem. Eur. J.* **19**: 5546-5550.

Ndlovu, H., Ashcroft, A., Radford, S. & Harris, S. A. (2013) Molecular dynamics simulations of mechanical failure in polymorphic arrangements of amyloid fibrils containing structural defects. *Beilstein J. Nanotechnol.* **4**: 429-440.

Nicol, C., Cesur, O., Forrest, S., Belyaeva, T., Bunka, D., Blair, G. & Stonehouse, N. (2013) An RNA aptamer provides a novel approach for the induction of apoptosis by targeting the hpv16 e7 oncoprotein. *PLoS One* **8:** 10.1371.

Oliver, R., Read, D., Harlen, O. & Harris, S. (2013) A stochastic finite element model for the dynamics of globular macromolecules. *J. Comput. Phys.* **239**: 147-165.

Ooi, N., Chopra, I., Eady, A., Cove, J., Bojar, R. & O'Neill, A. (2013) Antibacterial activity and mode of action of tert-butylhydroquinone (tbhq) and its oxidation product, tert-butylbenzoquinone (tbbq). *J. Antimicrob. Chemother.* **68**: 1297-1304.

Patching, S., Henderson, P., Sharples, D. & Middleton, D. (2013) Probing the contacts of a low-affinity substrate with a membrane-embedded transport protein using H^1-C^{13} cross-polarisation magic-angle spinning solid-state NMR. *Mol. Membr. Biol.* **30**: 129-137.

Pellizzaro, M., Fisher, J. & Wilson, A. (2013) Electronic substituent effects on hydrogen-bonding motifs modulate supramolecular polymerisation. *RSC Adv.* **3**: 3103-3108.

Pellizzaro, M., Houton, K. & Wilson, A. (2013) Sequential and phototriggered supramolecular self-sorting cascades using hydrogen-bonded motifs. *Chem. Sci.* **4**: 1825-1829.

Peyman, S., Abou-Saleh, R. & Evans, S. (2013) Research spotlight: Microbubbles for therapeutic delivery. *Therapeutic delivery* **4**: 539-542.

Postis, V., Rawlings, A., Lesiuk, A. & Baldwin, S. (2013) Use of *Escherichia coli* for the production and purification of membrane proteins. *Methods Mol. Biol.* **998**: 33-54.

Prabhakaran, P., Barnard, A., Murphy, N., Kilner, C., Edwards, T. & Wilson, A. (2013) Aromatic oligoamide foldamers with a "wet edge" as inhibitors of the -helix-mediated p53-hdm2 protein-protein interaction. *European J. Org. Chem.* 3504-3512.

Preston, G. & Wilson, A. (2013) Photo-induced covalent cross-linking for the analysis of biomolecular interactions. *Chem. Soc. Rev.* **42**: 3289-3301.

Pritchard, C., O'connor, G. & Ashcroft, A. (2013) The role of ion mobility spectrometry-mass spectrometry in the analysis of protein reference standards. *Anal. Chem.* **85**: 7205-7212.

Psencik, J., Arellano, J., Collins, A., Laurinmaki, P., Torkkeli, M., Loflund, B., Serimaa, R., Blankenship, R., Tuma, R. & Butcher, S. (2013) Structural and functional roles of carotenoids in chlorosomes. *J. Bacteriol.* **195**: 1727-1734.

Radou, G., Enciso, M., Krivov, S. & Paci, E. (2013) Modulation of a protein free-energy landscape by circular permutation. *J. Phys. Chem. B* **117**: 13743-13747.

Randall, C., Mariner, K., Chopra, I. & O'Neill, A. (2013) The target of daptomycin is absent from *Escherichia coli* and other gram-negative pathogens. *Antimicrob. Agents Chemother.* **57**: 637-639.

Randall, C., Oyama, L., Bostock, J., Chopra, I. & O'Neill, A. (2013) The silver cation (ag): Antistaphylococcal activity, mode of action and resistance studies. *J. Antimicrob. Chemother.* **68**: 131-138.

Remenyi, J., Van Den Bosch, M., Palygin, O., Mistry, R., Mckenzie, C., Macdonald, A., Hutvagner, G., Arthur, J., Frenguelli, B. & Pankratov, Y. (2013) Mir-132/212 knockout mice reveal roles for these miRNAs in regulating cortical synaptic transmission and plasticity. *PLoS One* **8:** e62509.

Ren, J., Wang, X., Hu, Z., Gao, Q., Sun, Y., Li, X., Porta, C., Walter, T., Gilbert, R., Zhao, Y., Axford, D., Williams, M., Mcauley, K., Rowlands, D., Yin, W., Wang, J., Stuart, D., Rao, Z. & Fry, E. (2013) Picornavirus uncoating intermediate captured in atomic detail. *Nat. Commun.* **4:** 1929.

Riches, K., Franklin, L., Maqbool, A., Peckham, M., Adams, M., Bond, J. Warburton, P., Feric, N., Koschinsky, M., O'Regan, D., Ball, S., Turner, N. & Porter, K. (2013) Apolipoprotein(a) acts as a chemorepellent to human vascular smooth muscle cells via integrin alphabeta3 and RhoA/ROCK-mediated mechanisms. *Int. J. Biochem. Cell Biol.* **45**: 1776-83

Rhys, N. H. & Dougan, L. (2013) The emerging role of hydrogen bond interactions in polyglutamine structure, stability and association. *Soft Matter* **9**: 2359-2364.

Roberts, A., Kon, T., Knight, P., Sutoh, K. & Burgess, S. (2013) Functions and mechanics of dynein motor proteins. *Nat. Rev. Mol. Cell Biol.* **14**: 713-726.

Ross-Thriepland, D., Amako, Y. & Harris, M. (2013) The C terminus of NS5A domain II is a key determinant of hepatitis C virus genome replication, but is not required for virion assembly and release. *J. Gen. Virol.* **94**: 1009-1018.

Rushworth, J., Griffiths, H., Watt, N. & Hooper, N. (2013) Prion protein-mediated toxicity of amyloid-beta oligomers requires lipid rafts and the transmembrane lrp1. *J. Biol. Chem.* **288**: 8935-8951.

Santos, S., Barcons, V., Christenson, H., Billingsley, D., Bonass, W., Font, J. & Thomson, N. (2013) Stability, resolution, and ultra-low wear amplitude modulation atomic force microscopy of DNA: small amplitude small set-point imaging. *Appl. Phys. Lett.* **103:** 063702.

Santos, S., Billingsley, D. & Thomson, N. (2013) Atomic force microscopy imaging of macromolecular complexes. *Methods Mol. Biol.* **950**: 315-341.

Sarell, C., Stockley, P. & Radford, S. (2013) Assessing the causes and consequences of co-polymerization in amyloid formation. *Prion* **7**: 359-368.

Sarell, C., Woods, L., Su, Y., Debelouchina, G., Ashcroft, A., Griffin, R., Stockley, P. & Radford, S. (2013) Expanding the repertoire of amyloid polymorphs by co-polymerization of related protein precursors. *J. Biol. Chem.* **288**: 7327-7337.

Saundh, B., Baker, R., Harris, M., Smith, M., Cherukuri, A. & Hale, A. (2013) Early BK polyomavirus (BKV) reactivation in donor kidney is a risk factor for development of BKV-associated nephropathy. *J. Infect. Dis.* **207**: 137-141.

Savage, V., Chopra, I. & O'Neill, A. (2013) Population diversification in *Staphylococcus aureus* biofilms may promote dissemination and persistence. *PLoS One* **8:** e62513.

Savage, V., Chopra, I. & O'Neill, A. (2013) *Staphylococcus aureus* biofilms promote horizontal transfer of antibiotic resistance. *Antimicrob. Agents Chemother.* **57**: 1968-1970.

Scarff, C., Sicorello, A., Tome, R., Macedo-Ribeiro, S., Ashcroft, A. & Radford, S. (2013) A tale of a tail: Structural insights into the conformational properties of the polyglutamine protein ataxin-3. *Int. J. Mass spectrom.* **345**: 63-70.

Schumann, S., Jackson, B., Baquero-Perez, B. & Whitehouse, A. (2013) Kaposi's sarcoma-associated herpesvirus orf57 protein: Exploiting all stages of viral mRNA processing. *Viruses* **5**: 1901-1923.

Settanni, G., Serquera, D., Marszalek, P., Paci, E. & Itzhaki, L. (2013) Effects of ligand binding on the mechanical properties of ankyrin repeat protein gankyrin. *PLoS Comp. Biol.* **9**.

Sevdali, M., Kumar, V., Peckham, M. & Sparrow, J. (2013) Human congenital myopathy actin mutants cause myopathy and alter z-disc structure in drosophila flight muscle. *Neuromuscul. Disord.* **23**: 243-255.

Shepherd, D., Holmes, K., Rowlands, D., Stonehouse, N. & Ashcroft, A. (2013) Using ion mobility spectrometry-mass spectrometry to decipher the conformational and assembly characteristics of the hepatitis b capsid protein. *Biophys. J.* **105**: 1258-1267.

Sheynis, T., Friediger, A., Xue, W.-F., Hellewell, A., Tipping, K., Hewitt, E., Radford, S. & Jelinek, R. (2013) Aggregation modulators interfere with membrane interactions of beta(2)-microglobulin fibrils. *Biophys. J.* **105**: 745-755.

Simmons, K., Gotfryd, K., Billesbolle, C., Loland, C., Gether, U., Fishwick, C. & Johnson, A. (2013) A virtual high-throughput screening approach to the discovery of novel inhibitors of the bacterial leucine transporter, LeuT. *Mol. Membr. Biol.* **30**: 184-194.

Skedelj, V., Perdih, A., Brvar, M., Kroflic, A., Dubbee, V., Savage, V., O'Neill, A., Solmajer, T., Bester-Rogac, M., Blanot, D., Hugonnet, J.-E., Magnet, S., Arthur, M., Mainardi, J.-L., Stojan, J. & Zega, A. (2013) Discovery of the first inhibitors of bacterial enzyme d-aspartate ligase from *Enterococcus faecium* (asl(fm)). *Eur. J. Med. Chem.* **67**: 208-220.

Song, C., Papachristos, K., Rawson, S., Huss, M., Wieczorek, H., Paci, E., Trinick, J., Harrison, M. & Muench, S. (2013) Flexibility within the rotor and stators of the vacuolar H^+-ATPase. *PLoS One* **8:** e82207.

Song, L., Ho, V., Chen, C., Yang, Z., Liu, D., Chen, R. & Zhou, D. (2013) Efficient, pH-triggered drug delivery using a pH-responsive DNA-conjugated gold nanoparticle. *Adv. Healthc. Mater.* **2**: 275-280.

Stec, J., Fomovska, A., Afanador, G., Muench, S., Zhou, Y., Lai, B.-S., El Bissati, K., Hickman, M., Lee, P., Leed, S., Auschwitz, J., Sommervile, C., Woods, S., Roberts, C., Rice, D., Prigge, S., Mcleod, R. & Kozikowski, A. (2013) Modification of triclosan scaffold in search of improved inhibitors for enoyl-acyl carrier protein (acp) reductase in *Toxoplasma gondii*. *ChemMedChem* **8**: 1138-1160.

Stewart, H., Walter, C., Jones, D., Lyons, S., Simmonds, P. & Harris, M. (2013) The non-primate hepacivirus 5 ' untranslated region possesses internal ribosomal entry site activity. *J. Gen. Virol.* **94**: 2657-2663.

Stockley, P., Ranson, N. & Twarock, R. (2013) A new paradigm for the roles of the genome in ssRNA viruses. *Future Virol.* **8**: 531-543.

Stockley, P., Twarock, R., Bakker, S., Barker, A., Borodavka, A., Dykeman, E., Ford, R., Pearson, A., Phillips, S., Ranson, N. & Tuma, R. (2013) Packaging signals in single-stranded RNA viruses: Nature's alternative to a purely electrostatic assembly mechanism. *J. Biol. Phys.* **39**: 277-287.

Stones, R., Benoist, D., Peckham, M. & White, E. (2013) Microtubule proliferation in right ventricular myocytes of rats with monocrotaline-induced pulmonary hypertension. *J. Mol. Cell. Cardiol.* **56**: 91-96.

Svobodova, M., Bunka, D., Nadal, P., Stockley, P. & O'Sullivan, C. (2013) Selection of 2 ' f-modified RNA aptamers against prostate-specific antigen and their evaluation for diagnostic and therapeutic applications. *Anal. Bioanal. Chem.* **405**: 9149-9157.

Thompson, S., Wilson, A. & Battersby, A. (2013) In celebration of the 60th birthday of Professor Andrew D. Hamilton FRS. *Organic & Biomolecular Chemistry* **11**: 6236-6241.

Timms, N., Windle, C., Polyakova, A., Ault, J., Trinh, C., Pearson, A., Nelson, A. & Berry, A. (2013) Structural insights into the recovery of aldolase activity in N-acetylneuraminic acid lyase by replacement of the catalytically active lysine with gamma-thialysine by using a chemical mutagenesis strategy. *ChemBioChem* **14**: 474-481.

Towey, J., Soper, A. K. & Dougan, L. (2013) What happens to the structure of water in cryoprotectant solutions? *Faraday Discuss.* **167**: 159-176.

Tych, K., Hoffmann, T., Brockwell, D. & Dougan, L. (2013) Single molecule force spectroscopy reveals the temperature-dependent robustness and malleability of a hyperthermophilic protein. *Soft Matter* **9**: 9016-9025.

Van Geersdaele, L., Stead, M., Harrison, C., Carr, S., Close, H., Rosbrook, G., Connell, S. & Wright, S. (2013) Structural basis of high-order oligomerization of the cullin-3 adaptor Spop. *Acta Crystallogr. D Biol. Crystallogr.* **69**: 1677-1684.

Vaziri, H., Baldwin, S., Baldwin, J., Adams, D., Young, J. & Postis, V. (2013) Use of molecular modelling to probe the mechanism of the nucleoside transporter NupG. *Mol. Membr. Biol.* **30**: 114-128.

Watt, N., Griffiths, H. & Hooper, N. (2013) Neuronal zinc regulation and the prion protein. *Prion* **7**: 203-208.

Whitehouse, I., Miners, J., Glennon, E., Kehoe, P., Love, S., Kellett, K. & Hooper, N. (2013) Prion protein is decreased in Alzheimer's brain and inversely correlates with Bace1 activity, amyloid-beta levels and BRAAK stage. *Plos One* **8:** e59554.

Wilson, A., Ault, J., Filby, M., Philips, H., Ashcroft, A. & Fletcher, N. (2013) Protein destabilisation by ruthenium(ii) tris-bipyridine based protein-surface mimetics. *Org. Biomol. Chem.* **11**: 2206-2212.

Wolny, M., Colegrave, M., Colman, L., White, E., Knight, P. & Peckham, M. (2013) Cardiomyopathy mutations in the tail of beta-cardiac myosin modify the coiled-coil structure and affect integration into thick filaments in muscle sarcomeres in adult cardiomyocytes. *J. Biol. Chem.* **288**: 31952-31962.

Woods, L., Radford, S. & Ashcroft, A. (2013) Advances in ion mobility spectrometry-mass spectrometry reveal key insights into amyloid assembly. *Biochim. Biophys. Acta* **1834**: 1257-1268.

Xu, J., Vanderlick, T. & Beales, P. (2013) Lytic and non-lytic permeabilization of cardiolipin-containing lipid bilayers induced by cytochrome c. *PLoS One* **8:** e69492.

Xue, W.-F.& Radford, S. (2013) An imaging and systems modeling approach to fibril breakage enables prediction of amyloid behavior. *Biophys. J.* **105**: 2811-2819.

Yeo, D., Warriner, S. & Wilson, A. (2013) Monosubstituted alkenyl amino acids for peptide "stapling". *Chem. Commun.* **49**: 9131-9133.

Yi, D., He, N., Kickstein, M., Metzner, J., Weiss, M., Berry, A. & Fessner, W.-D. (2013) Engineering of a cytidine 5 '-monophosphate-sialic acid synthetase for improved tolerance to functional sialic acids. *Adv. Synth. Catal.* **355**: 3597-3612.

Young, J., Yao, S., Baldwin, J., Cass, C. & Baldwin, S. (2013) The human concentrative and equilibrative nucleoside transporter families, slc28 and slc29. *Mol. Aspects Med.* **34**: 529-547.

Yule, I. & Fishwick, C. (2013) A simple, one-pot synthesis of n-alkyl and n-aryl thieno 2,3-d pyrimidinones from thiophene- and benzothiophene-2-yl-ureas. *Synth. Commun.* **43**: 337-344.

Yuzugullu, Y., Trinh, C., Fairhurst, L., Ogel, Z., McPherson, M. & Pearson, A. (2013) Investigating the active centre of the *Scytalidium thermophilum* catalase. *Acta Crystallogr. F Struct. Biol. Commun.* **69**: 369-375.

Yuzugullu, Y., Trinh, C., Smith, M., Pearson, A., Phillips, S., Sutay Kocabas, D., Bakir, U., Ogel, Z., & McPherson, M. (2013) Crystal structure, recombinant expression and mutagenesis studies of the bifunctional catalase-phenol oxidase from *Scytalidium thermophilum*. *Acta Crystallogr. D Biol. Crystallogr.* **69**: 398-408.

Zhang, H., Feng, G., Guo, Y. & Zhou, D. (2013) Robust and specific ratiometric biosensing using a copper-free clicked quantum dot-DNA aptamer sensor. *Nanoscale* **5**: 10307-10315.

Zhang, Y., Guo, Y., Quirke, P. & Zhou, D. (2013) Ultrasensitive single-nucleotide polymorphism detection using target-recycled ligation, strand displacement and enzymatic amplification. *Nanoscale* **5**: 5027-5035.

Zhang, Y., Pilapong, C., Guo, Y., Ling, Z., Cespedes, O., Quirke, P. & Zhou, D. (2013) Sensitive, simultaneous quantitation of two unlabeled DNA targets using a magnetic nanoparticle-enzyme sandwich assay. *Anal. Chem.* **85**: 9238-9244.